

Center for Computer Research in Music and Acoustics

May 29, 1987

Department of Music
Report No. STAN-M-39

MUSIC APPLICATIONS OF DIGITAL WAVEGUIDES

by

Julius O. Smith

This is an overview of Digital Waveguides as applied to music. Included are papers and viewgraphs describing Waveguide Reverberation, Waveguide Synthesis, Limit Cycle Elimination and Background Theory.

© 1987 by Julius O. Smith

This manuscript may be freely reproduced for nonprofit educational purposes.

Music Applications of Digital Waveguides

Julius O. Smith

Center for Computer Research in Music and Acoustics

Department of Music, Stanford University

Stanford, California 94305

TABLE OF CONTENTS

| | |
|-----------------------------------|-----|
| Waveguide Reverberation | 1 |
| Viewgraphs | 8 |
| Waveguide Synthesis | 29 |
| Viewgraphs | 35 |
| Limit Cycle Elimination | 47 |
| Viewgraphs | 79 |
| Background Theory | 108 |

**A New Approach to Digital Reverberation
using
Closed Waveguide Networks**

Julius O. Smith

*Center for Computer Research in Music and Acoustics (CCRMA)
Department of Music, Stanford University
Stanford, California 94305*

Abstract

This paper presents a new type of digital reverberator which is based on closed networks of intersecting *waveguides*. Each waveguide is a bi-directional delay line, of arbitrary length, and each intersection (of any number of waveguides) produces lossless signal scattering. By creating a closed network of waveguides, the total signal energy in the structure is preserved. A reverberator is constructed by introducing small losses in the network to achieve a desired reverberation time. The inputs and outputs can be chosen anywhere in the structure.

There are many reasons to construct reverberators (or any recursive digital filter for that matter) from lossless waveguide networks: (1) the scattering junctions can be made time varying without altering stored energy, (2) an "erector set" for lossless networks is obtained, allowing any number of branches to be fitted together in any desired configuration (with changes allowed in real time), (3) limit cycles and overflow oscillations are easily eliminated, regardless of interconnection, (4) an exact physical interpretation exists for all signals in the structure, and (5) the implementation is computationally efficient.

Introduction

Digital reverberation has been a standard post-processor for digital music synthesis since Schroeder's original papers in '61 and '62 [4,9]. The basic acoustics of reverberation and the design of concert halls has a long history covering many different approaches [1-24]. The basic goal of digital reverberation is to arrive at a digital filtering operation which simulates the effect of a good concert hall or "listening space" on the source sound. This goal is made difficult by the fact that typical listening spaces are inherently large-order systems which cannot be precisely simulated in real time using commonly available computing techniques. In architectural acoustics, the study of digital reverberation

aids in the design of concert halls with good "acoustics." In digitally synthesized music, the reverberator is a part of the instrumental ensemble, providing a direct enrichment to the sound quality. This paper is concerned with the latter application; while there is no need for a detailed physical model, it is desired to capture all musically important qualities of natural reverberation.

Digital room simulation has been implemented by simulating specular reflection in actual concert-hall geometries or some approximation thereto [17,10,16,8,12]. It has been found that the diffusive scattering of sound by natural listening environments cannot be neglected in high-quality models [16]. However, models which accommodate diffusing reflections are beyond the reach of present computing power when applied to listening spaces of nominal size over the audio frequency band.

Another implementation of digital reverberation is to record an approximation to the impulse response between two spatial points in a real hall. The effect of the hall on sound between these two points can be very accurately simulated by convolving the measured impulse response with the desired source signal [35]. Again this leads to a prohibitive computational burden (two to three orders of magnitude out of real time for typical mainframes).

We can easily summarize the current state of high-quality digital reverberation: it is well understood, but too expensive to compute. It would seem that much progress is possible, because there is much detail in natural reverberation that is not important perceptually. For example, it has been noted that convolving an unreverberated sound with exponentially decaying white noise gives the best known artificial reverberation [16]. The key to a successful digital reverberator design is to replace the details of a quantitative physical model by simple computations which retain all important qualitative behavior.

Some basic building blocks of presently pervasive digital reverberators, introduced by Schroeder [6], include cascaded allpass networks, recursive and non-recursive comb filters, tapped delay lines, and lowpass filters. The early reflections can be exactly matched [8,16] for a fixed source and listener position using a tapped delay line, and the late reverberation can be qualitatively matched using a combination of allpass chains, comb filters, and lowpass filters [8,16]. Using a lowpass filter in the feedback loop of a comb filter is used to simulate air absorption and non-specular reflection [16]. This overall strategy for reverberation, or some subset of it, has been the basis for reverberation design at CCRMA for more than a decade [13,15]. While these elements do not provide reverberation on par with excellent natural listening environments, they do a good job at providing some of the most essential aspects of reverberation—especially for smoothly varying sounds at low reverberation levels.

A New Approach

The proposed technique is to build digital reverberators as closed networks of lossless digital waveguides [46,47]. Such a network can be constructed from any given number of multiplies, additions, and delay elements. The available multiplies and additions determine how many signal-scattering nodes can be implemented, and the available delay elements determine the total delay which can be distributed among the branches interconnecting the various nodes. By choosing the number of intersecting branches and scattering coefficients appropriately, multiplies can be eliminated completely [46,47] (the scattering coefficients are reduced to a power of two or a simple function of powers of two such as $3/4 = 1/2 + 1/4$). There are simple rules for connecting branches to nodes in a way which preserves signal energy. The design variables (in the lossless prototype) are branch-connection topology, delay lengths, and the characteristic impedances of the individual waveguides.

The lossless prototype reverberator is augmented by one or more simple loss factors (of the form $1 - 2^{-n}$, typically) to set the reverberation decay time to any desired value. That is, T_{60} (the time over which the reverberation decays 60 dB) is infinite in the prototype, but arbitrary in the final network. This decoupling of reverberation time from structural aspects incurs no loss of generality.

Some branches can be fixed to give specific early reflections, while other branches may be chosen to provide a desirable texture in the late reverberation. An optimality

criterion for the late reverberation is to maximize homogeneity of the impulse response (make it look like exponentially decaying white noise). Waveguide networks allow every signal path to appear as a feedback branch around every other signal path. This connectivity richness facilitates development of dense late reverberation. Furthermore, the energy conserving properties of the waveguide networks can be maintained in the time-varying case [46,47]; this allows the breaking up of "patterns" in the late reverberation by subtly changing the reverberator in a way that does not modulate the reverberation decay profile. Finally, the explicit conservation of signal energy provides an easy way to completely suppress limit cycles and overflow oscillations.

Lossless Networks

A *network* is a closed interconnection of bi-directional signal paths. The signal paths are called *branches* and the interconnection points are called *nodes*. An example diagram of a simple network is shown in Fig. 1.

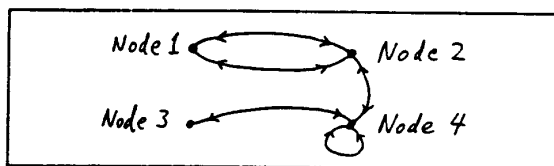


Figure 1. An example network diagram

Each signal path is *bi-directional*, meaning that in each branch there is a signal propagating in one direction and an independent signal propagating in the other direction. When a signal reaches a node, it is partially reflected back along the same branch, and partially transmitted into the other branches connected to the node. The relative strengths of the pieces of the "scattered" signal are determined by the relative characteristic impedances of the intersecting waveguides.

A *waveguide* is defined as a lossless bi-directional signal branch. In the simplest case, each branch in a waveguide network is merely a *bi-directional delay line*. The only computations in the network take place at the branch intersection points (nodes). More generally, a waveguide branch may contain any chain of cascade allpass filters. For practical reverberator design, we also introduce losses in the form of gain factors less than 1 and/or lowpass filters with frequency response strictly bounded by 1.

A lossless network preserves total stored signal energy. Energy is preserved if at each time instant the total energy stored in the network is the same as at any other time instant. The total energy at any time instant is found by summing the instantaneous power throughout the network. Each signal sample within the network contributes to instantaneous power. The instantaneous power of a stored sample is the squared amplitude times a scale factor, say g . If the signal is in units of "pressure," or equivalent, then $g = 1/Z$, where Z is the characteristic impedance of the waveguide medium. If the signal sample instead represents a "flow" variable, such as volume-velocity, then $g = Z$. In either case, the stored energy is a weighted sum of squared values of all samples stored in the digital network memory.

An N -port is a network in which N branches, called ports, leave the network to provide inputs and outputs. Figure 2 gives an example of a network with one port designated for input and two ports designated for output.

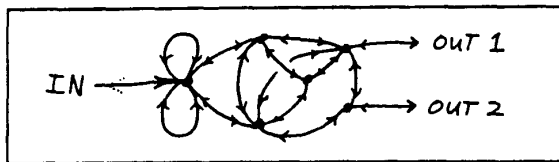


Figure 2. Example 3-port

Such a structure is suitable, for example, for providing stereo reverberation of a single channel of sound. Note, however, that really there are three inputs and three outputs. In an N -port, each branch leaving the network provides both an input and an output (because it is bi-directional). It is common practice in digital filtering applications [36] to use only one direction on a port branch as an input or output and ignore the other direction.

An N -port is lossless if at any time instant, the energy lost through the outputs (so far), equals the total energy supplied through the inputs (so far), plus the total stored energy. A lossless digital filter is obtained from a lossless N -port by using every port as both an input and output.

An N -port is linear if superposition holds. Superposition holds when the output in response to the sum of two input signals equals the sum of the outputs in response to each individual input signal. A network is linear if every N -port derived from it is linear. Only linear networks can be restricted to a large and well-understood class of energy conserving systems.

Lossless Scattering

Consider a parallel junction of N lossless waveguides of characteristic impedance Z_i (characteristic admittance $\Gamma_i = 1/Z_i$) as depicted in Fig. 3.

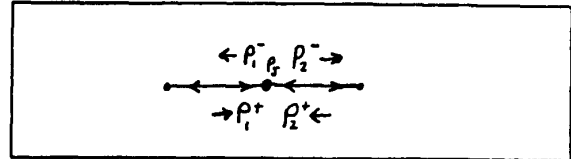


Figure 3. A junction of 2 waveguides.

If the incoming traveling pressure waves are denoted by P_i^+ , $i = 1, \dots, N$, the outgoing pressure waves are given by [46,47]

$$P_i^- = P_J - P_i^+ \quad (1)$$

where P_J is the resultant junction pressure,

$$P_J = 2 \frac{\sum_{i=1}^N \Gamma_i P_i^+}{\sum_{i=1}^N \Gamma_i} \quad (2)$$

The series flow-junction is equivalent to the parallel pressure-junction. The series pressure-junction or the parallel flow-junction can be found by use of duality [46,47].

Equation (1) is a computationally efficient way to implement an N -port scattering junction. In the case $N = 2$, the well-known one-multiplier lattice filter section (minus its unit delay) is obtained immediately from (1). More generally, an N -way intersection requires N multiplies and $N - 1$ additions to obtain P_J , and one addition for each outgoing wave, for a total of N multiplies and $2N - 1$ additions.

Normalized Waves

We can normalize the pressure and flow variables by the square root of the characteristic impedance to obtain propagation waves in units of root power:

$$\begin{aligned} \tilde{P}_i^+ &\triangleq P_i^+ \sqrt{\Gamma_i} & \tilde{P}_i^- &\triangleq P_i^- \sqrt{\Gamma_i} \\ \tilde{U}_i^+ &\triangleq U_i^+ \sqrt{Z_i} & \tilde{U}_i^- &\triangleq U_i^- \sqrt{Z_i} \end{aligned} \quad (3)$$

By restricting all waveguides to normalized waves, we obtain a generalization of the normalized ladder structure for digital filters [34,36,39]. The stored power in each section is unchanged if the characteristic impedance is changed (the pressure and flow variables are scaled in a complementary fashion). The use of normalized waves yields digital filter

structures whose signal energy is not modulated by time-varying coefficients [46,47]. Signal power and "coefficient power" are decoupled.

Energy and Power

The *instantaneous power* in a waveguide containing instantaneous pressure P and flow U is defined as the product of pressure and flow:

$$P = PU = (P^+ + P^-)(U^+ + U^-) = P^+ + P^- \quad (4)$$

where

$$\begin{aligned} P^+ &= P^+U^+ = Z(U^+)^2 = \Gamma(P^+)^2 \\ P^- &= P^-U^- = -Z(U^-)^2 = -\Gamma(P^-)^2 \end{aligned} \quad (5)$$

define the *right-going* and *left-going* power, respectively.

For the N -way waveguide junction, we have, using Kirchoff's node equations [26,27,46,47],

$$P_J \triangleq \sum_{i=1}^N P_i U_i = \sum_{i=1}^N P_J U_i = P_J \sum_{i=1}^N U_i = 0 \quad (6)$$

Thus, the N -way junction is *lossless*; no net power, active or reactive, flows into or away from the junction.

Quantization Effects

While the ideal waveguide junction is lossless, finite word-length effects can make exactly lossless networks unrealizable. In fixed-point arithmetic, the product of two numbers requires more bits (in general) for exact representation than either of the multiplicands. If there is a feedback loop around a product, the number of bits needed to represent exactly a circulating signal grows without bound. Therefore, some sort of round-off rule must be included in a finite-precision implementation. The guaranteed absence of limit cycles and overflow oscillations is tantamount to ensuring that all finite-wordlength effects result in power *absorption* at each junction, and never power creation. If *magnitude truncation* is used on all outgoing waves, then limit cycles and overflow oscillations are suppressed [32]. Magnitude truncation results in greater losses than necessary to suppress quantization effects. More refined schemes are possible. In particular, by saving and accumulating the low-order half of each multiply at a junction, energy can be exactly preserved in spite of finite precision computations [46,47].

Conclusions

A construction was presented parametrizing all lossless linear networks. The construction is free of overflow oscillations and limit cycles, and a valuable energy decoupling property is obtained for time-varying networks. The added complexity relative to the best pre-existing recursive filter architectures is negligible. Therefore, these structures are likely to become standard in the near future.

In addition to implementing robust reverberation and digital filtering, waveguide structures can provide accurate models of coupled vibrating strings, wind instruments, reed instruments, and many other physical systems. In these applications, the signals propagating in a waveguide are coupled to a nonlinear "excitation element," such as a reed, bow, switching air-jet, or lips [41]. On the other side of the excitation element, another waveguide network can be used to model the player windway, bow assembly, or other interacting resonating system.

Appendix—Application Notes

In this appendix, some practical tips are listed for obtaining good reverberation.

- 1000 echoes per second is considered sufficiently dense for late reverberation [8, p. 219].
- Because air absorption increases with spatial frequency, lowpass filters should be used here and there in the waveguides to give qualitatively the correct relative time constants of decay versus frequency.
- The scattering coefficients can be randomly modulated to better approach an exponentially decaying white noise impulse response. This places the signal in a closed, randomly changing maze.
- Modulating the scattering coefficients with sinusoids, FM, or other complex waveforms, produces an appealing “undulating” reverberator. A physical analogy is time-varying absorption coefficients in the walls of a concert hall (plus magic tunneling of absorbed energy into vibrational modes elsewhere). Increasing the modulation frequency to audio rates causes a kind of “sideband” generation in the reverberated sound, corresponding to weak amplitude modulation. This can be understood by considering that as a signal is reflecting from a junction, the amplitude of the reflection is directly proportional to the reflection coefficient. Therefore, all scattering coefficient modulation (random or not) should occur at frequencies below audible AM modulation rates in order to avoid this effect. Random switching should occur at sub-audio rates and employ proper audio fade-in/fade-out (e.g. 100ms fade time).
- The reverberation is generally less “colored” [6] when each output of the reverberator is taken to be a resultant pressure P_J at a junction of multiple waveguides.
- Setting branch delays to an interval of a Fibonacci series has given good results [45].
- Choosing equal reflection coefficients at a junction leads to an even energy distribution throughout the network. (A beam incident on the junction is scattered equally in all directions.) If the scattering coefficients are too disparate, “hot spots” or nearly lossless sub-paths may appear in the network. A uniform energy distribution helps to minimize the probability of overflow.
- Duality can be used to improve the dynamic range. In high-impedance waveguides, pressure tends to be large, while in low-impedance waveguides, flow is large (for a given signal power). Therefore, switching between pressure and flow for the propagating variable in each waveguide allows maximum use of the available dynamic range. This is the same thing as choosing the sign parameters in standard lattice filters [36]. Use of normalized waves eliminates the need to decide on pressure versus flow, and the signal level is always proportional to the root-power, independent of the characteristic impedance.
- Choosing a power of two for the number of branches of equal characteristic impedance intersecting at a node yields a multiplier-free realization.
- Physical analogies can give considerable insight into the operation of a waveguide network. For example, placing a finger on the midpoint of a freely vibrating string (making the tone rise one octave) is a physical analog to introducing a junction with rising reflection coefficient in the middle of a single waveguide with reflecting terminations. Another analogy is an optical waveguide containing beam-splitters in the form of partially silvered partitions. Visualizing more than two intersections is less easy; one example is to imagine waves along many taut wires of varying thickness welded together at a common point.
- It is possible to create the effect of moving walls by smoothly varying the delay-line lengths as well as the scattering coefficients. The basic technique for this is described in [44]. One way to avoid energy modulation is to effectively “slide” a junction along a line formed by two waveguides meeting at that junction. The delay lost by one waveguide is given to the other.
- A desirable reverberator property is that the density of resonant modes between any input/output point grow as the square of frequency [1]. The number of complex modes in any nondegenerate digital filter is equal to the total number of delay elements. Thus, a closed waveguide network always has as many complex resonances as there are stored samples. Finding exactly where the resonances are tuned as a function of the interconnection topology and scattering coefficients seems to be a difficult problem. Whenever a new input or output point is chosen, the zeros of transmission are changed. The poles of the point-to-point transfer function, however, are invariant under general conditions. Con-

sequently, if a realistic mode distribution is found, it can be used with a wide variety of input and output ports.

- Picking n_i in the branch loss factors $g_i = 1 - 2^{-n_i}$ as a function of T_{60} appears hard to do exactly. An approximate formula is to choose n_i so that $g_i^{T_{60}/D_i}$ close to 0.001, where D_i is the delay of the i th waveguide in seconds.
- Reverberation is realistically diffuse if the steady-state reverberator response to a sinusoidal input signal has a Rayleigh distributed amplitude throughout the delay elements of the reverberator [20]. Equivalently, the intensity is exponentially distributed, phase is uniformly distributed, and the real and imaginary parts of the sinusoidal response phasor are Gaussian distributed [20]. These distributions correspond physically to the excitation of many modes of vibration in the hall, yielding plane waves traveling in "all directions" with independent random phases. See also [1,7].
- Assuming a Rayleigh amplitude distribution allows calculation of probability of overflow as a function of the number of guard bits provided.

References

Reverberation and Architectural Acoustics

- [1] P. M. Morse, *Vibration and Sound*, published by the American Institute of Physics for the Acoustical Society of America, 1976 (1st ed. 1936, 2nd ed. 1948).
- [2] L. L. Beranek, *Acoustics*, McGraw-Hill, New York, 1954, 1960.
- [3] B. B. Bauer, "Stereophonic earphones and binaural loudspeakers," *J. Audio Eng. Soc.*, vol. 9, no. 2, pp. 148-151, April 1961.
- [4] M. R. Schroeder and B. F. Logan, "Colorless Artificial Reverberation," *J. Audio Eng. Soc.*, vol. 9, no. 3, pp. 192-, July 1961.
- [5] L. L. Beranek, *Music, Acoustics, and Architecture*, John Wiley and Sons, Inc., New York, 1962.
- [6] M. R. Schroeder, "Natural Sounding Artificial Reverberation," *J. Audio Eng. Soc.*, vol. 10, no. 3, pp. 219-223, July 1962.
- [7] P. M. Morse and U. Ingard, *Theoretical Acoustics*, McGraw-Hill, New York, 1968.
- [8] M. R. Schroeder, "Digital Simulation of Sound Transmission in Reverberant Spaces," *J. Acoust. Soc. Amer.*, vol. 47, no. 2, pp. 424-431 (part 1), Feb. 1970.
- [9] M. R. Schroeder, "Improved Quasi-Stereophony and Colorless Artificial Reverberation," *J. Acoust. Soc. Amer.*, vol. 33, pp. 1061- (part 1), Feb. 1970.
- [10] B. M. Gibbs and D. K. Jones, "A Simple Image Method for Calculating the Distribution of Sound Pressure Levels within an Enclosure," *Acustica*, vol. 26, pp. 24-32, 1972.
- [11] H. Kuttruff, *Room Acoustics*, Applied Science Publishers, London, 1973.
- [12] M. R. Schroeder, "Computer Models for Concert Hall Acoustics," *A. J. P.*, vol. 41, pp. 461-471, April 1973.
- [13] J. M. Chowning, J. M. Grey, L. Rush, and J. A. Moorer, "Computer Simulation of Music Instrument Tones in Reverberant Environments," Music Dept. Tech. Rep. STAN-M-1, Stanford University, 1974.
- [14] W. Jesteadt, C.C. Wier, and D.M. Green, "Intensity Discrimination as a Function of Frequency and Sensation Level," *J. Acoust. Soc. Amer.*, vol. 61, no. 1, pp. 169-177, Jan. 1977.
- [15] J. M. Chowning, J. M. Grey, L. Rush, J. A. Moorer, and L. Smith, "Simulation of Music Instrument Tones in Reverberant Environments: Final Report," Music Dept. Tech. Rep. STAN-M-8, Stanford University, 1978.
- [16] J. A. Moorer, "About this Reverberation Business," *Computer Music J.*, vol. 3, no. 2, pp. 13-28, 1979. Reprinted in [24].
- [17] J. B. Allen and D. A. Berkeley, "Image Method for Efficiently Simulating Small-Room Acoustics," *J. Acoust. Soc. Amer.*, vol. 65, no. 4, pp. 943-950, April 1979.
- [18] M. Barron and A. H. Marshall, "Spatial Impression due to Early Lateral Reflections in Concert Halls: the Derivation of a Physical Measure," *J. Sound Vib.*, vol. 77, no. 2, pp. 211-232, Feb. 1981.
- [19] M. R. Schroeder, "Modulation Transfer Function: Definition and Measurement," *Acustica*, vol. 49, pp. 179-182, 1981.
- [20] K. J. Ebeling, K. Freudenstein, and H. Alrutz, "Experimental Investigations of Statistical Properties of Diffuse Sound Fields in Reverberation Rooms," *Acustica*, vol. 51, no. 3, pp. 145-153, 1982.
- [21] C. Sheeline, "An Investigation of the Effects of Direct and Reverberant Signal Interactions on Auditory Distance Perception," Ph.D. Dissertation, Hearing and Speech Sc. Dept., Stanford University, Nov. 1982. Music Dept. Tech. Rep. STAN-M-13.

- [22] J. Borish, "Electronic Simulation of Auditorium Acoustics," Ph.D. Dissertation, Elec. Eng. Dept., Stanford University, Music Dept. Tech. Rep. STAN-M-18, 1984.
- [23] J. D. Polack, H. Alrutz, and M. R. Schroeder, "The Modulation Transfer Function of Music Signals and its Application to Reverberation Measurement," *Acustica*, vol. 54, pp. 257-265, 1984.
- [24] C. Roads and J. Strawn, eds., *Foundations of Computer Music*, MIT Press, Cambridge MA, 1985.
- Signal Processing
- [25] R. Bracewell, *The Fourier Transform and its Applications*, McGraw-Hill, New York, 1965.
- [26] V. Belevitch, *Classical Network Theory*, Holden Day, San Francisco, CA, 1968.
- [27] A. Fettweis, "Digital Filters Related to Classical Structures," *AEU: Archive für Elektronik und Übertragungstechnik*, vol. 25, pp. 79-89, Feb. 1971.
- [28] A. Fettweis, "Some Principles of Designing Digital Filters Imitating Classical Filter Structures," *IEEE Trans. on Circ. Theory*, vol. CT-18, pp. 314-316, March 1971.
- [29] J. L. Flanagan, *Speech Analysis, Synthesis, and Perception*, Springer-Verlag, New York, 1972.
- [30] A. Fettweis, "Pseudopassivity, Sensitivity, and Stability of Wave Digital Filters," *IEEE Trans. on Circ. Theory*, vol. CT-19, pp. 668-673, Nov. 1972.
- [31] K. Meerkötter and W. Wegener, "A New Second-Order Digital Filter without Parasitic Oscillations," *AEU: Archive für Elektronik und Übertragungstechnik*, vol. 29, pp. 312-314, Feb. 1975.
- [32] A. Fettweis and K. Meerkötter, "Suppression of Parasitic Oscillations in Wave Digital Filters," *IEEE Trans. Circ. and Sys.*, vol. CAS-22, No. 3, pp. 239-246, Mar. 1975.
- [33] A. Fettweis and K. Meerkötter, "On Adaptors for Wave Digital Filters," *IEEE Trans. on Acoust., Speech, and Signal Proc.*, vol. ASSP-23, pp. 516-525, Dec. 1975.
- [34] A. H. Gray and J. D. Markel, "A Normalized Digital Filter Structure," *IEEE Trans. on Acoust., Speech, and Signal Proc.*, vol. ASSP-23, pp. 268-277, June 1975.
- [35] L. R. Rabiner and B. Gold, *Theory and Application of Digital Signal Processing*, Prentice-Hall Inc., Englewood Cliffs, NJ, 1975.
- [36] J. D. Markel and A. H. Gray, *Linear Prediction of Speech*, Springer-Verlag, New York, 1976.
- [37] B. Noble, *Applied Linear Algebra*, Prentice-Hall Inc., Englewood Cliffs, NJ, 1969, 1977.
- [38] Digital Signal Processing Committee, ed., *Programs for Digital Signal Processing*, IEEE Press, New York, 1979.
- [39] A. H. Gray, "Passive Cascaded Lattice Digital Filters," *IEEE Trans. Circ. and Sys.*, vol. CAS-27, No. 5, pp. 337-344, May 1980.
- [40] B. Friedlander, "Lattice Filters for Adaptive Processing," *Proc. IEEE*, vol. 70, pp. 829-867, Aug. 1982.
- [41] M. E. McIntyre, R. T. Schumacher, and J. Woodhouse, "On the Oscillations of Musical Instruments," *J. Acoust. Soc. Amer.*, vol. 74, no. 5, pp. 1325-1345, Nov. 1983.
- [42] A. Fettweis, "Digital Circuits and Systems," *IEEE Trans. Circ. and Sys.*, vol. CAS-31, No. 1, pp. 31-48, Jan. 1984.
- [43] J. O. Smith, "Introduction to Digital Filter Theory," In J. Strawn, ed., *Digital Audio Signal Processing: An Anthology*. William Kaufmann, Inc., Los Altos, California, 1985.
- [44] J. O. Smith and B. Friedlander, "Adaptive Interpolated Time-Delay Estimation," *IEEE Trans. on Aerospace and Electronic Systems*, vol. AES-21, no. 2, pp. 180-199, May 1985.
- [45] P. Gossett, Private Communication.
- [46] J. O. Smith, "Waveguide Digital Filters," CCRMA, Dept. of Music, Stanford University, March 1985.
- [47] J. O. Smith, "Reverberation by means of Digital Waveguide Networks," in preparation.

WAVEGUIDE
DIGITAL
REVERBERATION

J. O. Smith

CCRMA

ICMC-85

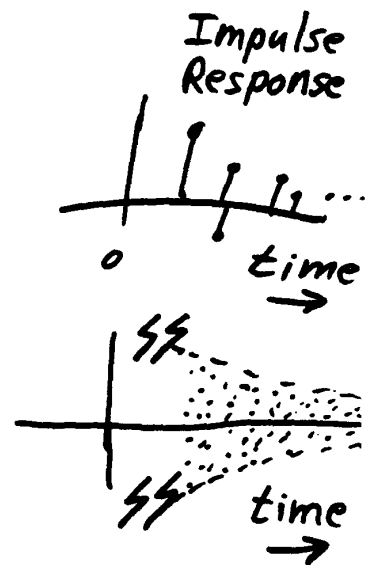
Aug. 22, 1985

GOAL of DIGITAL REVERB

- Simulate the filtering effects of a top-quality concert hall.

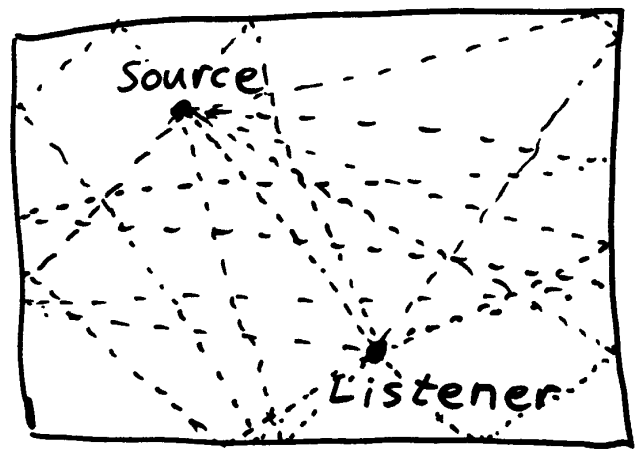


- ① Provide realistic "Early Reflections"
- ② Late Reverberation is highly diffuse

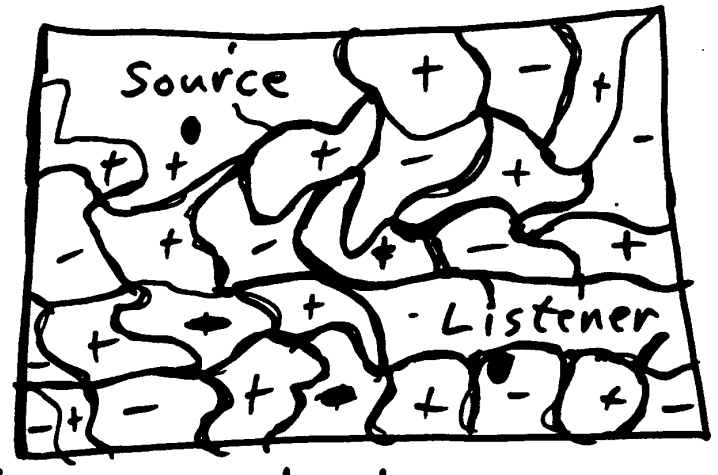


TWO VIEWS of NATURAL REVERB

Infinite
Series
of
Echoes



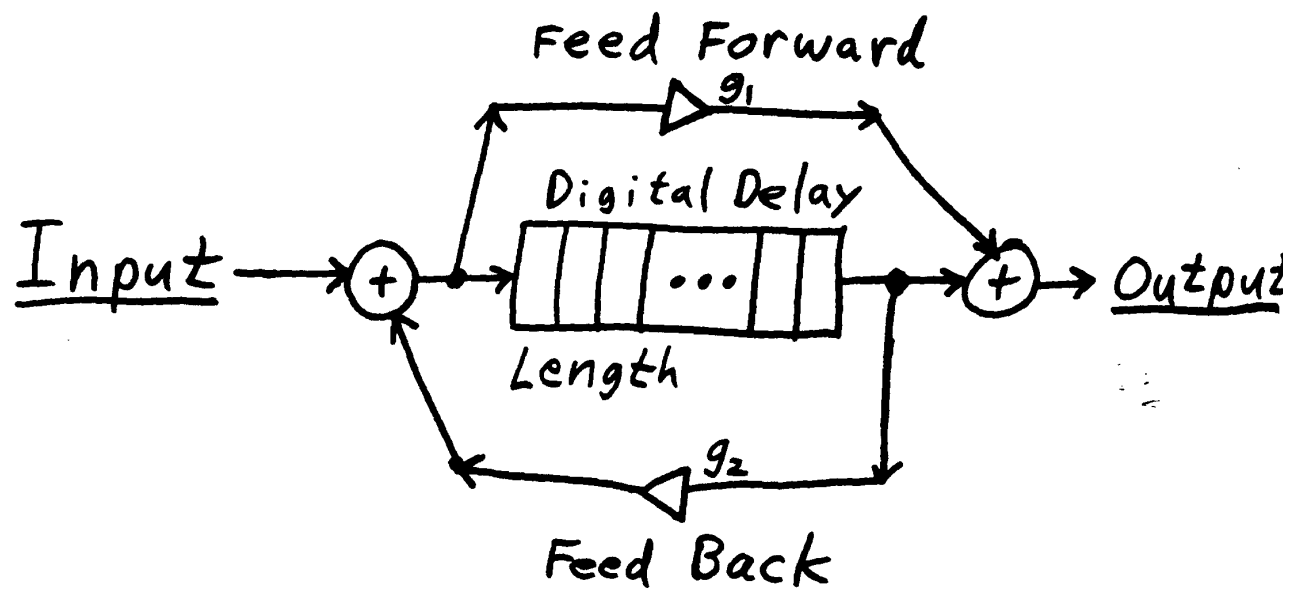
Random
sound
field at
Each
Frequency



$f \lambda \rightarrow$

ELEMENTS OF MUSIC

DIGITAL REVERBERATORS



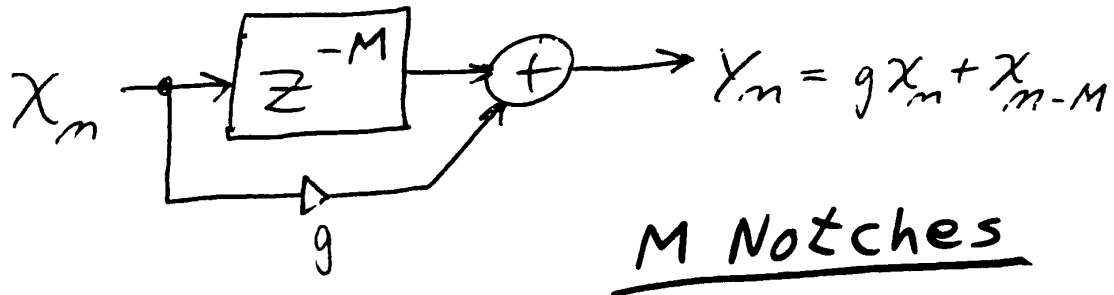
Universal Section

| g_1 | g_2 | Name |
|-------|-------|--------------------------|
| 0 | 0 | Delay Line |
| 0 | X | Feedback Comb Filter |
| X | 0 | Feed forward Comb Filter |
| X | -X | Allpass Filter |

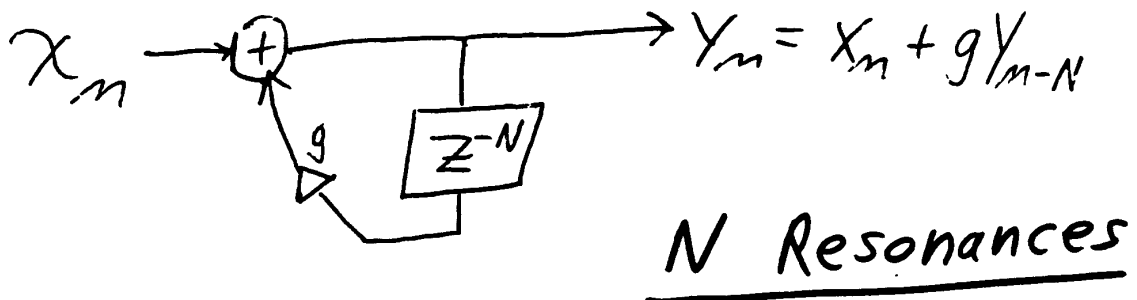
SPECIAL CASES

12

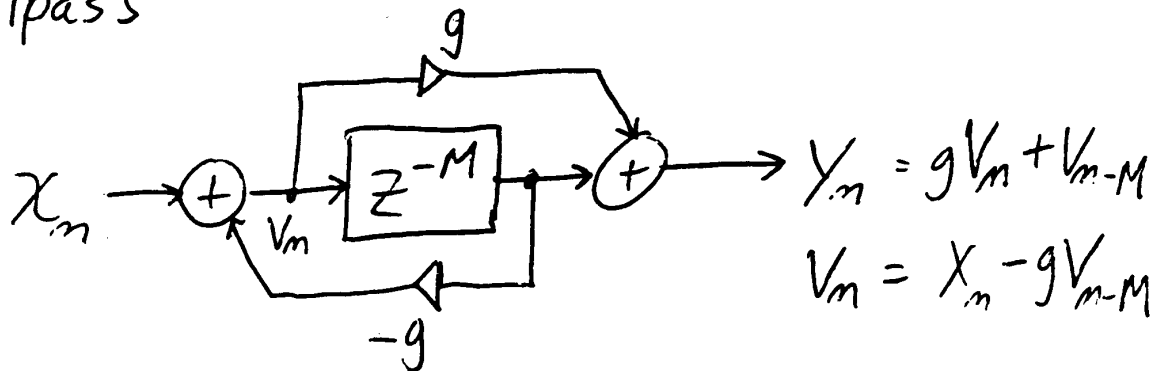
- Feed-forward Comb-Filter (FFC)



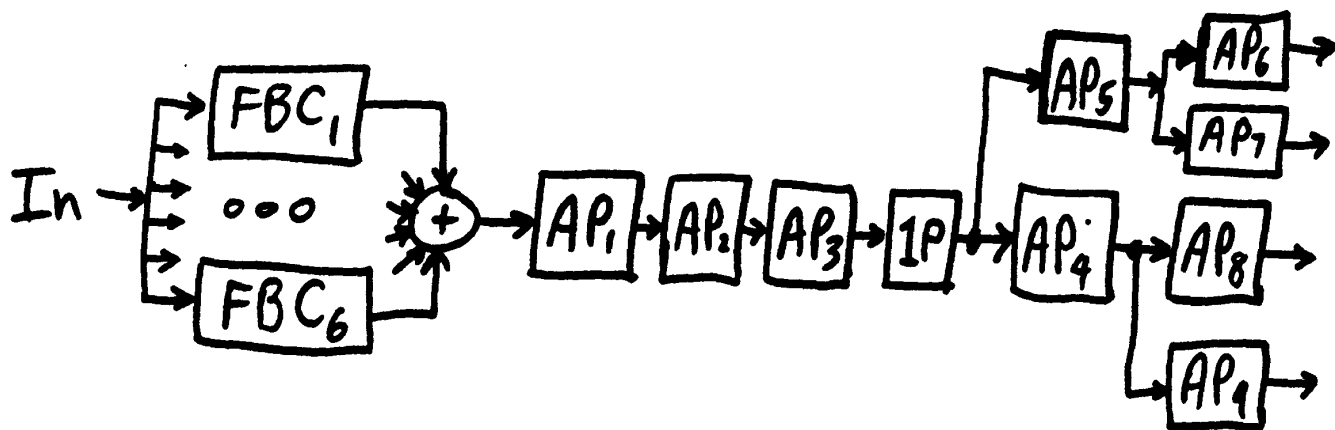
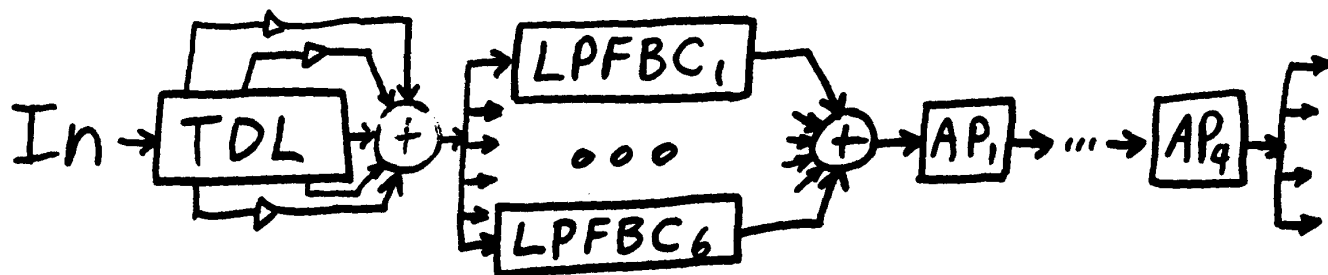
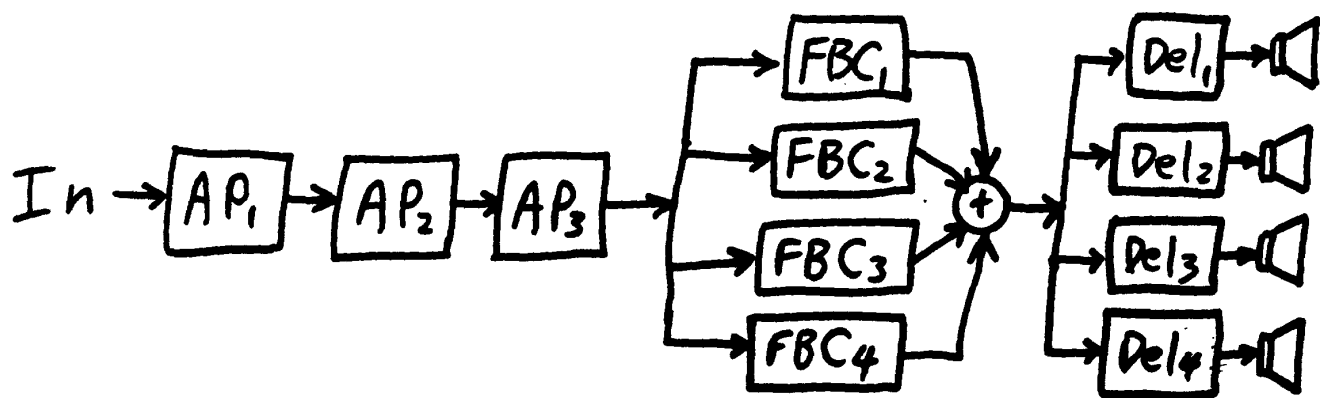
- Feedback Comb-Filter (FBC)



- Allpass



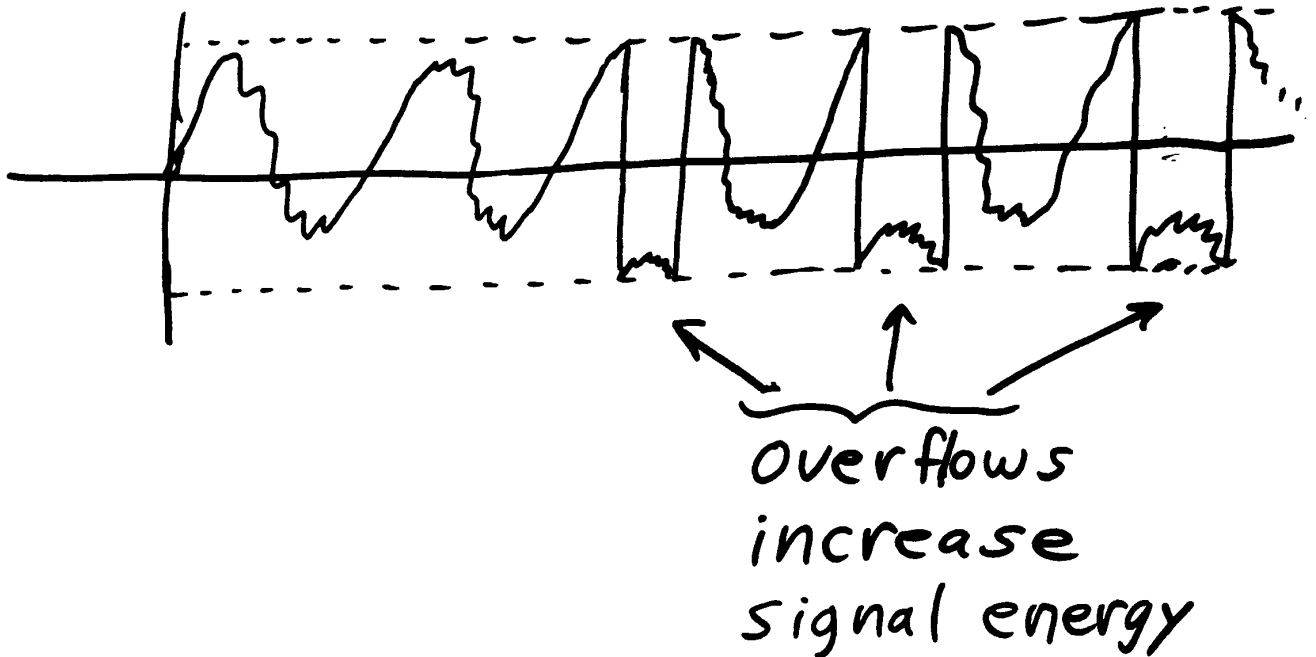
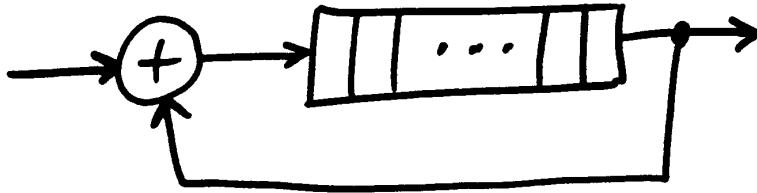
EXAMPLES of CONVENTIONAL REVERBERATORS



PROBLEMS WITH EXISTING REVERBERATORS

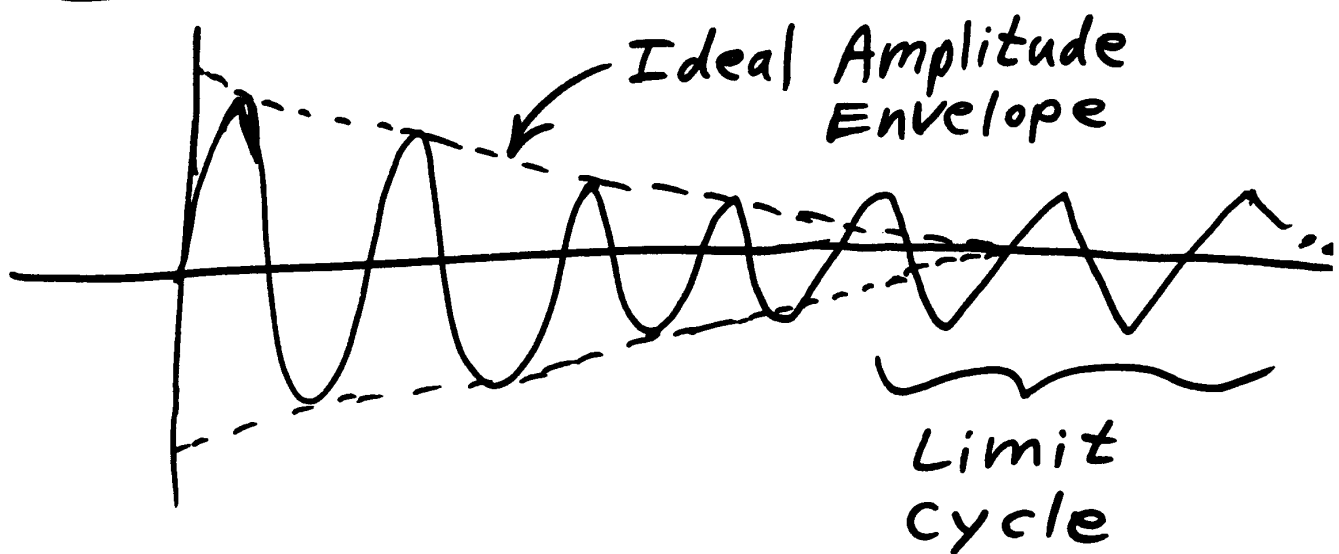
- Overflow
 - Overflow Oscillations
 - Limit Cycles
 - Sensitivity to Coefficients
 - Dynamic Range Requirements
 - Restriction to Forward Tree
-

Overflow Oscillations



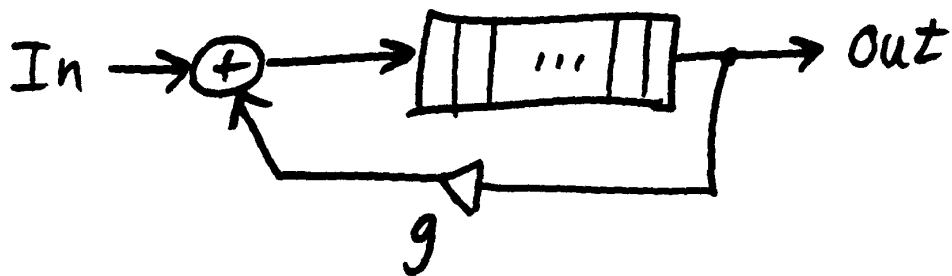
- Overflow in feedback can cause a chain reaction
- Even after input ceases, overflows can cause eternal output signal (highly unpleasant)

Limit Cycles



- Due to round-off error, signal output never decays all the way to zero.
 - Round-off error increases signal energy relative to the ideal (perfect precision) case.
-

Coefficient Sensitivity

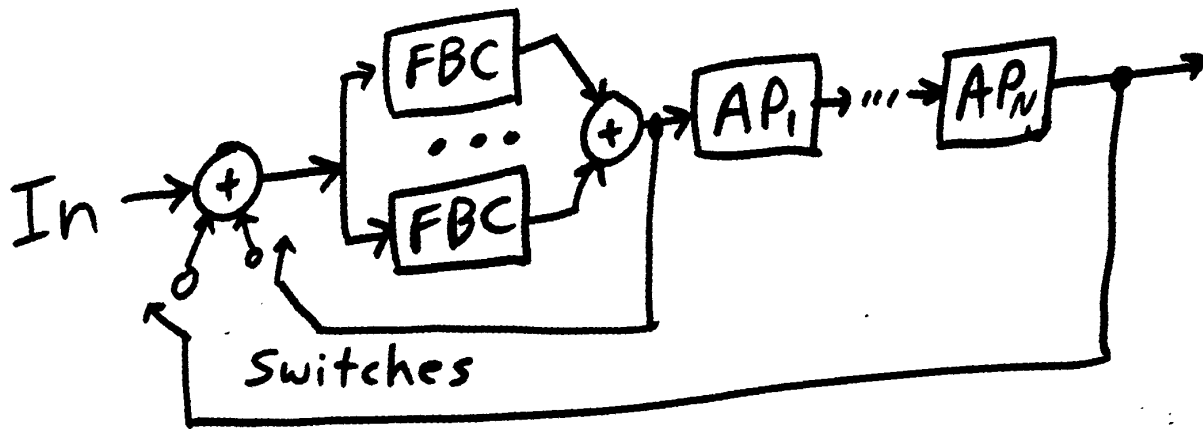


$$\frac{|Out|}{|In|} \approx \leq \frac{1}{1-g} \approx \text{Doubled output peak-amplitude for each halved distance to } g=1.$$

Dynamic Range

- N^{th} order allpass cancels resonances of size $\approx 1/(1-g)$ using notches of depth $\approx (1-g)$.
 - Resonances may reinforce unexpectedly in different parts of the structure.
-

Restriction to Forward Tree

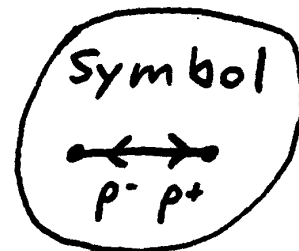
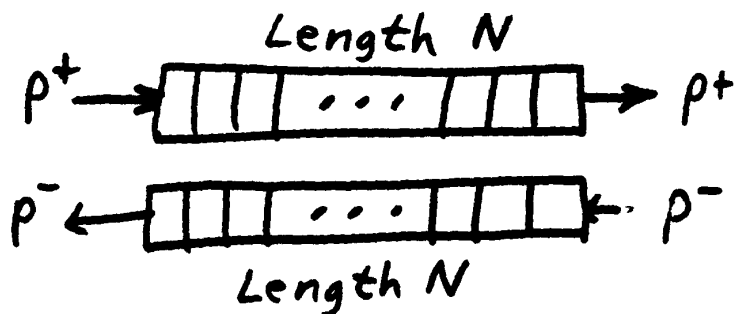


- Closing such a switch is very likely to make the structure unstable
- Use of feedback highly restricted
- No robust "Reverberator Construction Kit" exists.

Waveguide Reverberators¹⁹

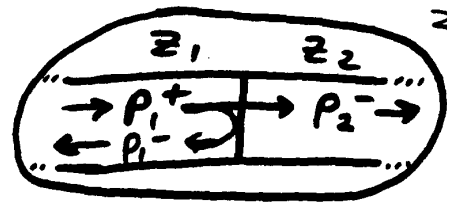
- Interconnect lossless "waveguides" to form a closed energy-conserving system.
 - Introduce slight losses to achieve desired reverberation time.
 - Same as finding a parametrization within the set of multi-input, multi-output allpass filters.
-

A Lossless Waveguide



- Explicitly represent left-going and right-going traveling waves using Bi-Directional Delay Lines
- Delay-Line values can be
 - pressure (p^+ , p^-)
 - velocity (u^+ , u^-)
 - Root Power ($\sqrt{p^+ u^+}$, $\sqrt{p^- u^-}$)

Lossless Scattering

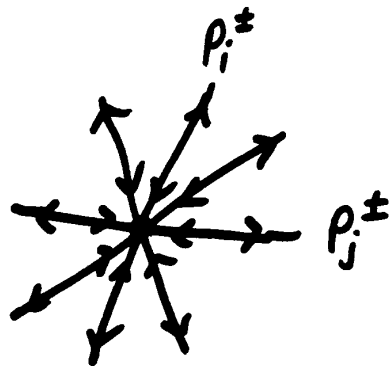


- To each waveguide is associated a characteristic impedance Z_i
 - The change in Z across a junction of two waveguides causes scattering, i.e., the incident wave is partially transmitted and partially reflected in an energy-conserving manner,
 - We can arrange that finite-precision calculations do not increase signal energy. This eliminates limit cycles and overflow oscillations.
-

Junction Intersection

"Kirchoff's Laws"

- ① Pressure is continuous across junction
 - ② Flows sum to zero at junction
- ① & ② \Rightarrow Junction is Lossless

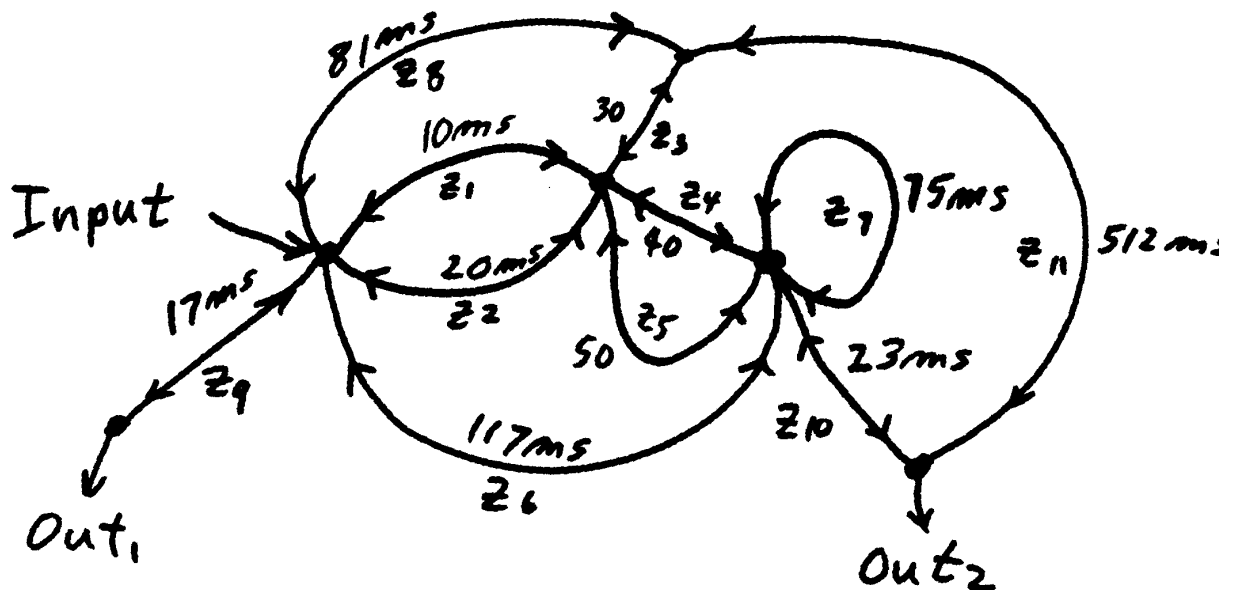


- ① Only one pressure at junction

$$P_J = P_i^+ + P_i^-$$
 - ② Flows cancel at junction: $\sum_i (u_i^+ + u_i^-) = 0$
-



A Reverberator Construction

- No matter how many waveguides are connected together, and no matter what the network looks like, signal energy is conserved.



Example Waveguide Reverberator

Features

- Limit Cycles suppressed
 - Overflow Oscillations suppressed
 - Good dynamic range distribution
 - Richer feedback structures
 - Every digital filter is a special case \rightarrow 
 - Every MIMO Allpass filter is a special case 
 - All results extend to time-varying impedances
 - True physical simulation
 - Can couple to reed/bow/jet/lip simulators
-

WAVEGUIDE REVERB

25

WAVE.OTL SOUND EXAMPLES

Approx 10 sec. leader

| # | Name | Ft End | DESCR |
|---|---------|--------|--|
| 0 | TD0 | 10 | DRY TOOT |
| 1 | TD1 | 25 | Unfiltered basic case |
| 2 | TD2 | 45 | Heavily filtered (-0.7) basic case |
| 3 | TD6 | 1:08 | 100Hz FM (turns to noise) |
| 4 | TD7end | 1:37 | Limit cycles |
| 5 | TD11 | 3:20 | Truncated time-varying case |
| 6 | CR.SNO | | MM: Various delay and input configurations |
| 7 | CR4.SNO | | " |
| 8 | CR8.SNO | | MM: Backwards |

Sound Examples

Sound example 0:

This example plays the original saxophone toot used in later examples 1 through 5.

Sound example 1:

A very basic case consisting of only three waveguides connected together at two nodes. The late reverberation is very metallic because there is no lowpass filtering in the waveguides. See viewgraph page 19 for a diagram of this structure.

Sound example 2:

Here we add a 1-pole lowpass filter in each waveguide branch. The filter coefficient (0.7) is somewhat extreme to illustrate the effect of lowpass filtering in an exaggerated manner. See viewgraph page 19.

Sound example 3:

In this example, the branches are varied with time as shown on page 19 of the viewgraphs. The principal delay loop varies sinusoidally between 224ms and 391ms. The variation frequency itself varies sinusoidally between 0Hz and 100Hz with a period of 10 seconds.

Sound example 4:

This sound example, diagrammed on page 20, shows the effect of limit cycles on the late reverberation. Again the original signal was the sax toot. The sound example is a snapshot of the limit cycles, due to rounding, which dominate the late reverberation. The limit cycles tend to have their energy concentrated at the mode frequencies of the structure. Because the structure is time varying, the resonance frequencies are changing over time. Thus, while this example is not something normally desirable, it has the interesting property of "tracing" the mode frequencies of the waveguide reverberator in a manner analogous to tracing blood circulation with radio active salts.

Sound example 5:

Here the three-waveguide network shown on page 20 of the viewgraphs is used to delay and recirculate the same original sax toot. The network varies sinusoidally as in example 3 except that the variation frequency itself varies randomly instead of sinusoidally.

Sound examples 6 and 7:

CCRMA composer Mike McNabb has taken the above example 5 and adapted it for his forthcoming piece "Invisible Cities". These examples demonstrate what can be done by carefully selecting the input signal, delay lengths, time variation frequencies, and filter coefficients.

Sound example 8:

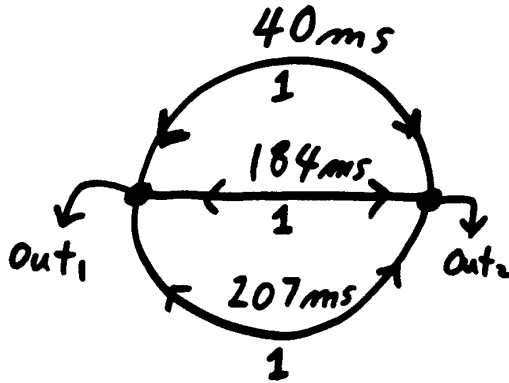
This is similar to examples 6 and 7 except that the final sound is played backwards. The sound goes from "gas" to "solid" instead of the other way around. This effect can also be achieved in hardware in real time.

Sound

Examples

(© Dry original)

①



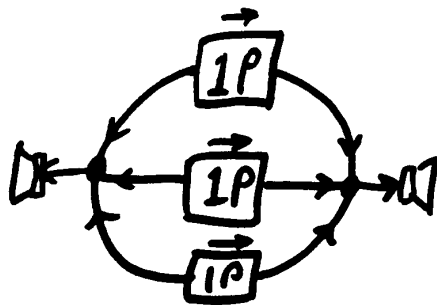
2 modes
3 branches

$$z_i = 1$$

$$LOSS_i = 0.7^{D_i/D_{max}}$$

$$f_s = 26063$$

②



* 1-Pole Lowpass

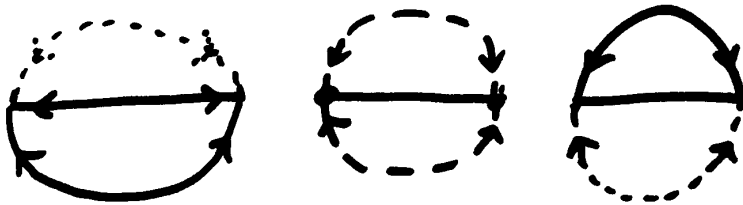
$$Y_m = (1-g)X_m + gY_{m-1}$$

$$g = 0.7$$

• Otherwise same as example ①

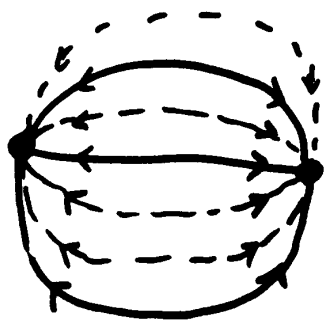
Like ② with $g = 0.3$

③



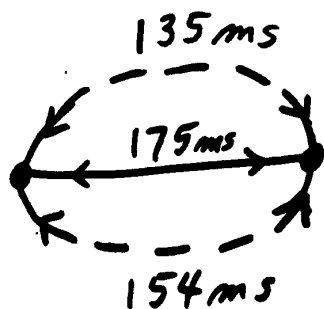
Oscillation at 0 to 100Hz (0.1 FM)

④



7 branches, 2 modes
Limit Cycles
Move with
changing
Resonant Modes

⑤



2 modes
 3 branches ($g=3$)

Time varying
 (slow)

characteristic impedances
 oscillate sinusoidally at
 frequencies between -3Hz
 and 3Hz . A new frequency
 is chosen at random every
 second.

Efficient Simulation of the Reed-Bore and Bow-String Mechanisms

Julius O. Smith

*Center for Computer Research in Music and Acoustics (CCRMA)
Department of Music, Stanford University
Stanford, California 94305*

Abstract

A method for simulating the reed of a wind instrument is described which requires only 1 multiply, 2 additions, and 1 (small) table lookup per sample of synthesized sound. The table contains only a constant and a ramp in the simplest case. An analogous method is described for simulating the interaction between a bow and string, requiring 2 more additions than the reed simulator.

1. Introduction

In [20], McIntyre and Woodhouse laid the foundations for efficient synthesis of a wide class of musical instruments, including most winds and strings. The synthesis architecture consists of a delay-line loop whose length is approximately one period of sound, a lowpass filter implementing various sources of signal loss, and a nonlinear element which converts control variables into oscillations in a way very much like a reed or bow, depending on the nonlinear function used. A review of the virtues of this model appears in [21]. Related applications have been developed in [13,12,30,31].

In [20], it was apparently first suggested to explicitly represent the left- and right-going traveling-wave components of a one-dimensional wave and to lump the round-trip losses into a low-order digital filter. This enables most of the string to be simulated with a simple delay line (or shift register). The delay loop model (also called the "method of the rounded corner" by Cremer [10]) is far more efficient than finite-element approaches employing numerical integration of the difference equations describing a system of masses and springs.

In 1953, Friedlander [11] and Keller [17] published papers containing the first [20] use of a successful graphical solution technique for the bow-string interaction. This technique consists of finding the intersection between two force-

versus-velocity curves, one given by the friction curve for the bow-string contact, and the other given by the characteristic impedance (radiation resistance) of the string.

The complete bowed-string model discussed in [20] consists of a Friedlander-Keller diagram solver, a low-order lowpass filter, and pure delay, configured as a traveling-wave loop. The scope of this model was later extended to single-reed oscillators such as the clarinet, and to switching air-jets such as flute, recorder, and organ pipe [21].

This paper presents a simplified implementation of the graphical Friedlander-Keller component of the model studied by McIntyre and Woodhouse. A table lookup and multiply replace the simultaneous solution of a linear and nonlinear equation at each sampling instant described in [21].

In the proposed technique, the reed is regarded as producing a time-varying reflection coefficient terminating the bore which is modeled as an ideal lossless waveguide or transmission line. A complete single-reed instrument with cylindrical bore (clarinet) can be built using the proposed reed mechanism together with a bore model requiring no multiplies, one addition, and variable delay lines whose length equals the sonic period in samples.

1.1. The Clarinet

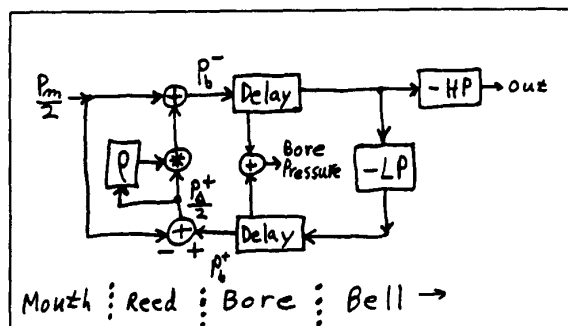


Figure 1. Model of a single-reed, cylindrical-bore woodwind.

A diagram of the basic clarinet model is shown in Fig. 1. The delay-lines carry left-going and right-going pressure samples P_b^+ and P_b^- (respectively) which sample the traveling pressure-wave components within the bore (cf. [30,12,31]). Pressure waves are chosen over velocity waves because the main control is mouth pressure rather than breath velocity.

Sound pressure in the bore at any point is obtained by adding the corresponding left-going pressure sample to the corresponding right-going pressure sample immediately opposite, as indicated in the figure. Tone-hole output can be implemented this way in the simplest case, and interpolating position along the bore can be accomplished using allpass filtering, as discussed in [30,12].

The lowpass filter at the right represents the bell or tone-hole losses as well as the round-trip attenuation losses from traveling back and forth in the bore. To a first order, the bell *reflects* incoming pressure waves (with a sign inversion) for wavelengths much greater than the bore diameter, and the bell *passes* traveling waves having wavelengths much shorter than the bore diameter. In other words, the bell splits the incoming signal (like a crossover network for audio speakers) into reflected low-frequency and transmitted high-frequency components. The radiated bell output is therefore highpass to the first order. The flare of the bell lowers the reflection/transmission cutoff frequency by decreasing the bore characteristic impedance toward the end in a non-reflecting manner; it serves the same function as a transformer coupling of two electrical transmission lines.

At the far left is the reed mouthpiece controlled by *mouth pressure* P_m . Another control is *embouchure*, changed by

modifying the contents of the reflection-coefficient look-up table $\rho(P_\Delta^+/2)$.

Figure 1 is drawn for the case of the lowest note (all tone holes closed); for higher notes the first few open tone holes jointly provide a bore termination [5] analogous to the bell (at which time the bell itself gets very little low-frequency energy). In this situation, it is convenient to model each important open tone hole as a three-port junction in the waveguide [31]. Since the tone hole diameters are small compared with audio frequency wavelengths, the three-port reflection and transmission coefficients can be implemented as constants rather than crossover filters.

1.2. The Bowed String

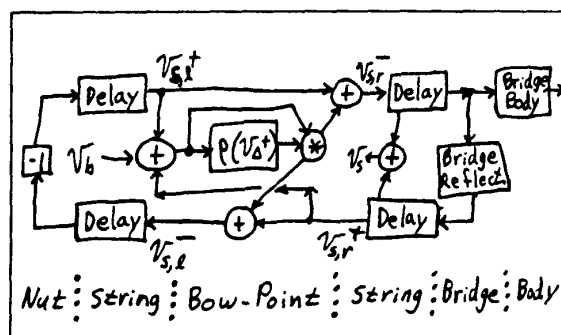


Figure 2. Basic model for a bowed string.

A diagram of the violin model is shown in Fig. 2. The right pair of delay-lines carry left-going and right-going velocity waves samples $v_{s,r}^+$ and $v_{s,r}^-$ (respectively) which sample the traveling-wave components within the string to the right of the bow (cf. [30,12,31]), and similarly for the section of string to the left of the bow. The choice of velocity waves instead of force waves is due to the fact that bow velocity

is the primary control variable.

String velocity at any point is obtained by adding a left-going velocity sample to the right-going velocity sample immediately opposite in the other delay line, as indicated in the figure. The lowpass filter at the right represents the losses at the bridge, bow, nut or finger-terminations (when stopped), and the round-trip attenuation/dispersion from traveling back and forth on the string. To a very good degree of approximation, the nut reflects incoming velocity waves (with a sign inversion) at all audio wavelengths. The bridge behaves similarly to a first order, but there are additional (complex) losses due to the finite bridge driving-point impedance (necessary for transducing sound from the string into the resonating body). Techniques for estimating the coefficients of this lowpass filter are discussed in [30].

Figure 2 is drawn for the case of the lowest note. For higher notes the delay lines between the bow and nut are shortened according to the distance between the bow and the finger termination. At the bowing point is the bow-string interface controlled by *differential velocity* v_{Δ}^+ which is the bow velocity minus the current string velocity. Other controls include *bow force and angle* which are changed by modifying the contents of the reflection-coefficient look-up table $\rho(v_{\Delta}^+)$. Bow position is changed by taking samples from one delay-line pair and appending them to the other delay-line pair. Again, allpass filters can be used to provide continuous change of bow position.

1.3. The Nonlinear Oscillation Mechanism

To provide practical insight, a step by step description of the oscillation build-up is described.

For definiteness, consider the case of a reed woodwind. To start the oscillation, the player applies a pressure at the mouthpiece which "biases" the reed in a "negative-resistance" region. (The pressure drop across the reed tends to close the air gap at the tip of the reed so that an increase in pressure will result in a net decrease in volume velocity—this is negative resistance.) The high-pressure front travels down the bore at the speed of sound until it encounters an open air hole or the bell. To a first approximation, the high-pressure wave reflects with a sign inversion and travels back up the bore. (In reality a lowpass filtering accompanies the reflection, and the complementary highpass filter shapes the spectrum that emanates away from the bore.

As the negated pressure wave travels back up the bore, it cancels the elevated pressure that was established by the passage of the first wave. When the negated pressure front gets back to the mouthpiece, it is reflected again, this time with no sign inversion (because the mouthpiece looks like a closed end to a first approximation). Therefore, as the wave travels back down to the bore, a *negative* pressure zone is left behind. Reflecting from the open end again with a sign inversion brings a return-to-zero wave traveling back to the mouthpiece. Finally the positive traveling wave reaches the mouthpiece and starts the second "period" of oscillation.

So far, we have produced oscillation without making any use of the negative-resistance of the reed aperture. This is merely the start-up transient. Since in reality there are places of pressure loss in the bore, some mechanism is needed to feed energy back into the bore and prevent the oscillation just described from decaying exponentially to zero. This is the function of the reed: When a traveling pressure-drop reflects from the mouthpiece, making pressure at the mouthpiece switch from high to low, the reed changes from open to closed (to a first order). The closing of the reed increases the reflection coefficient "seen" by the impinging traveling wave, and so as the pressure falls it is amplified by an increasing gain (whose maximum is unity when the reed shuts completely). This process sharpens the falling edge of the pressure drop. But this is not all. The closing of the reed also cuts back on the steady incoming pressure from the mouth. This causes the pressure to drop even more, potentially providing effective *amplification* by more than unity.

An analogous story can be followed through for a rising pressure appearing at the mouthpiece. However, in the rising pressure case, the reflection coefficient falls as the pressure rises, resulting in a progressive attenuation of the reflected wave; however, the increased pressure let in from the mouth amplifies the reflecting wave. It turns out that the reflection of a positive wave is boosted when the incoming wave is below a certain level and it is attenuated above that level. When the oscillation reaches a very high amplitude, it is limited on the negative side by the shutting of the reed, which sets a maximum reflective amplification for the negative excursions, and it is limited on the positive side by the attenuation described above. *Unlike* classical negative-resistance oscillators [25,22], in which the negative-resistance device is terminated by a simple resistance instead of a lossy transmission line, a *dynamic equilibrium* is established between the amplification of the negative excursion and the dissipation of the positive excursion.

In the first-order case, where the reflection-coefficient varies linearly with pressure drop, it is easy to obtain an exact quantitative description of the entire process. In this case it can be shown, for example, that amplification occurs only on the positive half of the cycle, and the amplitude of oscillation is typically close to half the incoming mouth pressure (when losses in the bore are small). The threshold blowing pressure (which is relatively high in this simplified case) can also be computed in closed form.

2. Single-Reed Simulation

The fundamental equation governing the action of the reed is *continuity of volume velocity*, i.e., $U_b = U_m$, where

$$U_m(P_\Delta) = \frac{P_\Delta}{Z_m(P_\Delta)} \quad (1)$$

is the flow out of the mouthpiece corresponding to the pressure-drop $P_\Delta = P_b - P_m$ from the bore to the mouth, $Z_m(P_\Delta)$ is the acoustic impedance of the reed opening (whose size depends on the pressure drop P_Δ across the reed), and

$$U_b(P_b^+, P_b^-) = \frac{P_b^+ - P_b^-}{Z_b} \quad (2)$$

is the volume velocity corresponding to the incoming pressure wave P_b^+ and outgoing pressure wave P_b^- . (The actual physical pressure in the bore at the mouthpiece is $P_b = P_b^+ + P_b^-$.) The characteristic impedance of the bore air-column (equal to air density times sound speed divided by cross-sectional area) is denoted Z_b .

In operation, the mouth pressure P_m and incoming traveling bore pressure P_b^+ are given, and the reed computation must produce an outgoing bore pressure P_b^- which satisfies (1) and (2), i.e., such that

$$\frac{P_\Delta}{Z_m(P_\Delta)} = \frac{P_b^+ - P_b^-}{Z_b}, \quad P_\Delta \triangleq P_b^+ + P_b^- - P_m \quad (3)$$

Such a solution for P_b^- is not immediately trivial because of the dependence of Z_m upon P_Δ which, in turn, depends upon P_b^- . A graphical solution technique has been proposed [11,17,20] which, in effect, consists of finding the intersection of the two sides of the equation as they are plotted individually on the same graph, varying P_b^- . It is helpful to normalize as follows: Defining $G(P_\Delta) = Z_b U_m(P_\Delta) = P_\Delta Z_b / Z_m(P_\Delta)$, and noting that $P_b^+ - P_b^- = 2P_b^+ - P_m - (P_b^+ + P_b^- - P_m) = P_\Delta - P_\Delta$, where $P_\Delta^+ \triangleq 2P_b^+ - P_m$, (3) can be written

$$G(P_\Delta) = P_\Delta^+ - P_\Delta, \quad P_\Delta^+ \triangleq 2P_b^+ - P_m \quad (4)$$

where a solution for P_Δ is required given P_Δ^+ . The solution is obtained by plotting $G(P_\Delta)$ and $P_\Delta^+ - P_\Delta$ on the same graph, finding the point of intersection $G(P_\Delta^+)$, and taking $P_b^- = P_\Delta^+ - P_b^+ + P_m$ as the desired outgoing pressure wave.

2.1. A Table Lookup Technique

One approach to reducing the computational burden is to prepare a table containing $P_\Delta^+(P_\Delta^+/2) = P_\Delta^+(P_b^+ - P_m/2)$. This reduces the total computations to three additions and the table lookup. While such a technique can be very fast, the table may be prohibitively large. For example, if P_b^+ and P_b^- are 16-bit signal samples, the table would contain on the order of 64K 16-bit P_Δ^+ samples. Clearly, some compression of this table would be desirable. Since $P_\Delta^+(P_b^+/2)$ is smoothly varying, significant compression is in fact possible. However, because the table is directly in the signal path, comparatively little compression can be done while maintaining full audio quality (such as 16-bit accuracy).

2.2. A Scattering Theory Approach

From (3) we can write

$$P_b^- = \rho(P_\Delta) P_b^+ + \frac{1 - \rho(P_\Delta)}{2} P_m \quad (5)$$

where

$$\rho(P_\Delta) \triangleq \frac{1 - r(P_\Delta)}{1 + r(P_\Delta)}, \quad r(P_\Delta) \triangleq \frac{Z_b}{Z_m(P_\Delta)}$$

We can interpret $\rho(P_\Delta)$ as a *signal-dependent reflection coefficient*. Let h denote half-pressure $P/2$, e.g., $h_m = P_m/2$ and $h_\Delta^+ = P_\Delta^+/2$. Also let

$$\hat{\rho}(h_\Delta^+) = \rho(P_\Delta^+(h_\Delta^+)) = \frac{P_\Delta^+(h_\Delta^+)}{h_\Delta^+} - 1$$

denote the reflection coefficient stored as a function of h_Δ^+ . Then (5) can be written

$$P_b^- = \hat{\rho}(h_\Delta^+) \cdot h_\Delta^+ + h_m \quad (6)$$

This is the equation proposed for implementation. The control variable is mouth half-pressure h_m , and $h_\Delta^+ = P_b^+ -$

h_m is computed from the incoming bore pressure using only a single subtraction. The table is indexed by h_{Δ}^+ , and the result of the lookup is then multiplied by h_{Δ}^+ . Finally, h_m is added to the result of the multiplication. Because the table contains a coefficient rather than a signal value, it can be more heavily quantized both in address space and word length. The total complexity is only two additions, one multiply, and a simplified table lookup.

Good results have been obtained at CCRMA using

$$\hat{\rho}(h_{\Delta}^+) = \begin{cases} 1, & h_{\Delta}^+ \leq h_{\Delta}^c \\ 1 - m(h_{\Delta}^+ - h_{\Delta}^c), & h_{\Delta}^+ > h_{\Delta}^c \end{cases} \quad (7)$$

where h_{Δ}^c is the pressure difference corresponding to reed closure. Embouchure and reed stiffness correspond to the choice of h_{Δ}^c and m .

3. The Bow-String Mechanism

An analogous derivation is possible for the simulation of the bow-string interaction. The final result is as follows.

$$\begin{aligned} v_{s,r}^- &= v_{s,l}^+ + \hat{\rho}(v_{\Delta}^+) \cdot v_{\Delta}^+ \\ v_{s,l}^- &= v_{s,r}^+ + \hat{\rho}(v_{\Delta}^+) \cdot v_{\Delta}^+ \end{aligned} \quad (8)$$

where $v_{s,r}$ denotes transverse velocity on the segment of the bowed string to the *right* of the bow, and $v_{s,l}$ denotes velocity waves to the *left* of the bow. In addition we have $v_{\Delta}^+ = v_b - (v_{s,r}^+ + v_{s,l}^+)$, where v_b is bow velocity, and

$$\hat{\rho}(v_{\Delta}^+) = \frac{r(v_{\Delta}(v_{\Delta}^+))}{1 + r(v_{\Delta}(v_{\Delta}^+))}$$

The impedance ratio is defined as $r(v_{\Delta}) = 0.25Z_b(v_{\Delta})/Z_s$, where $v_{\Delta} = v_b - v_s$ is the velocity of the bow minus that of the string, $v_s = v_{s,l}^+ + v_{s,l}^- = v_{s,r}^+ + v_{s,r}^-$ is the string velocity in terms of traveling waves, Z_s is the characteristic impedance of the string (equal to the geometric mean of tension and density), and $Z_b(v_{\Delta})$ is the friction coefficient for the bow against the string, i.e., bow force $F_b(v_{\Delta}) = Z_b(v_{\Delta}) \cdot v_{\Delta}$. (Force and velocity point in the same direction when they have the same sign.)

Nominally, $Z_b(v_{\Delta})$ is constant (the so-called static coefficient of friction) for $|v_{\Delta}| \leq v_{\Delta}^c$, where v_{Δ}^c is the break-away differential velocity, and for $|v_{\Delta}| > v_{\Delta}^c$, $Z_b(v_{\Delta})$ falls quickly to a low dynamic coefficient of friction.

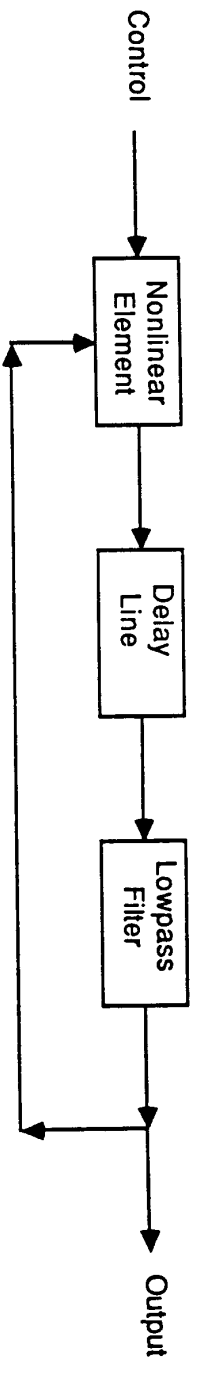
References

The references marked with "*" are especially recommended for first reading. The most comprehensive single reference is [21].

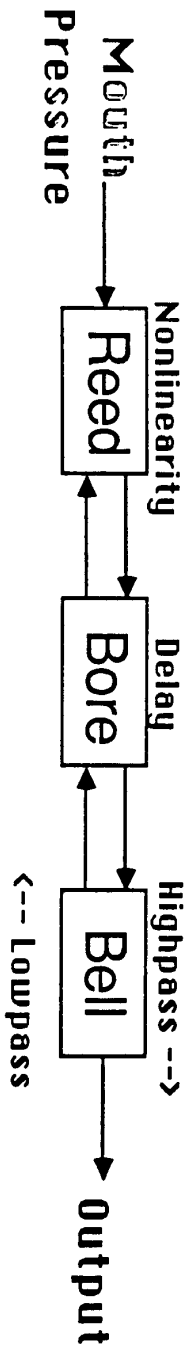
- [1] J. M. Adrian and X. Rodet, "Physical Models of Instruments — a Modular Approach, Application to Strings," *Proc. Int. Computer Music Conf.*, 1985.
- [2]* J. Backus, "Small-Vibration Theory of the Clarinet," *J. Acoust. Soc. Amer.*, vol. 35, no. 3, pp. 305-313, March 1963.
- [3] J. Backus, "Input Impedance Curves for the Reed Woodwind Instruments," *J. Acoust. Soc. Amer.*, vol. 56, no. 4, pp. 1266-1279, Oct. 1974.
- [4] J. Backus, "Input Impedance Curves for the Brass Instruments," *J. Acoust. Soc. Amer.*, vol. 60, no. 2, pp. 470-480, Aug. 1976.
- [5]* A. H. Benade, *Fundamentals of Musical Acoustics*, Oxford University Press, New York, 1976.
- [6] A. H. Benade and C. O. Larson, "Requirements and Techniques for Measuring the Musical Spectrum of the Clarinet," *J. Acoust. Soc. Amer.*, vol. 78, no. 5, pp. 1475-1498, Nov. 1985.
- [7] C. Chafe, "Bowed String Synthesis and Its Control From a Physical Model," Music Dept. Tech. Rep. STAN-M-32, Stanford University, July 1985.
- [8] L. Cremer, "Bow Pressure Influence on the Self-Excited Vibrations of a String During Contact," *Acustica*, vol. 30, no. 3, pp. 119-136, March 1974.
- [9] "Fate of the Secondary Waves During Self-Excitation of String Instruments," *Acustica*, vol. 42, no. 3, pp. 133-148, May 1979.

- [10]* L. Cremer, *The Physics of the Violin*, MIT Press, Cambridge MA, 1984.
- [11] F. G. Friedlander, "On the Oscillations of the Bowed String," *Proc. Cambridge Philos. Soc.*, vol. 49, pp. 516-530, 1953.
- [12]* D. Jaffe and J. O. Smith, "Extensions of the Karplus-Strong Plucked String Algorithm," *Computer Music J.*, vol. 7, no. 2, pp. 56-69, 1983.
- [13]* K. Karplus and A. Strong, "Digital Synthesis of Plucked String and Drum Timbres," *Computer Music J.*, vol. 7, no. 2, pp. -55, 1983.
- [14] D. H. Keefe, "Theory of the Single Woodwind Tone Hole," *J. Acoust. Soc. Amer.*, vol. 72, no. 3, pp. 676-687, Sep. 1982.
- [15] D. H. Keefe, "Experiments on the Single Woodwind Tone Hole," *J. Acoust. Soc. Amer.*, vol. 72, no. 3, pp. 688-699, Sep. 1982.
- [16] D. H. Keefe, "Acoustic Streaming, Dimensional Analysis of Nonlinearities, and Tone Hole Mutual Interactions in Woodwinds," *J. Acoust. Soc. Amer.*, vol. 72, no. 3, pp. 688-699, Sep. 1982.
- [17] J. B. Keller, "Bowling of Violin Strings," *Comm. Pure Applied Math.*, vol. 6, pp. 483-495, 1953.
- [18] W. E. Kock, "The Vibrating String Considered as an Electrical Transmission Line," *J. Acoust. Soc. Amer.*, vol. 8, pp. 227, 1937.
- [19] J. D. Markel and A. H. Gray, *Linear Prediction of Speech*, Springer-Verlag, New York, 1976.
- [20]**M. E. McIntyre and J. Woodhouse, "On the Fundamentals of Bowed String Dynamics," *Acustica*, vol. 43, no. 2, pp. 93-108, Sep. 1979.
- [21]**M. E. McIntyre, R. T. Schumacher, and J. Woodhouse, "On the Oscillations of Musical Instruments," *J. Acoust. Soc. Amer.*, vol. 74, no. 5, pp. 1325-1345, Nov. 1983.
- [22] J. Millman and H. Taub, *Pulse, Digital, and Switching Waveforms*, Chapters 12 and 13, McGraw-Hill, New York, 1965.
- [23]* P. M. Morse, *Vibration and Sound*, published by the American Institute of Physics for the Acoustical Society of America, 1976 (1st ed. 1936, 2nd ed. 1948).
- [24] P. M. Morse and K. U. Ingard, *Theoretical Acoustics*, McGraw-Hill, New York, 1968.
- [25] J. M. Petit and M. M. McWhorter, *Electronic Switching, Timing, and Pulse Circuits*, Chapter 8, McGraw-Hill, New York, 1970. (Use of a transmission line as an oscillator timing element is treated in Chapter 9.)
- [26] C. V. Raman, "On the Mechanical Theory of Vibrations of Bowed Strings, etc.," *Indian Assoc. Cult. Sci. Bull.*, vol. 15, pp. 1-158, 1918.
- [27]* P. M. Ruiz, "A Technique for Simulating the Vibrations of Strings with a Digital Computer," *M. Music Diss.*, Univ. Ill., Urbana, 1969.
- [28] R. T. Schumacher, "Ab Initio Calculations of the Oscillations of a Clarinet," *Acustica*, vol. 48, no. 2, pp. 71-85, May 1981.
- [29] J. O. Smith, "Synthesis of Bowed Strings," In *Proc. 1982 Int. Computer Music Conf.*, T. Blum and J. Strawn, eds., Computer Music Assoc., San Francisco, 1983.
- [30] J. O. Smith, "Techniques for Digital Filter Design and System Identification with Application to the Violin," Ph.D. Dissertation, Elec. Eng. Dept., Stanford University, June 1983.
- [31] J. O. Smith, "Waveguide Digital Filters," Center for Computer Research in Music and Acoustics (CCRMA), Dept. of Music, Stanford University, March 1985.
- [32]* S. E. Stewart and W. J. Strong, "Functional Model of a Simplified Clarinet," *J. Acoust. Soc. Amer.*, vol. 68, no. 1, pp. 109-120, July 1980.

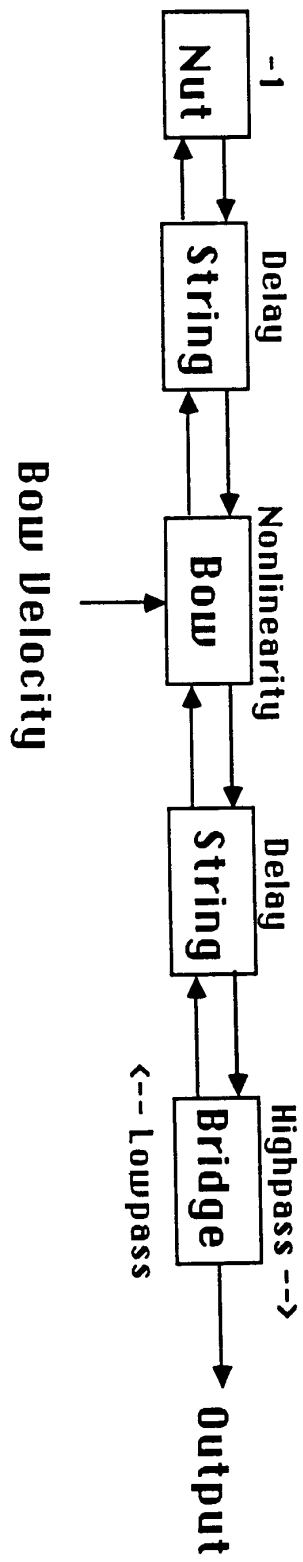
Synthesizer Architecture



The Clarinet

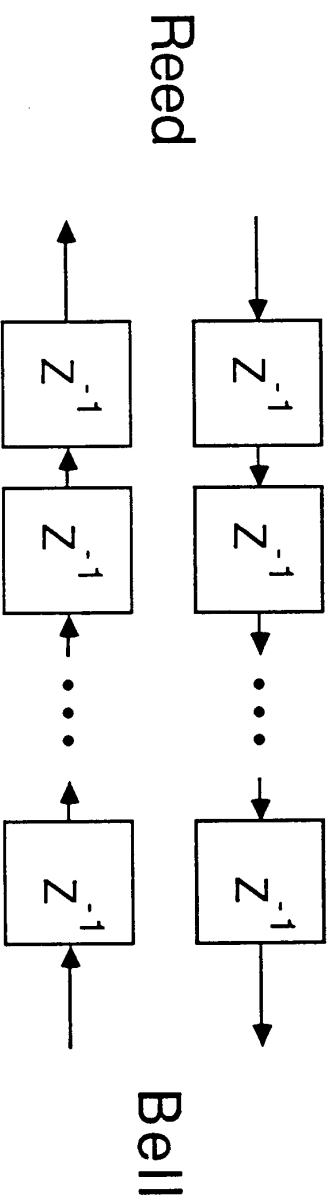


The Violin



Clarinet Bore = Digital Waveguide (Bi-Directional Delay Line)

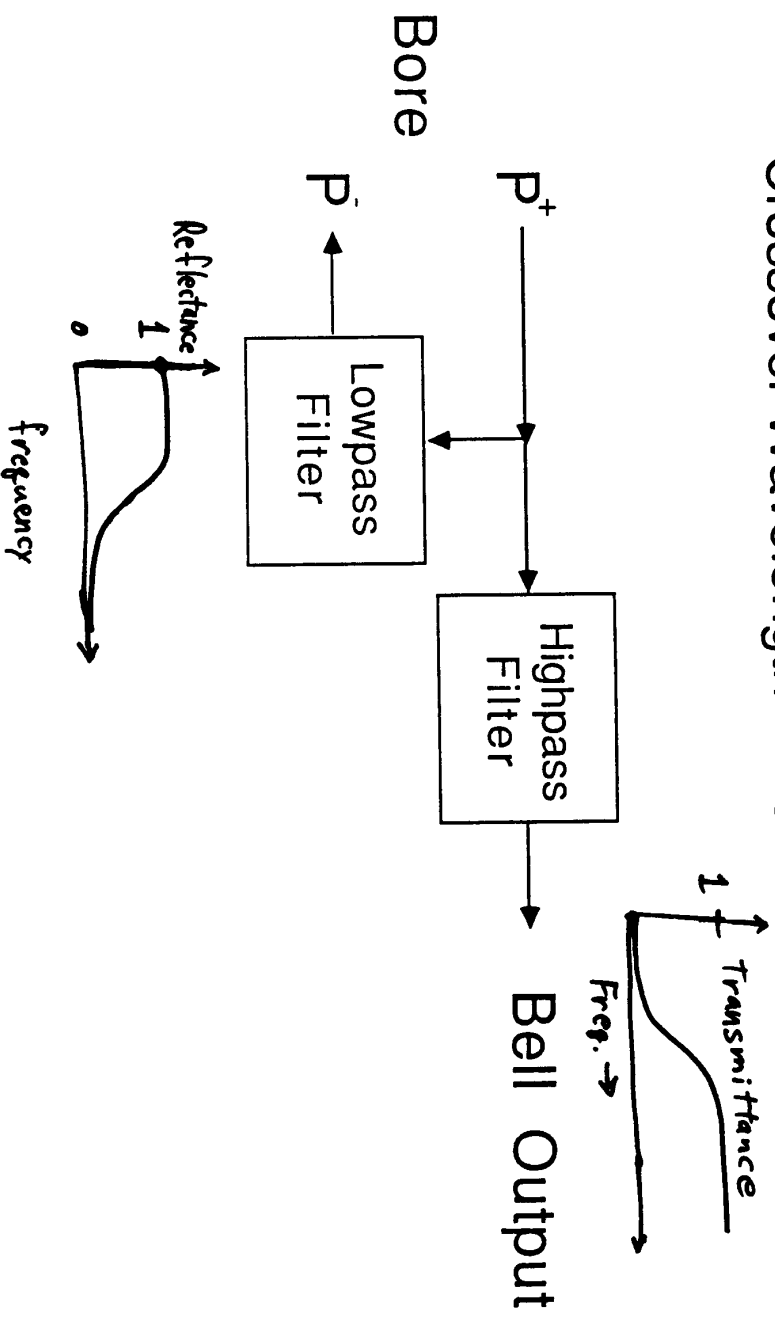
Right-Going Traveling Pressure Waves -->



<-- Left-Going Traveling Pressure Waves

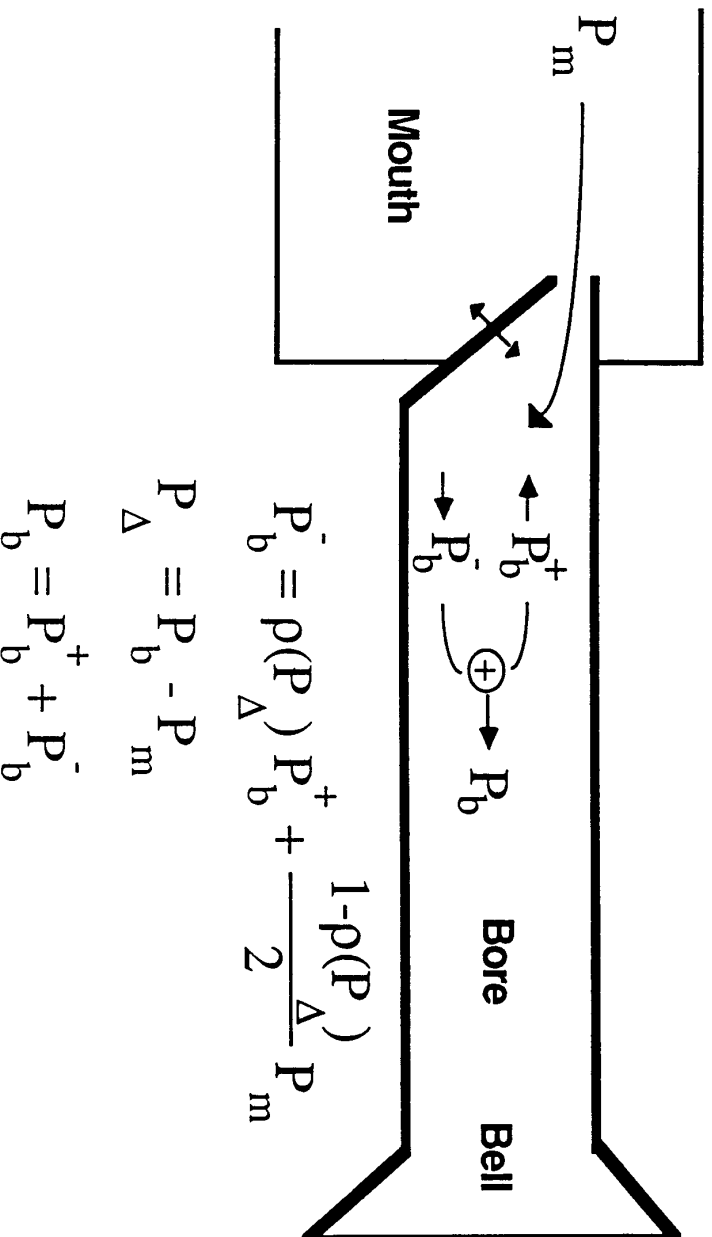
Bell = Crossover Network

Crossover Wavelength = Bore Diameter

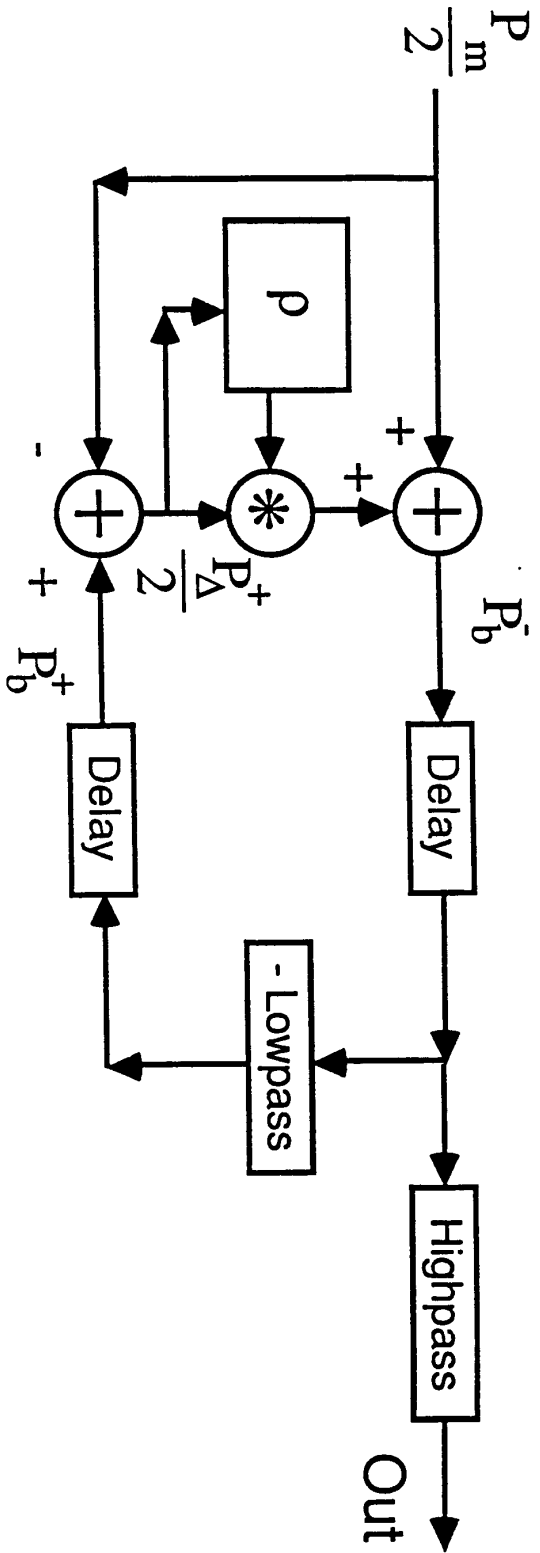


Reed = Pressure-Controlled Valve

Bore sees a time-varying reflection-coefficient
plus a time-varying mouth-pressure input

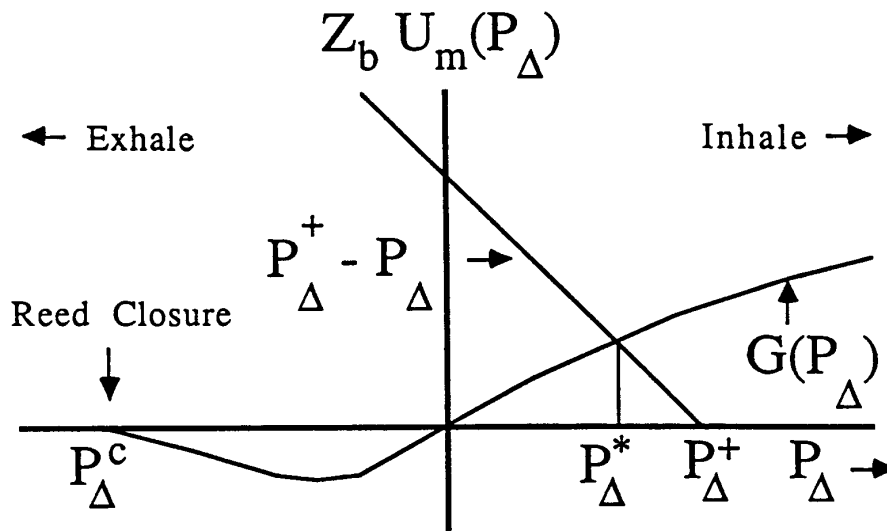


Proposed Clarinet Implementation



$$P_b^- = \rho \left(\frac{P_m^+}{2} \right) \frac{P_m^+}{2} + \frac{P_m^+}{2}$$

Flow versus Pressure Drop (Reed Woodwind)



$$G(P_\Delta) \triangleq Z_b U_m(P_\Delta) = P_\Delta^+ - P_\Delta$$

$$P_\Delta = P_b - P_m = \text{Pressure Drop Across Reed}$$

$$P_\Delta^+ = 2 P_b^+ - P_m = \text{Closed-Reed Pressure Drop}$$

$$P_b = P_b^+ + P_b^- = \text{Bore Pressure}$$

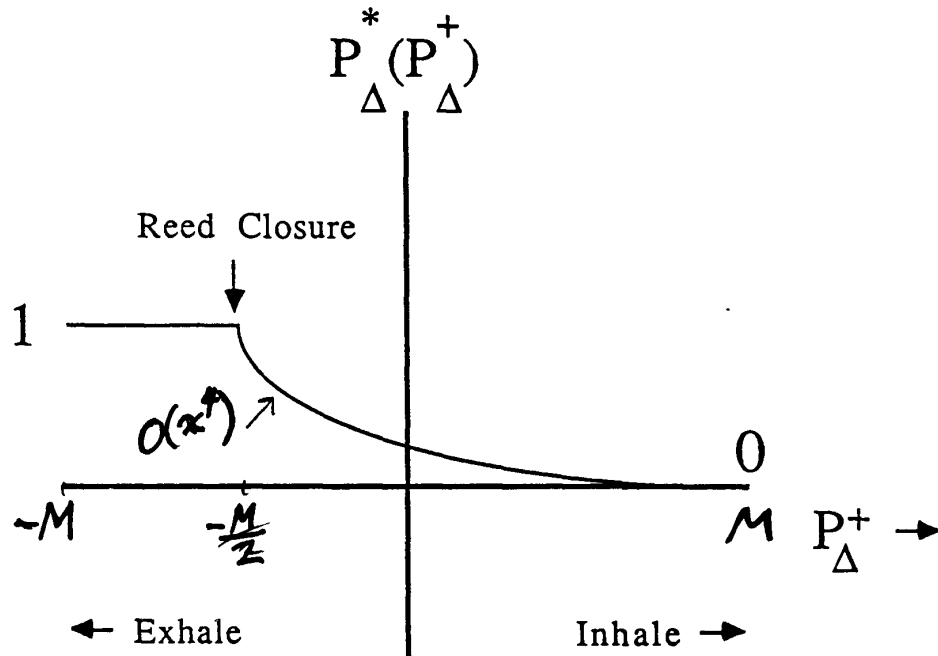
$$P_b^+, P_b^- = \text{Traveling Pressure Waves}$$

$$Z_b = \text{Bore Characteristic Impedance}$$

$$P_m = \text{Mouth Pressure}$$

$$U_m = \text{Mouthpiece Flow}$$

Reflection Coefficient vs Incident (Relative Quantization Error)



$$\rho(P_{\Delta}^+) = 2 \frac{P_{\Delta}^*(P_{\Delta}^+)}{P_{\Delta}^+} - 1$$

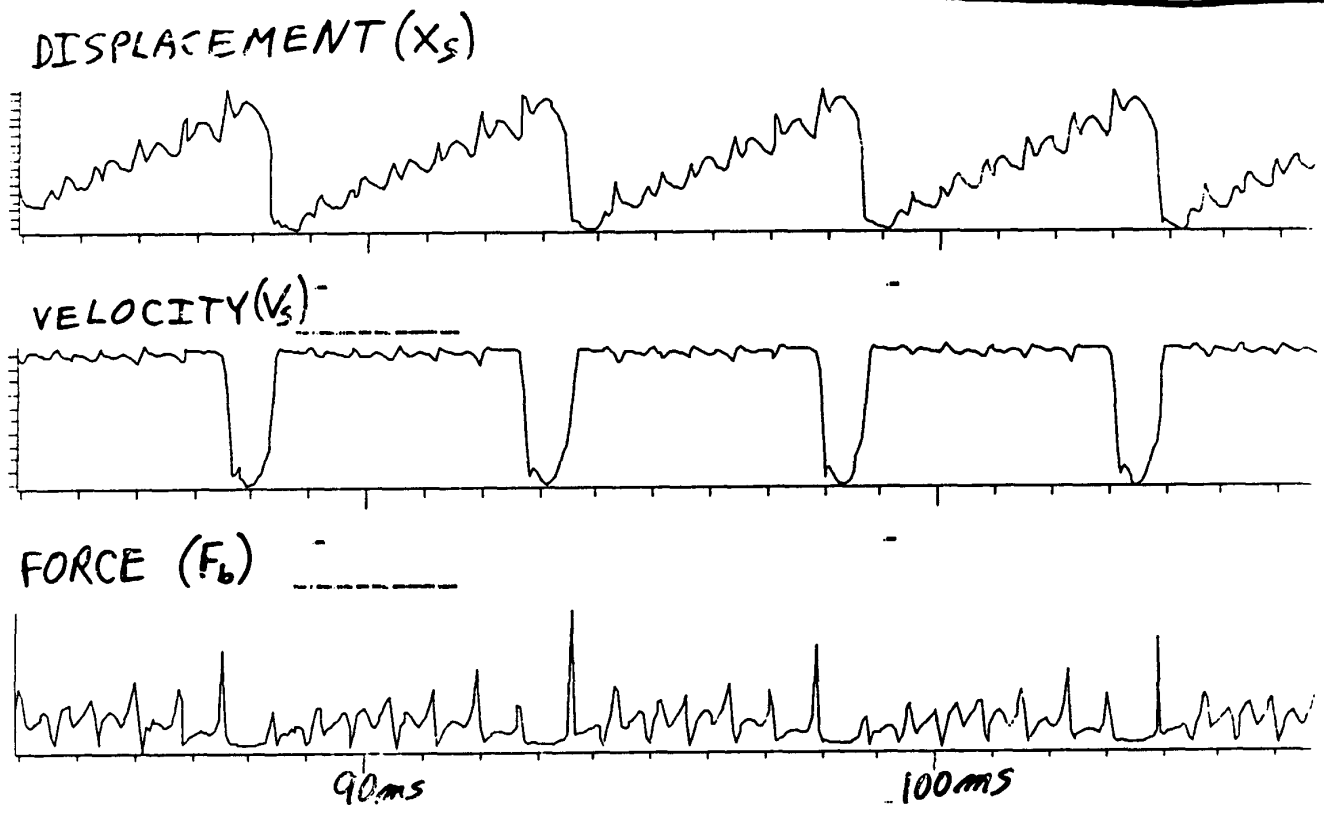
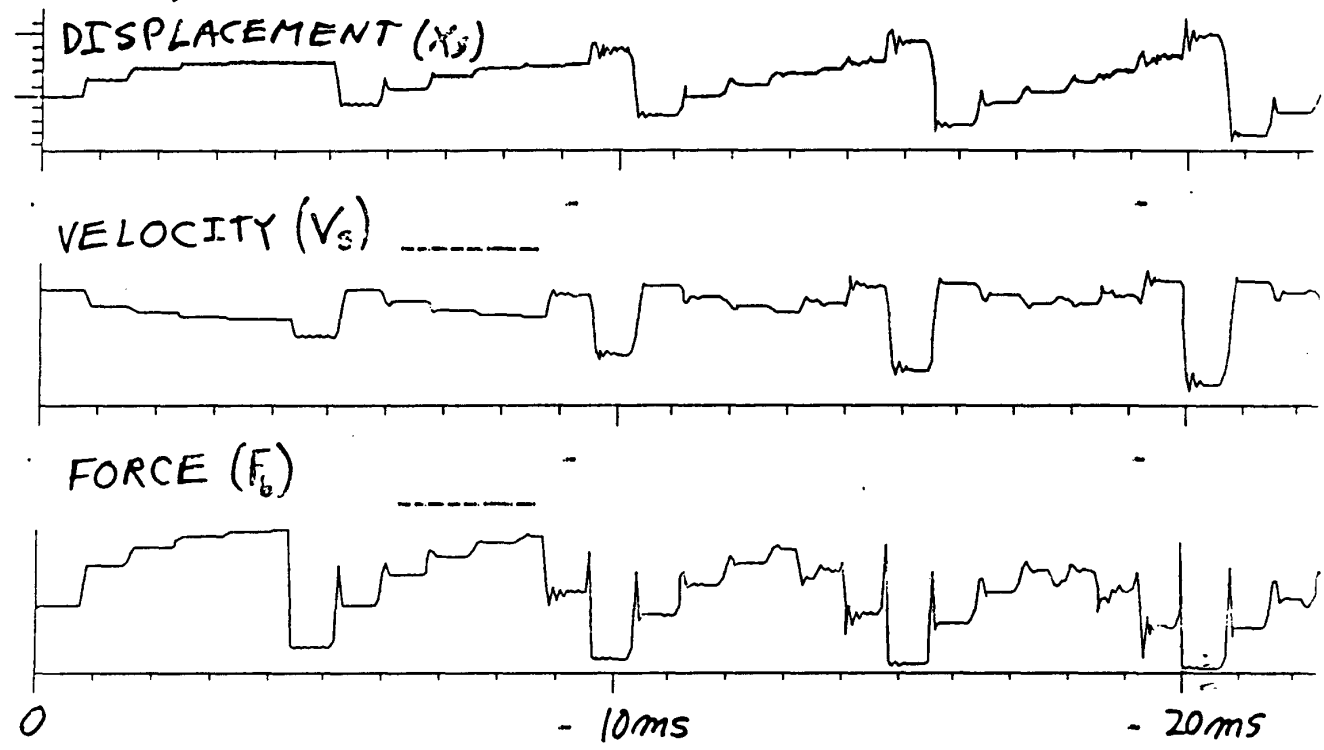
$$P_b^- = \rho(P_{\Delta}^+) P_b^+ + \frac{1 - \rho(P_{\Delta}^+)}{2} P_m$$

$$P_b^- = \rho(P_{\Delta}^+) \frac{P_{\Delta}^+}{2} + \frac{P_m}{2}$$

VIOLIN WAVEFORMS

44

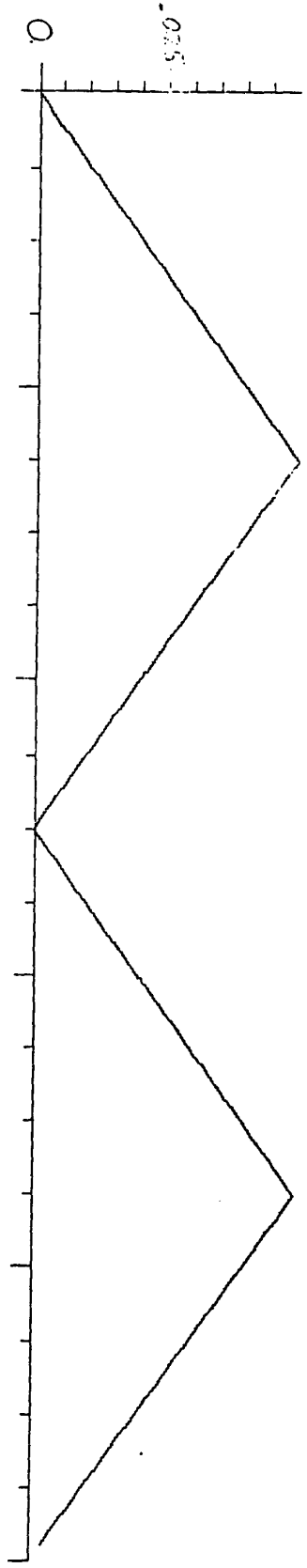
ATTACK) UDP2: VS, SAI [LIB, JOS] DEFAULT CASE



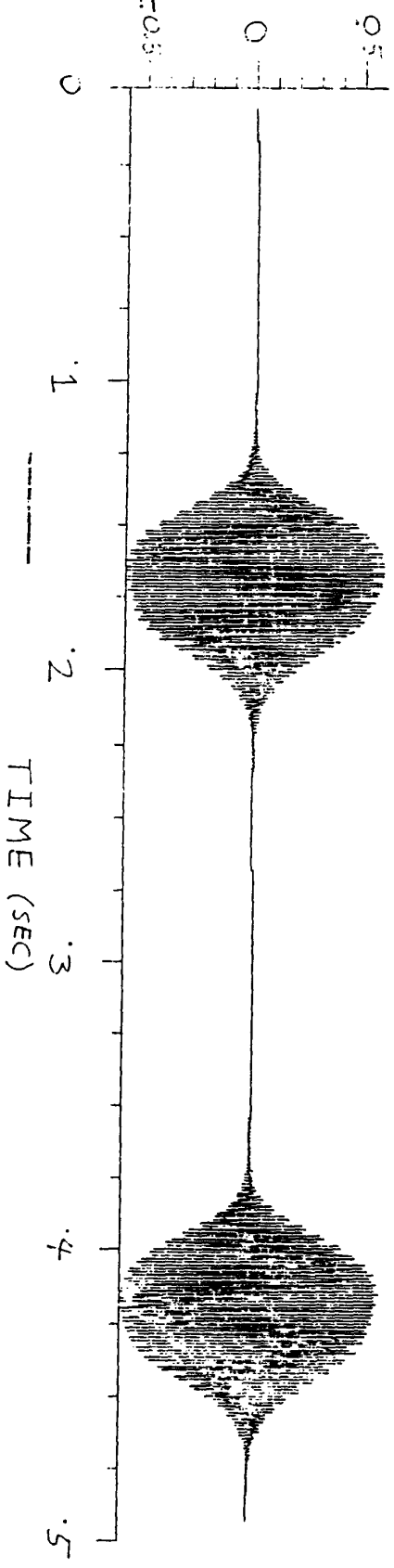
(STEADY STATE)

SAM CLARINET WAVEFORMS
3/21/86 J05

Mouth Pressure

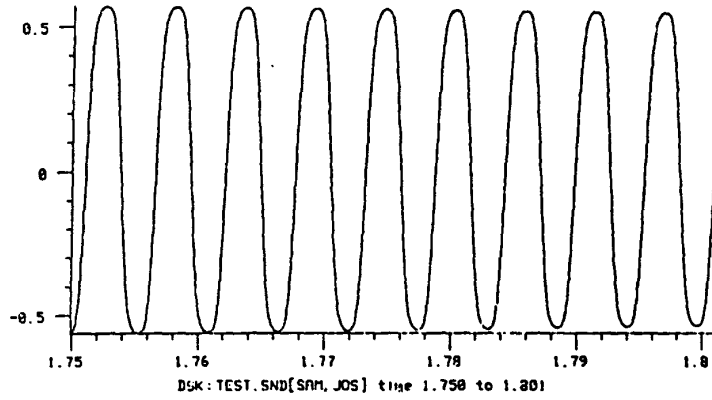


Bore Pressure

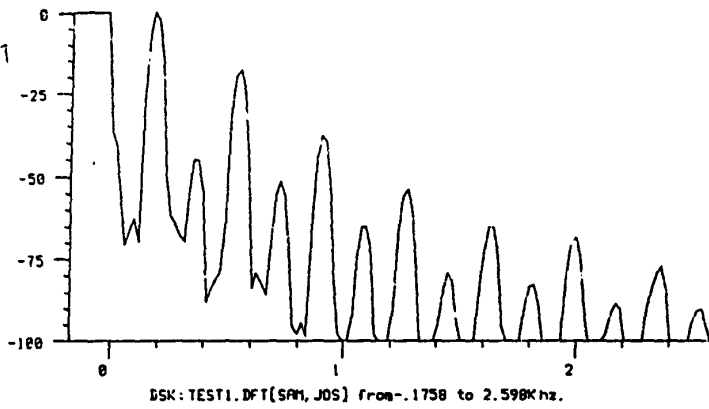


Clarinet

Time waveform



Spectrum



**Elimination of Limit Cycles and Overflow Oscillations
in
Time-Varying Lattice and Ladder Digital Filters**

Julius O. Smith*

Systems Control Technology

1801 Page Mill Rd., Palo Alto CA, 94303, Tel: (415)494-2233

Abstract

A construction is presented which shows that limit cycles and overflow oscillations can be eliminated in all prevalent forms of lattice and ladder digital filter structures, whether or not they are time varying, and whether or not the input signal is zero. In particular, the computationally efficient one-multiply lattice section can be made free of limit cycles and overflow oscillations in the time-varying, nonzero-input case. These results derive from a simplified formulation of digital filters in terms of cascade transmission-line segments.

Another byproduct of the formulation is a new normalized ladder filter (NLF) structure which has only three multiplies per section instead of four. The new NLF is, in principle, a transformer-coupled one-multiply section.

* Work supported in part by the Rome Air Development Foundation under contract no. F30602-84-C-0016 and (at CCRMA, Stanford University) by the System Development Foundation.

1. Introduction

Nonlinear effects of numerical roundoff error and overflow have plagued many applications of digital filters, including, for example, signal acquisition and conditioning systems. Artifacts can be particularly severe in the case of recursive filters. For example, overflow can cause a "chain reaction" of overflows due to the presence of feedback (an *overflow oscillation*), and roundoff error can result in a persistent, non-decaying "buzz" or "whistle" which lasts forever after the input signal ceases (a *limit cycle*).

Limit cycles and overflow oscillations can be suppressed by ensuring that the effects of overflow and roundoff error do not increase "signal power" relative to that of the ideal (infinite-precision) signal. Defining signal power and energy density on the level of individual signal samples is possible by following closely the basic physics of waves [2] or classical network theory [1].

The key point of this paper is that when digital filters are implemented in the form of classical cascade transmission line networks, a one-to-one correspondence can be found between each signal sample within the filter and a physical voltage or current level in an ideal transmission-line. In this context, it is quite clear how to define signal power for each delay register and for each sampling instant everywhere within the filter network. From there, ensuring "passive" computations is quite simple, even under arbitrary time-varying conditions. The only remaining task is then to show that all lattice and ladder filter structures can be obtained from the cascade transmission-line structure using network transformations which preserve exactly the signal power associated with each sample in spite of roundoff error and possible overflow.

The essential argument in eliminating limit cycles and overflow oscillations is as follows. Once finite-precision computations are adjusted to avoid increasing signal power on roundoff or overflow, the signal power in the digital filter becomes *bounded above* by the signal power in the corresponding infinite-precision filter. In this way, the infinite-precision signal power at each internal node serves as a

Lyapunov function for each internal node of the finite-precision filter. This means that the signal power at each delay element for each sampling instant within the finite-precision filter can never be larger than in the ideal case. Consequently, we can interpret all numerical artifacts as attenuating distortion of the original signal—no signal can persist beyond the ideal output as is characteristic of limit cycles and overflow oscillations.

2. Background

One of the earliest treatments connecting the scattering formulation of classical network theory to digital filter theory was carried out by Fettweis [3,4,5,7]. He has used the term “wave digital filters” (WDF) for the filter structures obtained by carrying classical continuous-time “wave variables” associated with networks of capacitors, inductors, and resistors, into the discrete-time domain. Wave variables are typically defined as $x = v + Ri$ and $y = v - Ri$, where v and i denote the voltage and current at a terminal of an N -port network, and R is an arbitrary “reference impedance.” In wave digital filter theory, the analog frequency variable is mapped to the digital frequency variable via the bilinear conformal mapping $s = (z - 1)/(z + 1)$. In this formulation, it is not obvious to what extent the well-known physical properties of the analog prototype filters have been carried over to the discrete-time domain, particularly in the time-varying case. However, Fettweis [5] and Meerkötter [9] have made use of “pseudo-passivity” conditions to develop digital filter structures which are guaranteed to be free of limit cycles and overflow oscillations in the time-invariant, zero-input case.

The well-known ladder and lattice filters used in speech modeling and spectrum estimation [8,10,11,13,16] and the more recent “orthogonal filters” deriving from state-space and Nerode projection techniques [14,15] can also be derived from classical scattering theory. Gray [10,13] has used a type of pseudo-passivity (Lyapunov) theory to demonstrate that the major existing ladder and lattice filter structures can be made free of limit cycles and overflow oscillations, in the time-invariant,

zero-input case, by using extended internal precision within each section and using magnitude truncation for the final outgoing pair of samples [6,13]. Moreover, Gray proved [13] that the normalized ladder filter (NLF) is free of limit cycles and overflow oscillations even in the *time-varying*, zero-input case.

In this paper, we extend the results of Fettweis, Meerkötter, Gray, and others to include all of the well-known ladder and lattice filter structures in the time-varying, nonzero-input case. Analogous results have been obtained also for generalized multi-input, multi-output lattice filter structures [17]. These results are immediate from a reformulation of the basic theory at the most fundamental level. The formulation is closely related to the classical scattering theory, except that (1) the wave variables are pure voltage or current on a transmission-line—not linear combinations of the two, and (2) scattering points are formed by coupling transmission-line sections rather than “adapting” two RLC networks of differing “reference impedance” together. The resulting filter structure is termed a *waveguide filter* (WGF), and the WGF can be transformed into common ladder and lattice structures by network equivalence operations. The advantage of working with the WGF structure is that it corresponds *exactly* to a physical interconnection of uniform transmission-lines. This enables immediate determination of true passivity, as opposed to “pseudo-passivity.”

3. The Waveguide Filter Structure

A single waveguide section between two partial sections is shown in Fig. 1. The sections are numbered 1 through 3 from left to right. For definiteness, suppose that the waveguide is *acoustic*, and that the signal variables are pressure and volume velocity. A more elaborate treatment of the acoustic tube can be found in [11]. Each waveguide section is characterized by a real, positive *characteristic impedance* $Z_i(t)$ which is allowed to vary with time, but which is constant across a waveguide section at any given instant. In the i th section, there are two pressure traveling waves: P_i^+ traveling to the right at speed c and P_i^- traveling to the left at speed c .

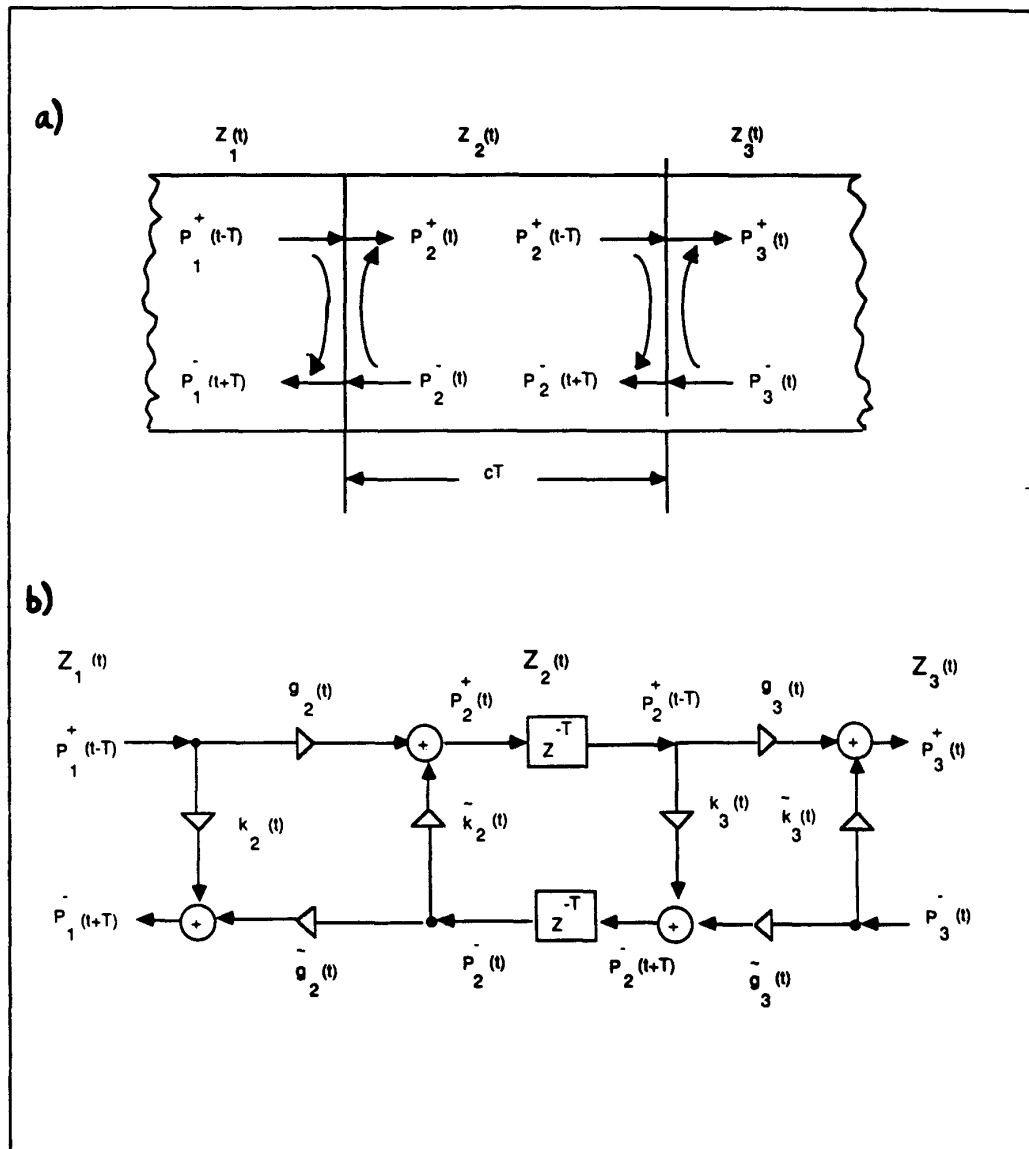


Figure 1. A waveguide section between two partial sections.

a) Physical picture indicating traveling waves in a continuous medium whose characteristic impedance changes from Z_1 to Z_2 to Z_3 .

b) Digital simulation diagram for the same situation. The section traversal delay is denoted as z^{-T} . The behavior at an impedance discontinuity is characterized by forward and reverse transmission ($\tau_i, \bar{\tau}_i$) and reflection (k_i, \bar{k}_i) coefficients.

For minimization of dynamic range requirements, we may sometimes choose instead left- and right-going *velocity waves*, U_i^- , U_i^+ , respectively, as the signal variables.

The fundamental equations relating the traveling waves and characteristic impedance in the i th section are

$$\begin{aligned} P_i^+ &= Z_i U_i^+ \\ P_i^- &= -Z_i U_i^- \end{aligned} \quad (1)$$

These will be referred to below as *Ohm's law* for unidirectional traveling waves. More precisely, $P_i^+(x, t) = Z_i(x, t)U_i^+(x, t)$ and $P_i^-(x, t) = -Z_i(x, t)U_i^-(x, t)$, where x is horizontal position along the waveguide axis and t is time. However, since (1) holds at any fixed point in space and time within each section, the arguments ' x, t ' can be dropped in the general case for simplicity of notation.

If the characteristic impedance Z_i is constant, the shape of a traveling wave is not altered as it propagates from one end of a section to the other. In this case we need only consider P_i^+ and P_i^- at one end of each section as a function of time. As shown in Fig. 1, we define $P_i^\pm(t)$ as the pressure at the *extreme left* of section i . Therefore, at the extreme right of section i , we have the traveling waves $P_i^+(t - T)$ and $P_i^-(t + T)$, where T is the travel time from one end of a section to the other.

When the characteristic impedances are time-varying, a number of possibilities exist which satisfy Ohm's law (1). For the moment, we will assume the traveling waves at the extreme right of section i are still given by $P_i^+(t - T)$ and $P_i^-(t + T)$. This definition, however, implies the velocity varies inversely with the characteristic impedance. As a result, signal energy is "pumped" into the waveguide by a changing characteristic impedance. The appendix describes normalization strategies which holds signal power fixed in the time-varying case.

The physical instantaneous pressure and velocity in section i are obtained by

summing the left- and right-going traveling wave components:

$$\begin{aligned} P_i &= P_i^+ + P_i^- \\ U_i &= U_i^+ + U_i^- \end{aligned} \quad (2)$$

Again this relationship is instantaneous with respect to space and time. Let $P_i(x, t)$ denote the instantaneous pressure at position x and time t in section i , where x is measured from the extreme left of section i (i.e., $0 \leq x \leq cT$). Then we have, for example, $P_i(0, t) \triangleq P_i^+(t) + P_i^-(t)$ and $P_i(cT, t) \triangleq P_i^+(t - T) + P_i^-(t + T)$ at the boundaries of section i .

Conservation of energy and mass dictate that the instantaneous pressure and velocity must be continuous across an impedance discontinuity, i.e.,

$$\begin{aligned} P_{i-1}(cT, t) &= P_i(0, t) \\ U_{i-1}(cT, t) &= U_i(0, t) \end{aligned} \quad (3)$$

Equations (1,2,3) imply the following *scattering equations*:

$$\begin{aligned} P_i^+(t) &= [1 + k_i(t)]P_{i-1}^+(t - T) - k_i(t)P_i^-(t) \\ P_{i-1}^-(t + T) &= k_i(t)P_{i-1}^+(t - T) + [1 - k_i(t)]P_i^-(t) \end{aligned} \quad (4)$$

where

$$k_i(t) \triangleq \frac{Z_i(t) - Z_{i-1}(t)}{Z_i(t) + Z_{i-1}(t)} \quad (5)$$

is called the i th *reflection coefficient*.

The scattering equations are illustrated in Fig. 2.* This scattering configuration is used in the *Kelly-Lochbaum* acoustic tube model [11].

* In the case of traveling velocity waves, the forward and reverse transmission coefficients are interchanged. However, we cannot mix pressure and velocity sections in the time-varying case unless we interject a "transformer" when changing from pressure to velocity as discussed in the appendix.

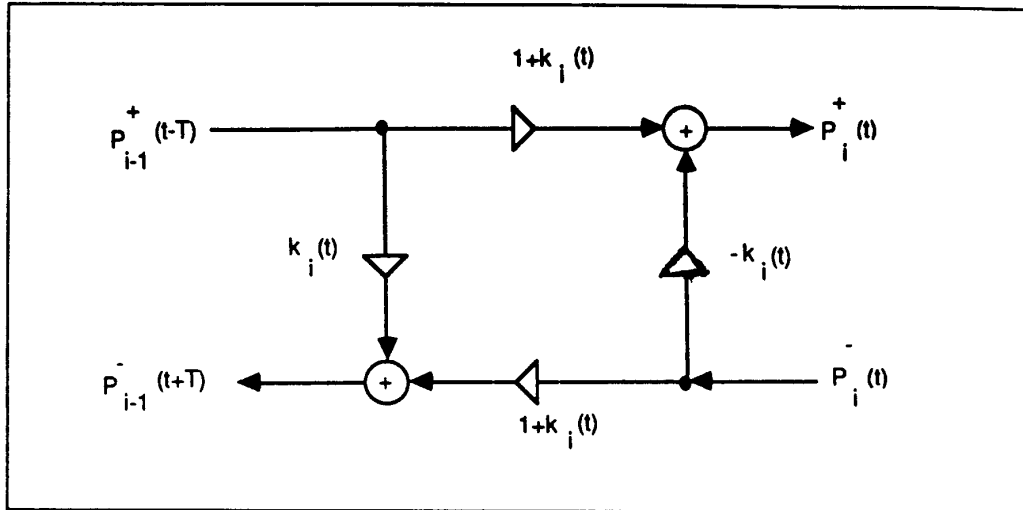


Figure 2. The Kelly-Lochbaum scattering junction.

By factoring out $k_i(t)$ in each equation of (4), we can write

$$\begin{aligned} P_i^+(t) &= P_{i-1}^+(t-T) + P_\Delta(t) \\ P_{i-1}^-(t+T) &= P_i^-(t) + P_\Delta(t) \end{aligned} \quad (6)$$

where

$$P_\Delta(t) = k_i(t) \left[P_{i-1}^+(t-T) - P_i^-(t) \right] \quad (7)$$

Thus, only one multiplication is actually necessary to compute the reflected waves from the incoming waves in the Kelly-Lochbaum junction. This computation is shown schematically in Fig. 3, and it is known as the *one-multiply* scattering junction [11]. In fixed-point implementations, the only source of error would typically be in single multiplication within the computation of P_Δ .

Another one-multiply form is obtained by organizing (4) as

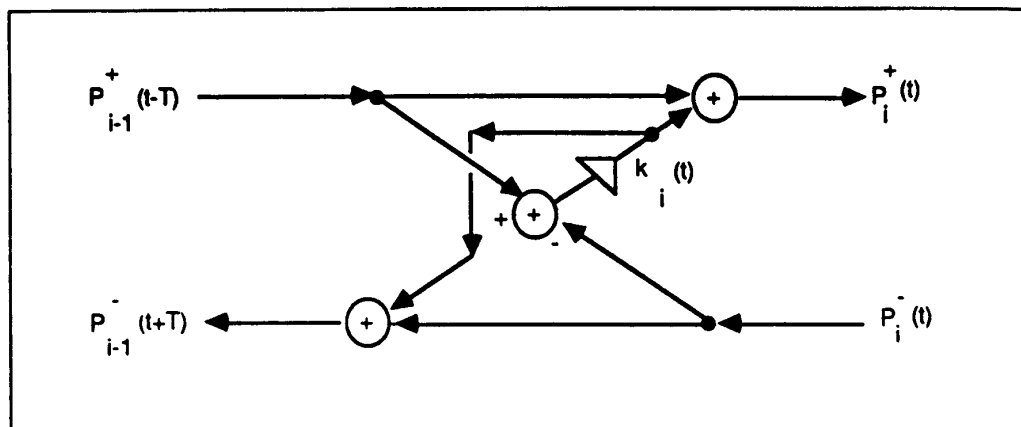


Figure 3. The one-multiply scattering boundary.

$$\begin{aligned}
 P_i^+(t) &= P_i^-(t) + \alpha_i(t)\tilde{P}_\Delta(t) \\
 P_{i-1}^-(t+T) &= P_i^+(t) - \tilde{P}_\Delta(t)
 \end{aligned}
 \tag{8}$$

where

$$\begin{aligned}
 \alpha_i(t) &\triangleq 1 + k_i(t) \\
 \tilde{P}_\Delta(t) &\triangleq P_{i-1}^+(t-T) - P_i^-(t)
 \end{aligned}
 \tag{9}$$

As in the previous case, only one multiplication and three additions are required per junction.

It is easy to show using the formulas of the next section that for junction passivity, the single section parameter k_i of (6) must lie between -1 and 1 , while in (8), the parameter α_i must lie between 0 and 2 .

4. Signal Power

The *instantaneous power* in a waveguide section containing instantaneous pressure $P_i(x, t)$ and velocity $U_i(x, t)$ is defined as the product of pressure and velocity:

$$I_i(x, t) = P_i(x, t)U_i(x, t) \quad (10)$$

An analogous definition (using the para-Hermitian conjugate of P_i) works out very well for the generalized case in which P_i^\ddagger and U_i^\ddagger are q by m matrices of meromorphic transfer functions [17].

The *right-going* and *left-going* power at the extreme left of the i th waveguide section are defined, respectively, by

$$\begin{aligned} I_i^+(t) &= P_i^+(t)U_i^+(t) = \frac{[P_i^+(t)]^2}{Z_i(t)} \\ I_i^-(t) &= P_i^-(t)U_i^-(t) = -\frac{[P_i^-(t)]^2}{Z_i(t)} \end{aligned} \quad (11)$$

From (10), we have $I_i(0, t) = I_i^+(t) + I_i^-(t)$ for the net power flow into the i th waveguide section from the left. The power equation completes the basic picture of interconnected waveguide sections.

5. Junction Passivity

A junction is passive if the power flowing away from it does not exceed the power flowing into it. Referring to equations (4) and (11), the total power flowing away from the i th junction is bounded by the incoming power if

$$\frac{[P_i^+(t)]^2}{Z_i(t)} + \frac{[P_{i-1}^-(t+T)]^2}{Z_{i-1}(t)} \leq \frac{[P_{i-1}^+(t-T)]^2}{Z_{i-1}(t)} + \frac{[P_i^-(t)]^2}{Z_i(t)} \quad (12)$$

which is true if and only if $I_{i-1}(cT, t) \geq I_i(0, t)$. Let \hat{P} denote the finite-precision version of P . Then a *sufficient* condition for junction passivity is

$$\begin{aligned} |\hat{P}_i^+(t)| &\leq |P_i^+(t)| \\ |\hat{P}_{i-1}^-(t+T)| &\leq |P_{i-1}^-(t+T)| \end{aligned} \quad (13)$$

Thus, if the junction computations do not increase either of the output pressure amplitudes, no signal power is created. An analogous conclusion is reached for velocity scattering junctions.

6. Passive Arithmetic

In a finite-precision implementation, only the junction output signals $\hat{P}_i^+(t)$ and $\hat{P}_{i-1}^-(t+T)$ need to be examined as possible sources of increased signal power. Quantized reflection coefficients $\hat{k}_i(t)$ (between 0 and 1) can be regarded as error-free (insofar as passivity is concerned) because to each sequence of quantized reflection coefficients, $\hat{k}_i(t), i = 1, \dots, M$, there corresponds a sequence of exact characteristic impedances $\hat{Z}_i(t) = \hat{Z}_{i-1}(t)[1 + \hat{k}_i(t)]/[1 - \hat{k}_i(t)], i = 1, \dots, M + 1$, where \hat{Z}_0 is arbitrary and \hat{Z}_{M+1} is infinity. The quantized input signals $\hat{P}_{i-1}^+(t-T)$ and $\hat{P}_i^-(t)$ are simply delayed outputs from adjoining junctions, and the intervening delay lines introduce no further quantization.

In view of the previous paragraph and equation (13), a general means of obtaining passive junctions is to compute exact results internally using extended precision, and apply saturation and magnitude truncation to the final outgoing waves. Let

$$\begin{aligned} n &\triangleq \text{Number of bits per signal sample} \\ m &\triangleq \text{Number of bits per reflection-coefficient} \end{aligned} \quad (14)$$

We assume fractional two's complement arithmetic is used, although analogous results exist for other number systems. Both the signal variables P_i^\pm and the

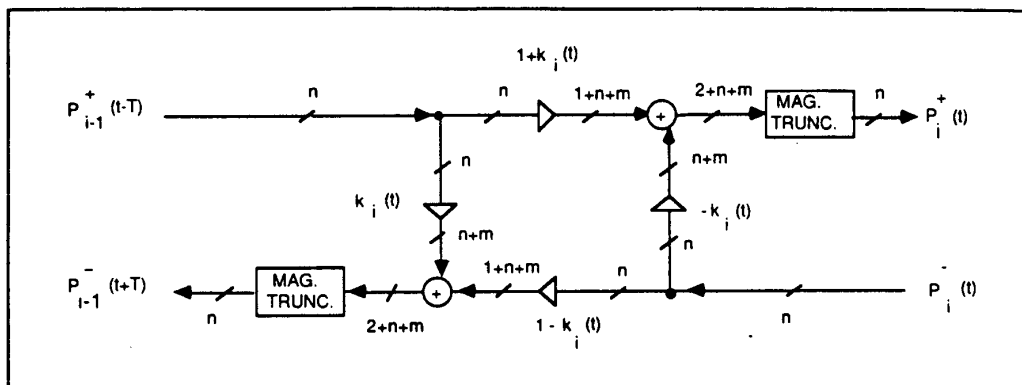


Figure 4. Bit allocations in the passive, finite-precision, Kelly-Lochbaum junction.

reflection coefficients k_i are assumed to lie between -1 and 1 so that the binary point is at the far left in every case.

7. The Passive Kelly-Lochbaum Junction

Figure 4 shows the number of bits needed to implement a passive Kelly-Lochbaum junction. The forward and reverse transmission coefficients each require $m + 1$ bits in order that $1 \pm \hat{k}_i(t)$ be represented exactly relative to $\hat{k}_i(t)$. When an n -bit value is multiplied by an m -bit value, the complete product contains $n+m$ bits, in general. Similarly, an n -bit value added to an m -bit value requires $1 + \max\{n, m\}$ bits to represent exactly all possible results.

The error-free junction outputs occupy $2 + n + m$ bits. The 2 most-significant bits (MSB's) and the m least-significant bits (LSB's) must be discarded. When the 3 MSB's are not equal, overflow has occurred. The 2 MSB's can simply be discarded (resulting in "wrap-around" on overflow), or they can be used replace the output value by the maximum-magnitude number in n -bit two's complement having the correct sign ("saturation" on overflow). The 3 MSB's determine the appropriate

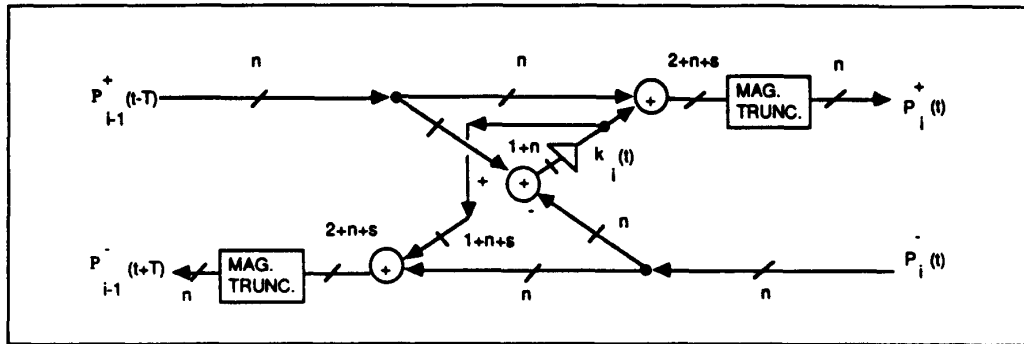


Figure 5. Bit allocations in the passive, finite-precision, one-multiply junction.

action to take in a saturating adder. With either overflow-handling strategy, the signal amplitude is reduced upon overflow. Consequently, by (13), signal power is always decreased by output adder overflow, even in the otherwise disastrous case of two's complement "wrap-around."

The magnitude truncation function discards the low-order (least significant) m bits of the result if it is positive. The low-order m bits are also discarded if they are all zero. If the extended-precision result is negative and any of the m low-order bits is nonzero, then the smallest positive number (2^{-n+1}) is added to the value obtained by discarding the low-order m bits. Thus, the number is always *truncated toward zero*.

A simpler magnitude truncation scheme which loses the LSB with probability 2^{-m} is to simply discard the low-order m bits in all cases, and always add 2^{-n+1} to the n -bit result if it is negative.

8. The Passive One-Multiply Junction

Figure 5 shows the number of bits needed to implement a passive one-multiply junction. The adder before the reflection coefficient increases the signal width by

one bit, and the reflection coefficient itself adds m bits, for a total of $1 + n + m$ bits going into each of the two final adders. The final output signal again occupies $2 + n + m$ bits. Output overflow considerations are exactly the same as in the Kelly-Lochbaum junction. However, the magnitude truncation is less expensive in the present case. Notice in Fig. 5 that *every adder has at least one operand consisting of only n bits*. Consequently, the low-order m bits at the input to the two output adders will be summed with zeros and passed through unchanged. Hence, the adders need not accept the low-order m bits. The logical OR of all of the m LSB's of the multiplier output (denoted s in Fig. 5) can be fed directly to the magnitude truncation unit, without increasing the adder complexity at all. In the simplified magnitude truncation scheme, the low-order m bits from the multiplier can be ignored completely. With some multiplier chips, the low-order product must be extracted on a separate output tri-state enable; in this situation, the simplified magnitude truncation scheme may double throughput.

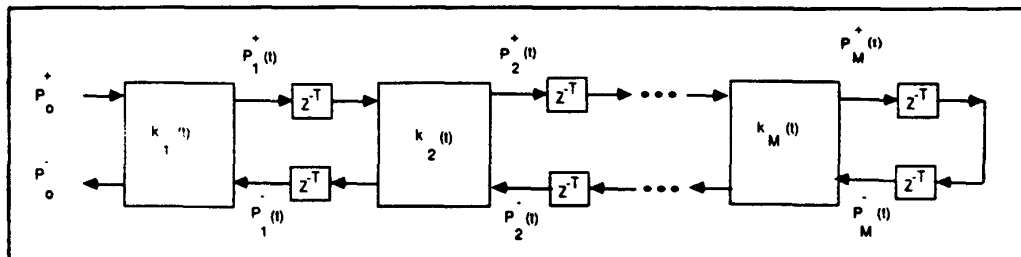


Figure 6. Waveguide digital filter structure.

9. Reduction to Standard Forms

The basic WGF we have been considering is shown in Fig. 6. Each box enclosing the symbol $k_i(t)$ denotes a scattering junction characterized by $k_i(t)$. While we have mentioned only the Kelly-Lochbaum and one-multiply junction, any type of ^{passive} ~~lossless~~ junction will do. In particular, the two-multiply lattice and normalized ladder scattering junctions [11] can appear in these boxes. *The WGF employs delays between each scattering junction along both the top and bottom signal paths, unlike conventional ladder and lattice filters. Reduction to the standard forms is merely a matter of pushing delays along the top rail around to the bottom rail, so that each bottom-rail delay becomes $2T$ seconds instead of T seconds. Such an operation is possible because of the termination at the right by an infinite (or zero) characteristic impedance.

In the time-varying case, pushing a delay through a multiply results in a corresponding time advance of the multiplier coefficient, as shown in Fig. 7.

* According to lore, when the diagram within each junction box is a planar graph, as in the Kelly-Lochbaum and normalized ladder junction, the resulting system is called a ladder filter. When the junction scattering diagrams are nonplanar, as in the one-multiply or two-multiply cases, the term lattice filter is used. However, this definition appears not to be universal.

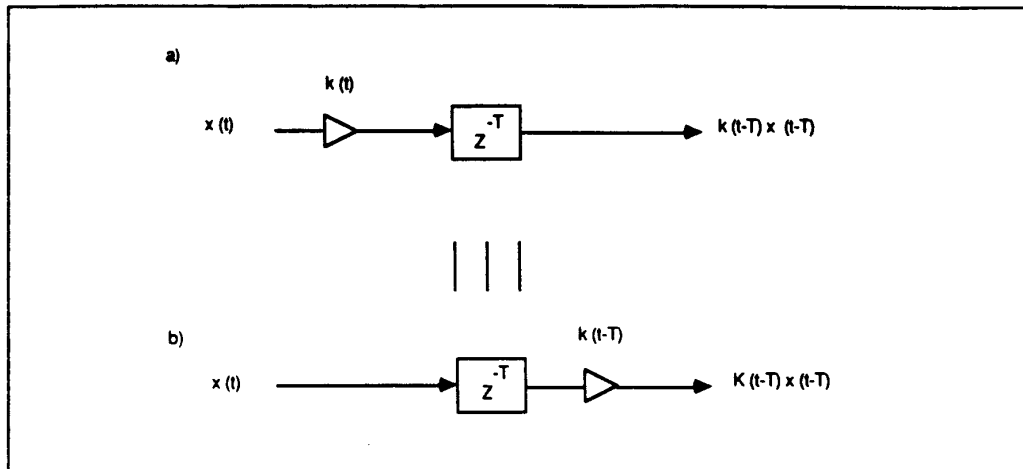


Figure 7. Commuting a delay with a multiplier coefficient in the time-varying case.

Imagine each delay element in Fig. 6 being divided into halves, and let q denote a delay of $T/2$ seconds. Then any WGF can be built from sections such as shown in Fig. 8a.

The series of transformations shown in Fig. 8 push the two input-signal delays through the junction to the two output delays. A similar sequence of moves pushes the two output delays into the two input branches. Consequently, we can replace any WGF section of the form shown in Fig. 9a by a section of the form shown in Fig. 9b or c.

By alternately choosing the structure of Fig. 9b and c, the filter structure of Fig. 10 is obtained. This structure has some advantages worth considering: (1) it consolidates delays to length $2T$ as do conventional lattice/ladder structures, (2) it does not require a termination by an infinite characteristic impedance, allowing it to be extended to networks of arbitrary topology (e.g., multiport branching, intersection, and looping), and (3) there is no long delay-free signal path along the upper rail as in conventional structures—a pipeline segment is only two sections long. This structure, termed the “half-rate waveguide filter” [17], appears to

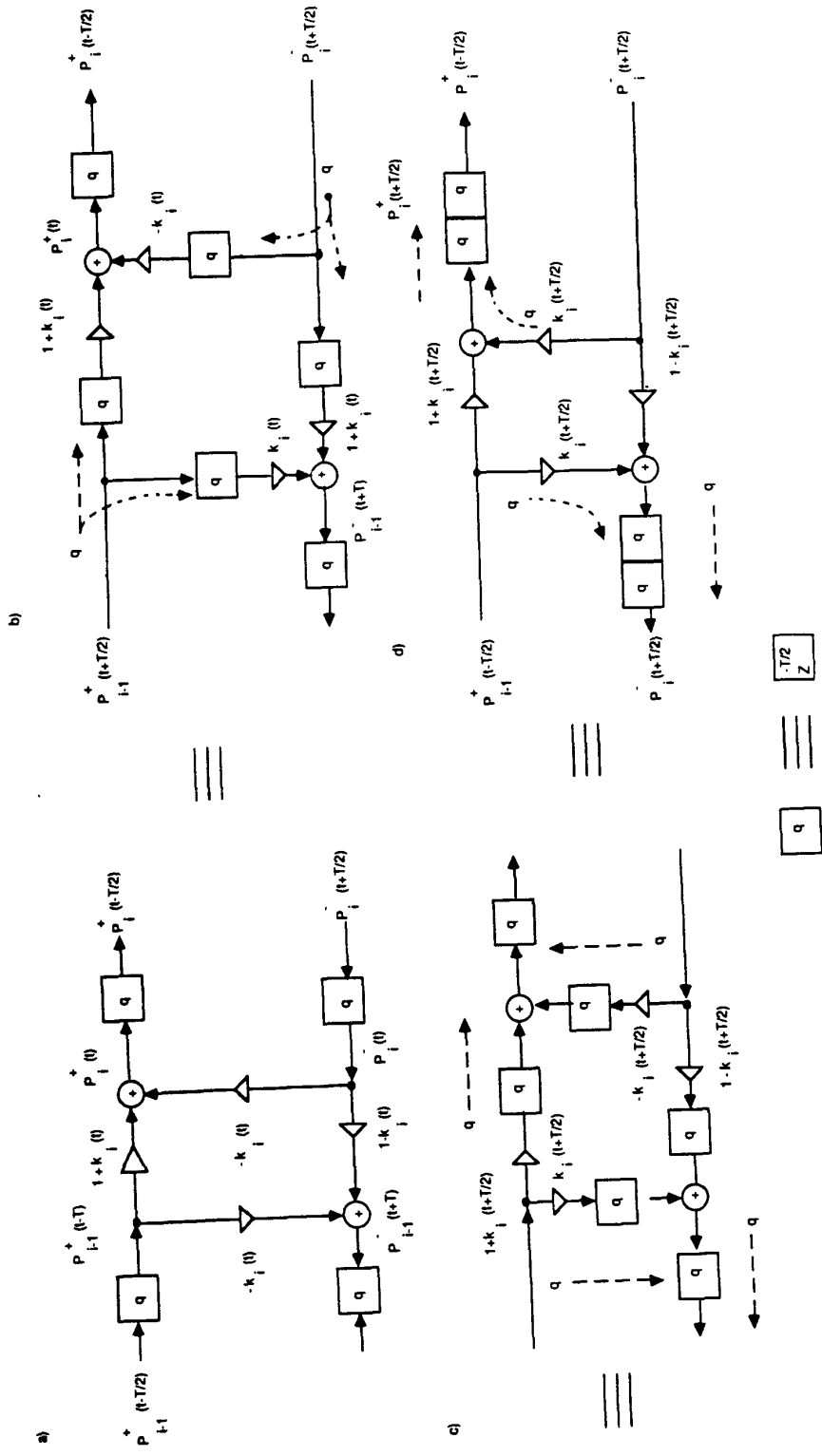


Figure 8. Consolidating delays by pushing through the junction.

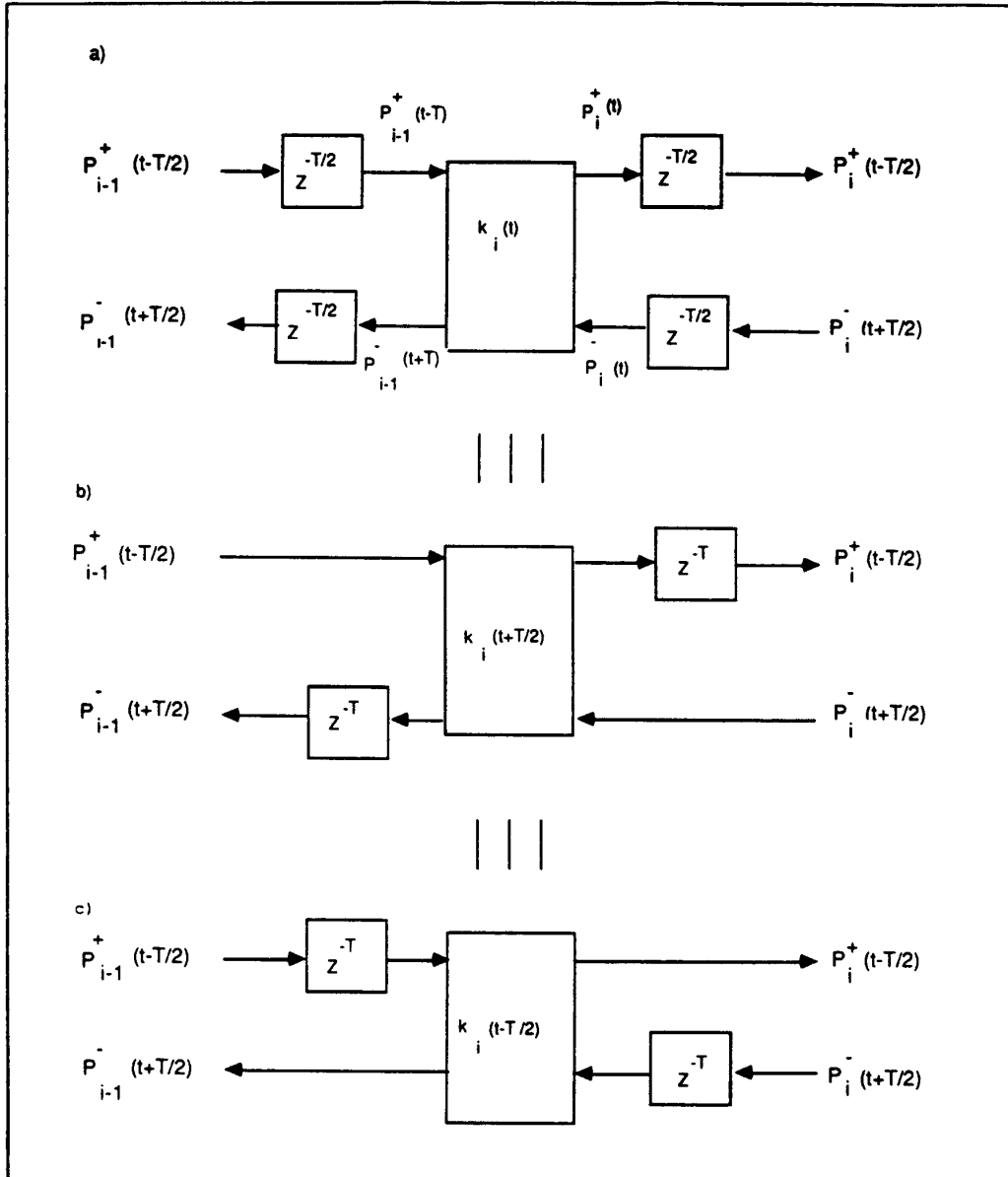


Figure 9. Equivalent waveguide filter sections.

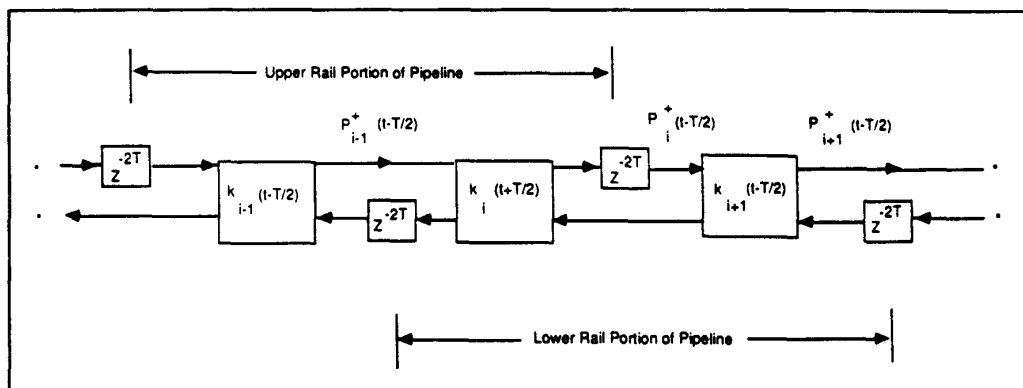


Figure 10. Pipelineable, physically extendible, consolidated-delay, waveguide filter.

have better overall characteristics than any other digital filter structure for many applications. Advantage (2) makes it especially valuable for modeling physical systems.

Finally, successive substitutions of the section of Fig. 9b and reapplication of the delay consolidation transformation lead to the structure of Fig. 11. This is the conventional ladder or lattice filter structure. The termination at the right by a total reflection is required to obtain this structure. Consequently, conventional lattice filters cannot be extended on the right in a physically meaningful way. Also, creating network topologies more complex than a simple series (or acyclic tree) of waveguide sections is not immediately possible because of the delay-free path along the top rail. For example, the output cannot be fed back to the input. Nevertheless, the conventional structure enjoys the same physical interpretation as the more general WGF structures, including the same simple passivity conditions in the time-varying, nonzero-input case.

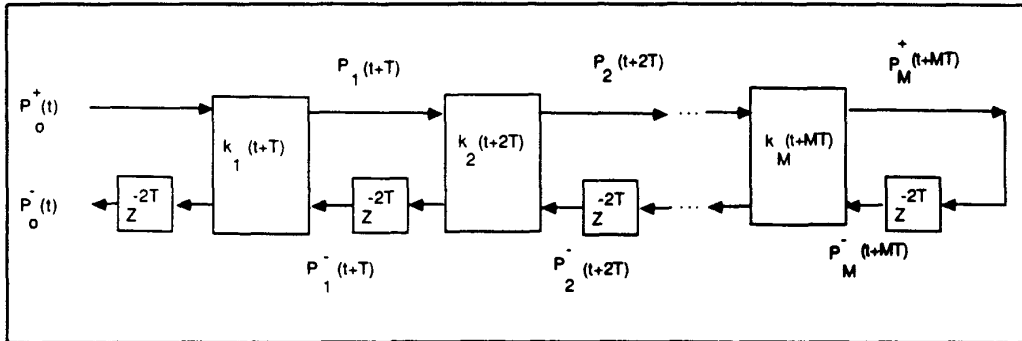


Figure 11. Conventional ladder/lattice filter structure.

10. Appendix — Power-Normalized Waveguide Filters

Above, we adopted the convention that the time variation of the characteristic impedance did not alter the traveling pressure waves P_i^\pm . In this case, the power represented by a traveling pressure wave is modulated by the changing characteristic impedance as it propagates. The actual power becomes inversely proportional to characteristic impedance:

$$I_i(x, t) = I_i^+(x, t) + I_i^-(x, t) = \frac{[P_i^+(x, t)]^2 - [P_i^-(x, t)]^2}{Z_i(t)} \quad (15)$$

This power modulation causes no difficulties in the Lyapunov theory because it occurs identically in both the finite-precision and infinite-precision filters. However, in some applications (e.g. [18]), it may be desirable to compensate for the power modulation so that changes in the characteristic impedances of the waveguides do not affect the power of the signals propagating within.

Consider an arbitrary point in the i th waveguide at time t and distance $x = ct$ measured from the left boundary, as shown in Fig. 12. The right-going pressure is $P_i^+(x, t)$ and the left-going pressure is $P_i^-(x, t)$. In the absence of scaling, the

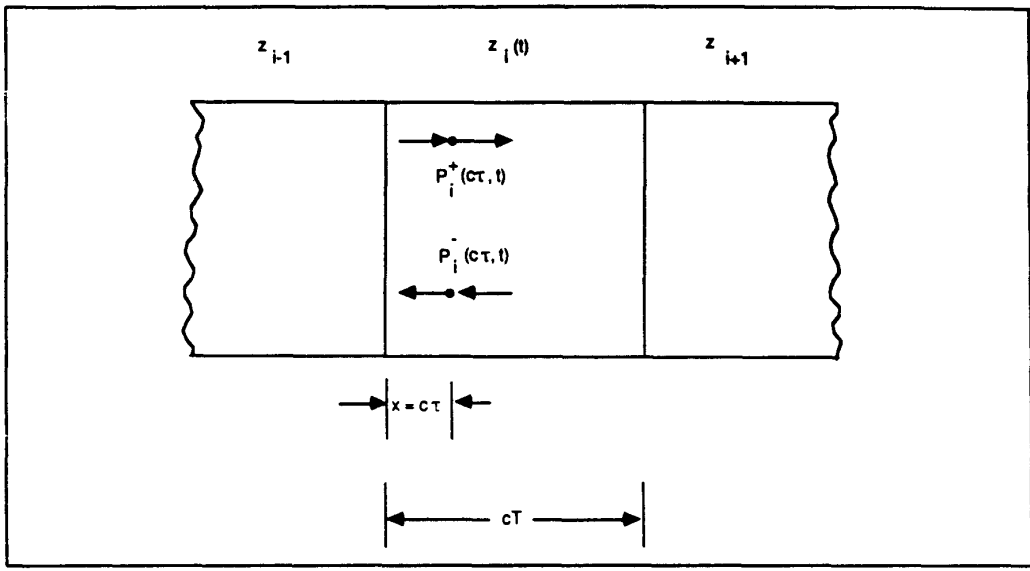


Figure 12. Traveling pressure waves at a general point within a waveguide section.

waveguide section behaves (according to our definition of the propagation medium properties) as a pressure delay line, and we have $P_i^+(x, t) = P_i^+(0, t - \tau)$ and $P_i^-(x, t) = P_i^-(0, t + \tau) = P_i^-(cT, t - T + \tau)$. The left-going and right-going components of the signal power are $[P_i^+(x, t)]^2/Z_i(t)$ and $[P_i^-(x, t)]^2/Z_i(t)$, respectively.

Below, three methods are discussed for making signal power *invariant* with respect to time-varying branch impedances.

10.1. Normalized Waveguides

Suppose we are willing to scale the traveling waves as the characteristic impedance changes in order to hold signal power fixed. We can choose any position as a reference, but perhaps it is most natural to fix the power of each wave to that which it had upon entry to the section. In this case, it is quickly verified that the

proper scaling is

$$\begin{aligned}\bar{P}_i^+(x, t) &= \left(\frac{Z_i(t)}{Z_i(t-\tau)} \right)^{1/2} P_i^+(0, t-\tau), & x = c\tau \\ \bar{P}_i^-(x, t) &= \left(\frac{Z_i(t)}{Z_i(t-T+\tau)} \right)^{1/2} P_i^-(cT, t-T+\tau)\end{aligned}\quad (16)$$

In practice, there is no need to perform the scaling until the signal actually reaches a junction. Thus, we implement

$$\begin{aligned}\bar{P}_i^+(cT, t) &= g_i(t) P_i^+(0, t-T) \\ \bar{P}_i^-(0, t) &= g_i(t) P_i^-(cT, t-T)\end{aligned}\quad (17)$$

where

$$g_i(t) = \sqrt{\frac{Z_i(t)}{Z_i(t-T)}}$$

Since
In the single-argument notation used earlier, (17) becomes

$$\begin{aligned}\bar{P}_i^+(t-T) &= g_i(t) P_i^+(t-T) \\ \bar{P}_i^-(t) &= g_i(t) P_i^-(t)\end{aligned}\quad (18)$$

A diagram of this normalization strategy is shown in Fig. 13. It has the property that the time-varying waveguides (as well as the junctions) conserve signal power. If the scattering junctions are implemented with one-multiply structures, then the number of multiplies per section rises to three when power is normalized. There are three additions as in the unnormalized case. In some situations (such as in the two-stage structure of Fig. 10), it may be acceptable to normalize at fewer points; the normalizing multiplies can be pushed through the scattering junctions and combined with other normalizing multiplies, much in the same way delays were pushed through the junctions to obtain standard ladder/lattice forms. In physical

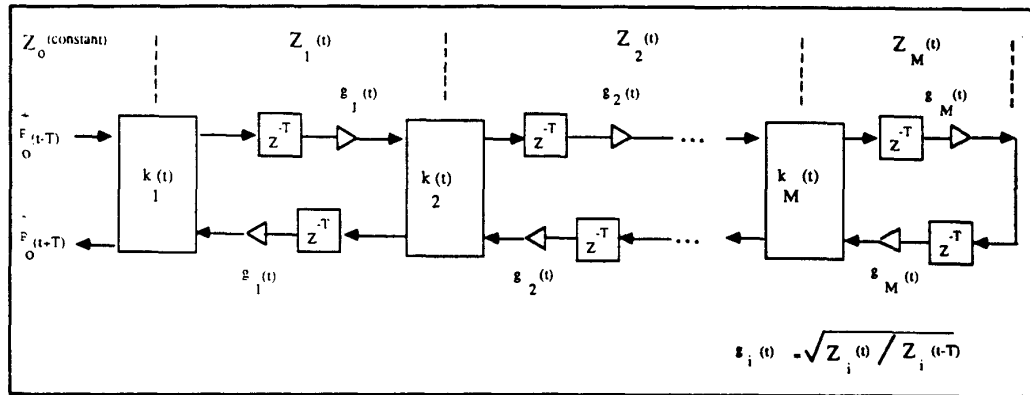


Figure 13. Normalized-waveguide digital filter structure.

modeling applications, normalization can be limited to opposite ends of a long cascade of sections with no interior output “taps.”

To ensure passivity of a normalized-waveguide with finite-precision calculations, it suffices to perform magnitude truncation after multiplication by $g_i(t)$. Alternatively, extended precision can be used within the scattering junction.

10.2. Normalized Waves

Another approach to normalization is to propagate *rms-normalized waves* in the waveguide. In this case, each delay-line contains

$$\begin{aligned} \tilde{P}_i^+(x, t) &= P_i^+(x, t) / \sqrt{Z_i(t)} \\ \tilde{P}_i^-(x, t) &= P_i^-(x, t) / \sqrt{Z_i(t)} \end{aligned} \tag{19}$$

We now consider \tilde{P}^\pm (instead of P^\pm) to be invariant with respect to the character-

istic impedance. In this case,

$$\tilde{P}_i^+(cT) = \frac{P_i^+(cT, t)}{\sqrt{Z_i(t)}} = \frac{P_i^+(0, t-T)}{\sqrt{Z_i(t-T)}} = \tilde{P}_i^+(t-T)$$

The scattering equations (4) become

$$\begin{aligned} \sqrt{Z_i(t)}\tilde{P}_i^+(0, t) &= [1 + k_i(t)]\sqrt{Z_{i-1}(t)}\tilde{P}_{i-1}^+(cT, t) - k_i(t)\sqrt{Z_i(t)}\tilde{P}_i^-(0, t) \\ \sqrt{Z_{i-1}(t)}\tilde{P}_{i-1}^-(cT, t) &= k_i(t)\sqrt{Z_{i-1}(t)}\tilde{P}_{i-1}^+(ct, T) + [1 - k_i(t)]\sqrt{Z_i(t)}\tilde{P}_i^-(t) \end{aligned} \quad (20)$$

or, solving for \tilde{P}_i^\pm ,

$$\begin{aligned} \tilde{P}_i^+(0, t) &= [1 + k_i(t)]\sqrt{\frac{Z_{i-1}(t)}{Z_i(t)}}\tilde{P}_{i-1}^+(cT, t) - k_i(t)\tilde{P}_i^-(0, t) \\ \tilde{P}_{i-1}^-(cT, t) &= k_i(t)\tilde{P}_{i-1}^+(ct, T) + [1 - k_i(t)]\sqrt{\frac{Z_i(t)}{Z_{i-1}(t)}}\tilde{P}_i^-(t) \end{aligned} \quad (21)$$

But, from (5),

$$\frac{Z_{i-1}(t)}{Z_i(t)} = \frac{1 - k_i(t)}{1 + k_i(t)} \quad (22)$$

whence

$$[1 + k_i(t)]\sqrt{\frac{Z_{i-1}(t)}{Z_i(t)}} = [1 - k_i(t)]\sqrt{\frac{Z_i(t)}{Z_{i-1}(t)}} = \sqrt{1 - k_i^2(t)} \quad (23)$$

The final scattering equations for normalized waves are

$$\begin{aligned} \tilde{P}_i^+(0, t) &= c_i(t)\tilde{P}_{i-1}^+(cT, t) - s_i(t)\tilde{P}_i^-(0, t) \\ \tilde{P}_{i-1}^-(cT, t) &= s_i(t)\tilde{P}_{i-1}^+(ct, T) + c_i(t)\tilde{P}_i^-(t) \end{aligned} \quad (24)$$

where

$$\begin{aligned} s_i(t) &\triangleq k_i(t) \\ c_i(t) &\triangleq \sqrt{1 - k_i^2(t)} \end{aligned} \quad (25)$$

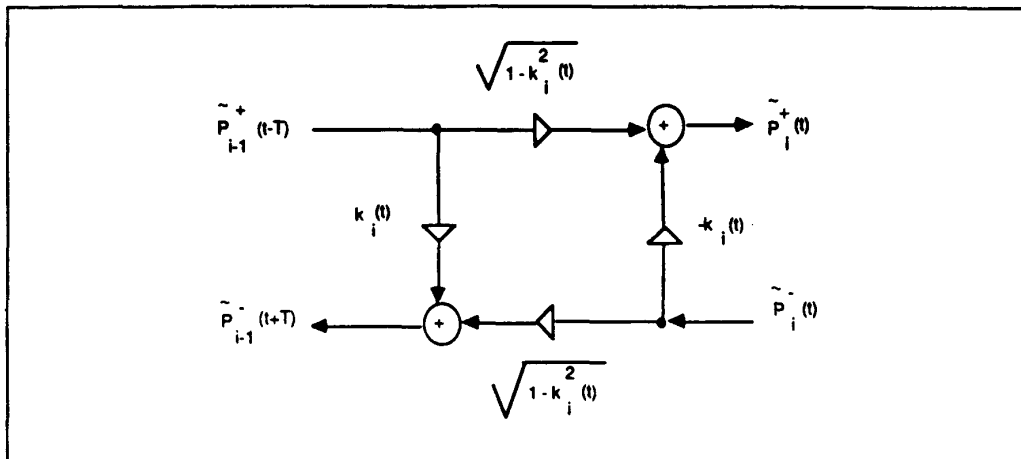


Figure 14. Wave-normalized waveguide junction.

can be viewed as the sine and cosine, respectively, of a single angle $\theta_i(t) = \sin^{-1}[k_i(t)]$ which characterizes the junction. Figure 14 illustrates the Kelly-Lochbaum junction as it applies to normalized waves. This time we cannot factor out $k_i(t)$ to obtain a one-multiply structure. The four-multiply structure of Fig. 14 is used in the *normalized ladder filter* (NLF) suggested by Gray and Markel [10,11,13].

Note that normalizing the output of the delay lines (as discussed in the previous subsection) saves one multiply relative to the NLF which propagates normalized waves. However, there are other differences to consider. In the case of normalized waves, duals are easier; i.e., changing the propagation variable from pressure to velocity or vice versa in the i th section requires no signal normalization, and the forward and reverse reflection coefficients are unchanged. Only sign-reversal is required for the reverse path. Also, in the case of normalized waves, the rms signal level is the same whether or not pressure or velocity is used. While appealing from a "balance of power" standpoint, normalizing all signals by their rms level can be a disadvantage: In the case of normalized delay-line outputs, dynamic range can be minimized by choosing the smaller of pressure and velocity as the variable of propagation.

10.3. Transformer-Coupled Waveguides

Still another approach to the normalization of time-varying waveguide filters is perhaps the most convenient of all. So far, the least expensive normalization technique is the normalized-waveguide structure of Fig. 13, requiring only three multipliers per section rather than four in the normalized-wave case. Unfortunately, in the normalized-waveguide case, changing the characteristic impedance of section i results in a changing of the reflection coefficients in *both* adjacent scattering junctions. Of course, a single junction can be modulated in isolation by changing all downstream characteristic impedances by the same ratio. But this does not help if the filtering network is not a cascade chain or acyclic tree of waveguide sections. A cleaner local variation in characteristic impedance can be obtained using *transformer coupling*. A transformer joins two waveguide sections of differing characteristic impedance in such a way that signal power is preserved and no scattering occurs. It turns out that filter structures built using the transformer-coupled waveguide are *equivalent* to those using the normalized-wave junction described in the previous subsection, but one of the four multipliers can be traded for an addition.

From Ohm's law (1) and the power equation (11), we see that to bridge an impedance discontinuity with no power change and no scattering requires the relations

$$\begin{aligned} \frac{|P_i^+|^2}{Z_i(t)} &= \frac{|P_{i-1}^+|^2}{Z_{i-1}(t)} \\ \frac{|P_i^-|^2}{Z_i(t)} &= \frac{|P_{i-1}^-|^2}{Z_{i-1}(t)} \end{aligned} \quad (26)$$

Therefore, the junction equations for a *transformer* [1] can be chosen as

$$\begin{aligned} P_i^+ &= g_i(t)P_{i-1}^+ \\ P_{i-1}^- &= g_i^{-1}(t)P_i^- \end{aligned} \quad (27)$$

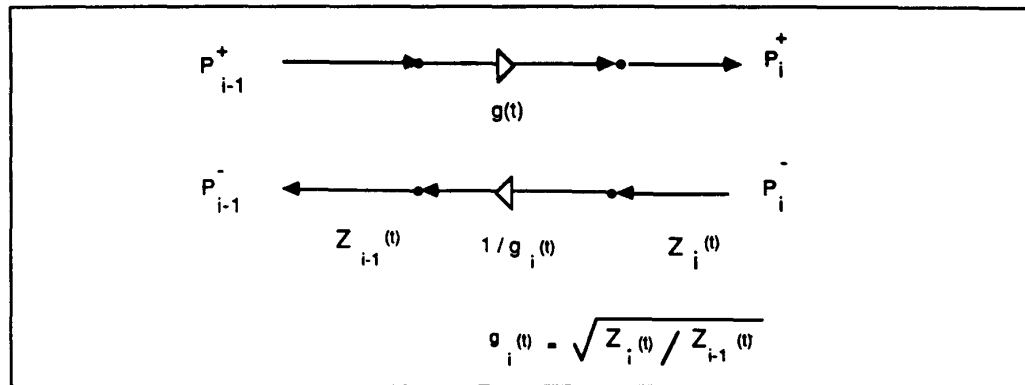


Figure 15. a) Transformer junction.

(depicted in Fig. 15) where, from (22),

$$g_i(t) \triangleq \sqrt{\frac{Z_i(t)}{Z_{i-1}(t)}} = \sqrt{\frac{1 + k_i(t)}{1 - k_i(t)}} \quad (28)$$

The choice of a negative square root corresponds to the *gyrator* [1]. The gyrator is equivalent to a transformer in cascade with a dualizer [17]. A dualizer is a direct implementation of Ohm's law (1) (to within a scale factor): the forward path is unchanged while the reverse path is negated. On one side of the dualizer there are pressure wave, and on the other side there are velocity waves. Ohm's law is a gyrator in cascade with a transformer whose scale factor equals the characteristic admittance.

The transformer-coupled WGF junction is shown in Fig. 16a. We can now modulate a single junction, even in arbitrary network topologies, by inserting a transformer immediately to the left or right of the junction. Conceptually, the characteristic impedance is not changed over the delay-line portion of the waveguide section; instead, it is changed to the new time-varying value just before (or after) it meets the junction. When velocity is the wave variable, the coefficients g_i and g_i^{-1} in Fig. 16a are swapped (or inverted).

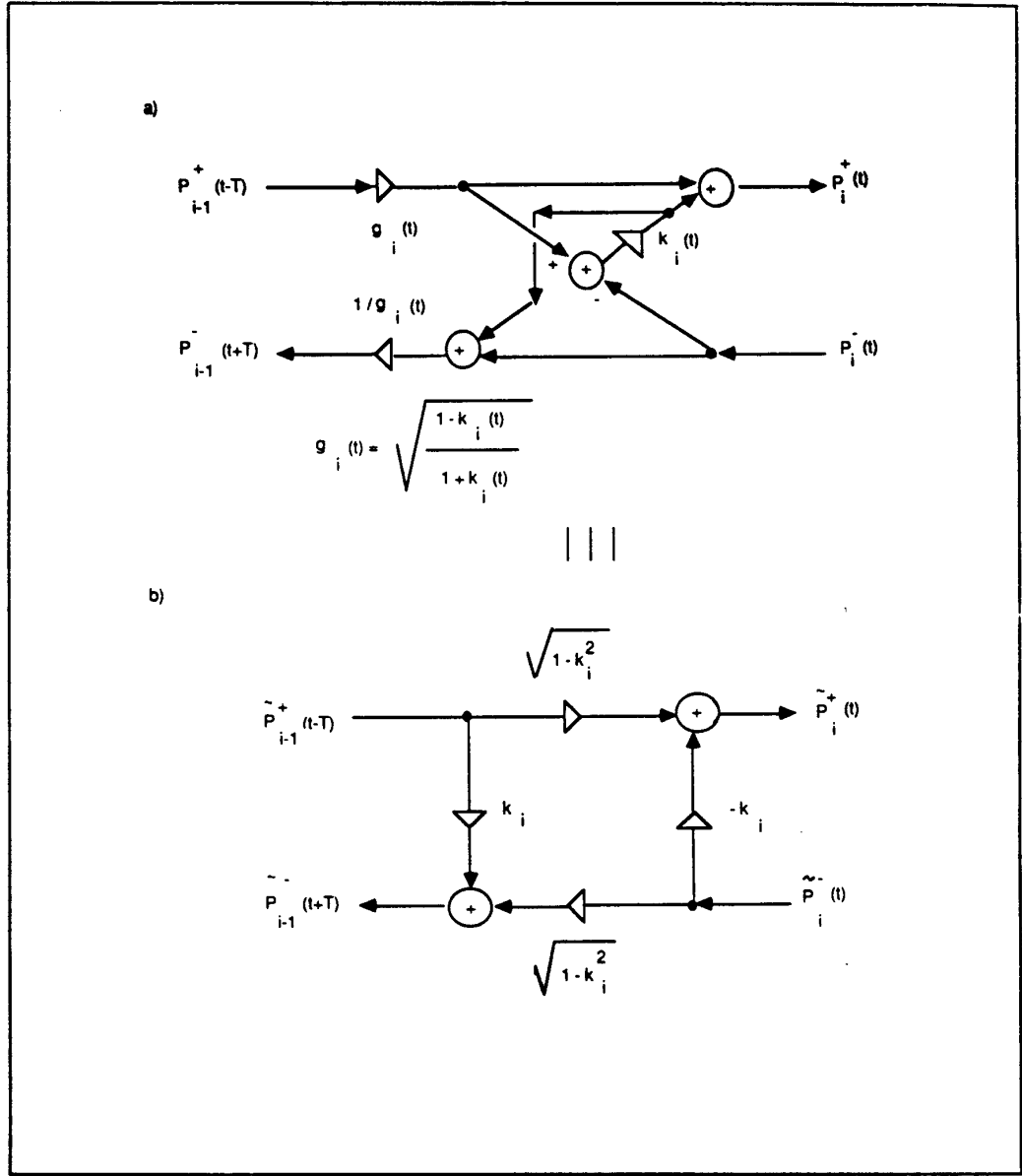


Figure 16. a) Transformer-coupled waveguide digital filter section, for transformer on left of junction. b) Normalized ladder filter section. The two are equivalent.

So, as in the normalized waveguide case, for the price of two extra multiplies per section, we can implement time-varying digital filters which do not modulate stored signal energy. Moreover, transformers enable the scattering junctions to be varied independently, without having to propagate time-varying impedance ratios throughout the waveguide network.

It is interesting to note that the transformer-coupled WGF and the wave-normalized WGF (shown in Fig. 16b) are equivalent. One simple proof is to start with a transformer and a Kelly-Lochbaum junction, move the transformer scale factors inside the junction, combine terms, and arrive at Fig. 16b. The practical importance of this equivalence is that the normalized ladder filter (NLF) can be implemented with only three multiplies and three additions instead of four multiplies and two additions.

11. Conclusions

It has been shown that limit cycles and overflow oscillations are easily eliminated in a waveguide filter (WGF) structure, which precisely simulates a sampled interconnection of ideal transmission line sections. Furthermore, the WGF can be transformed into all well-known ladder and lattice filter structures simply by pushing delays around to the bottom rail in the special case of a cascade, reflectively terminated WGF network. Therefore, aside from some time skew in the signal and filter coefficients, the samples computed in the WGF and the samples computed in other ladder/lattice filters are identical.

The WGF structure gives a precise implementation of physical wave phenomena in time-varying media. This property may be valuable in its own right for simulation purposes. It was shown how to delay or advance time-varying coefficient streams in order to obtain physically correct time-varying waveguide (or acoustic tube) simulations using standard lattice/ladder structures; also, the necessary time corrections for the traveling waves, needed to output a simulated pressure or velocity, were shown.

A reduction in the required number of multiplies per section was obtained for the well-known normalized ladder filter (NLF). While the three-multiply structure can be obtained from the four-multiply structure using network equivalence operations, its discovery is due to the simplified theoretical formulation presented in this paper.

12. References

- [1] V. Belevitch, *Classical Network Theory*, Holden Day, San Francisco, CA, 1968.
 - [2] P. M. Morse and K. U. Ingard, *Theoretical Acoustics*, McGraw-Hill, New York, 1968.
 - [3] A. Fettweis, "Digital Filters Related to Classical Structures," *AEU: Archive für Elektronik und Übertragungstechnik*, vol. 25, pp. 79-89, Feb. 1971.
 - [4] A. Fettweis, "Some Principles of Designing Digital Filters Imitating Classical Filter Structures," *IEEE Trans. on Circ. Theory*, vol. CT-18, pp. 314-316, March 1971.
 - [5] A. Fettweis, "Pseudopassivity, Sensitivity, and Stability of Wave Digital Filters," *IEEE Trans. on Circ. Theory*, vol. CT-19, pp. 668-673, Nov. 1972.
 - [6] K. Meerkötter and W. Wegener, "A New Second-Order Digital Filter without Parasitic Oscillations," *AEU: Archive für Elektronik und Übertragungstechnik*, vol. 29, pp. 312-314, Feb. 1975.
 - [7] A. Fettweis and K. Meerkötter, "On Adaptors for Wave Digital Filters," *IEEE Trans. on Acoust., Speech, and Signal Proc.*, vol. ASSP-23, pp. 516-525, Dec. 1975.
 - [8] A. H. Gray and J. D. Markel, "Digital Lattice and Ladder Filter Synthesis," *IEEE Trans. on Audio Electroacoust.*, vol. AU-21, pp. 491-500, Dec. 1973.
 - [9] A. Fettweis and K. Meerkötter, "Suppression of Parasitic Oscillations in Wave Digital Filters," *IEEE Trans. Circ. and Sys.*, vol. CAS-22, No. 3, pp. 239-246, Mar. 1975.
-

A reduction in the required number of multiplies per section was obtained for the well-known normalized ladder filter (NLF). While the three-multiply structure can be obtained from the four-multiply structure using network equivalence operations, its discovery is due to the simplified theoretical formulation presented in this paper.

12. References

- [1] V. Belevitch, *Classical Network Theory*, Holden Day, San Francisco, CA, 1968.
 - [2] P. M. Morse and K. U. Ingard, *Theoretical Acoustics*, McGraw-Hill, New York, 1968.
 - [3] A. Fettweis, "Digital Filters Related to Classical Structures," *AEU: Archive für Elektronik und Übertragungstechnik*, vol. 25, pp. 79-89, Feb. 1971.
 - [4] A. Fettweis, "Some Principles of Designing Digital Filters Imitating Classical Filter Structures," *IEEE Trans. on Circ. Theory*, vol. CT-18, pp. 314-316, March 1971.
 - [5] A. Fettweis, "Pseudopassivity, Sensitivity, and Stability of Wave Digital Filters," *IEEE Trans. on Circ. Theory*, vol. CT-19, pp. 668-673, Nov. 1972.
 - [6] K. Meerkötter and W. Wegener, "A New Second-Order Digital Filter without Parasitic Oscillations," *AEU: Archive für Elektronik und Übertragungstechnik*, vol. 29, pp. 312-314, Feb. 1975.
 - [7] A. Fettweis and K. Meerkötter, "On Adaptors for Wave Digital Filters," *IEEE Trans. on Acoust., Speech, and Signal Proc.*, vol. ASSP-23, pp. 516-525, Dec. 1975.
 - [8] A. H. Gray and J. D. Markel, "Digital Lattice and Ladder Filter Synthesis," *IEEE Trans. on Audio Electroacoust.*, vol. AU-21, pp. 491-500, Dec. 1973.
 - [9] A. Fettweis and K. Meerkötter, "Suppression of Parasitic Oscillations in Wave Digital Filters," *IEEE Trans. Circ. and Sys.*, vol. CAS-22, No. 3, pp. 239-246, Mar. 1975.
-

- [10] A. H. Gray and J. D. Markel, "A Normalized Digital Filter Structure," *IEEE Trans. on Acoust., Speech, and Signal Proc.*, vol. ASSP-23, pp. 268-277, June 1975.
 - [11] J. D. Markel and A. H. Gray, *Linear Prediction of Speech*, Springer-Verlag, New York, 1976.
 - [12] S. S. Lawson, "On a Generalization of the Wave Digital Filter Concept," *Int. J. Circuit Theory Appl.*, vol. 6, pp. 107-120, 1978.
 - [13] A. H. Gray, "Passive Cascaded Lattice Digital Filters," *IEEE Trans. Circ. and Sys.*, vol. CAS-27, No. 5, pp. 337-344, May 1980.
 - [14] P. DeWilde and H. Dym, "Schur Recursions, Error Formulas, and Convergence of Rational Estimators for Stationary Stochastic Estimators," *IEEE Trans. on Info. Theory*, vol. IT-27, pp. 446-461, July 1981.
 - [15] P. H. Delsarté, Y. V. Genin, and Y. Kamp, "On the Role of the Nevanlinna-Pick Problem in Circuit and System Theory," *Int. J. Circuit Theory Appl.*, vol. 9, no. 2, pp. 177-187, April 1981.
 - [16] B. Friedlander, "Lattice Filters for Adaptive Processing," *Proc. IEEE*, vol. 70, pp. 829-867, Aug. 1982.
 - [17] J. O. Smith, "Waveguide Digital Filters," Center for Computer Research in Music and Acoustics (CCRMA), Dept. of Music, Stanford University, March 1985.
 - [18] J. O. Smith, "A New Approach to Digital Reverberation using Closed Waveguide Networks," *Proc. 1985 Int. Conf. Computer Music*, Vancouver Canada, Computer Music Assoc., 1985. Music Dept. Tech. Rep. STAN-M-31, Stanford University, July 1985.
-

**ELIMINATION OF LIMIT CYCLES AND OVERFLOW
OSCILLATIONS IN TIME-VARYING LATTICE AND
LADDER DIGITAL FILTERS**

Elimination of Limit Cycles in Time-Varying Lattice/Ladder Filters

Julius O. Smith III

RESULTS:

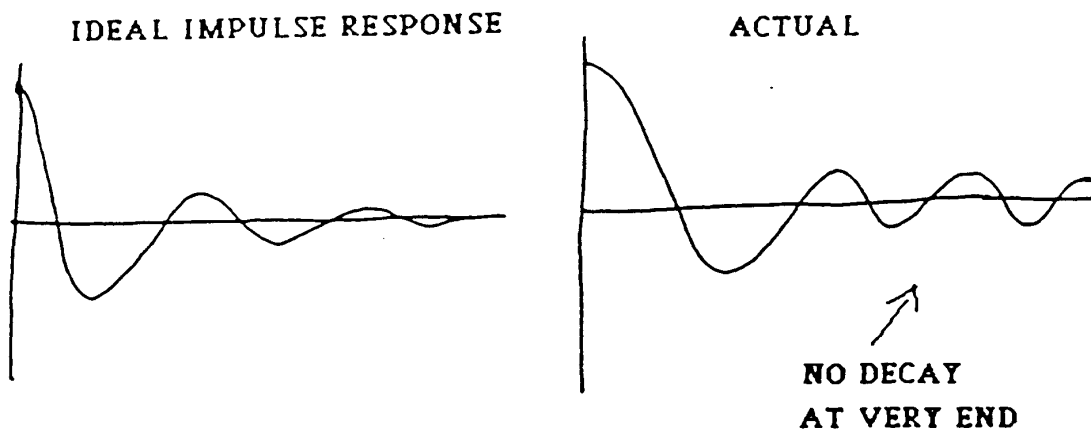
- o All time-varying lattice and ladder digital filter structures can be made free of limit cycles and overflow oscillations by applying magnitude truncation to the output of each scattering junction, where computations internal to a scattering junction are performed in extended (error free) precision.
- o Pointwise passivity is guaranteed irrespective of coefficient or input signal behavior.
- o Three-multiply normalized lattice section discovered as a byproduct

DERIVATION SUMMARY:

- Lattice and ladder digital filters are shown to be numerically equivalent to a digital transmission-line simulation in which physical signal power is defined **instantaneously** with respect to space and time.
- Magnitude truncation results in non-increasing instantaneous signal power, even in the time-varying case.
- Signal power in the finite-precision filter is bounded above by signal power in the infinite-precision filter at each instant of time and at each internal storage location.
- Hence, limit cycles and overflow oscillations cannot occur, regardless of filter coefficient or input signal behavior.

LIMIT CYCLE \triangleq Nonterminating response to a terminating input signal.

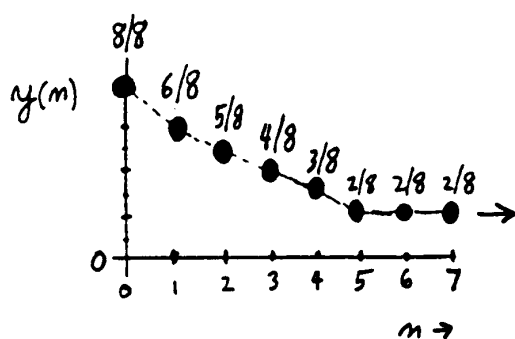
- o Typical cause is "rounding"
- o Not defined for periodic or otherwise nonterminating input signal



A FIRST-ORDER LIMIT-CYCLE EXAMPLE

- $y(n) = g \cdot y(n-1) + x(n)$
- $x(n) = 1, 0, 0, \dots$
- Assume 3-bit arithmetic with rounding
- $g = 3/4$ (decimal) = 0.110 (binary)

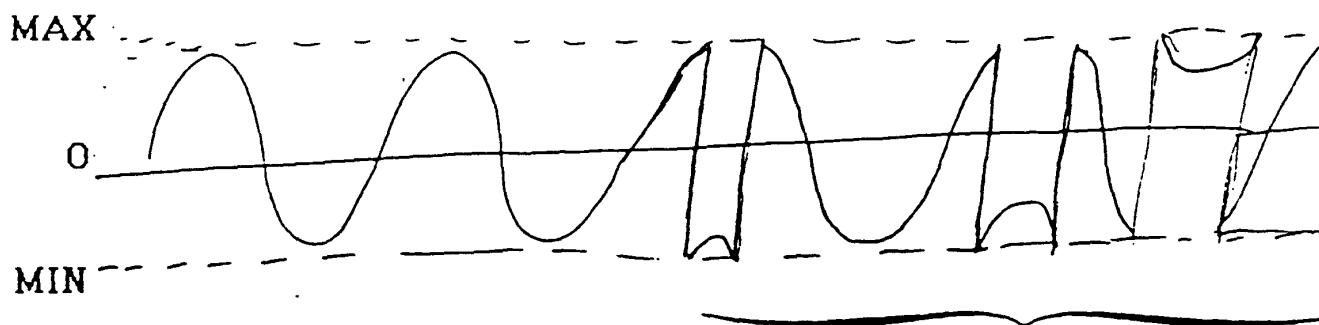
| n | 0 | 1 | 2 | 3 | 4 | 5 | 6 | 7 |
|-----------------|-------|-------|-------|-------|-------|-------|-------|-------|
| (binary) $y(n)$ | 1.000 | 0.110 | 0.101 | 0.100 | 0.011 | 0.010 | 0.010 | 0.010 |



LIMIT CYCLE
BEGINS IN IMPULSE
RESPONSE

OVERFLOW OSCILLATION =
"Chain reaction" of overflows in a recursive
filter

EXAMPLE: TYPICAL 2'S COMPLEMENT
WRAP-AROUND



WRAP-AROUND UPON
OVERFLOW PRODUCES
INCREASED SIGNAL
POWER. FED-BACK EXTRA
POWER CAN CAUSE
FURTHER OVERFLOW.

PASSIVE ARITHMETIC

If a nonlinear operation such as round-off or overflow cannot increase signal power, relative to the linear ideal, then limit cycles and overflow oscillations cannot be introduced by these nonlinearities.

ACOUSTIC TUBE VARIABLES

$P = P^+ + P^-$ = Physical pressure (or
voltage, E field, force)

$U = U^+ + U^-$ = Volume velocity (current,
B field, displacement)

X^+ = Right-going traveling-wave
component of X

X^- = Left-going traveling-wave component of X

Z = Characteristic impedance of propagation medium

FUNDAMENTAL INSTANTANEOUS RELATIONS

- o Ohm's Law (for unidirectional traveling waves)

$$P^+ = Z U^+$$

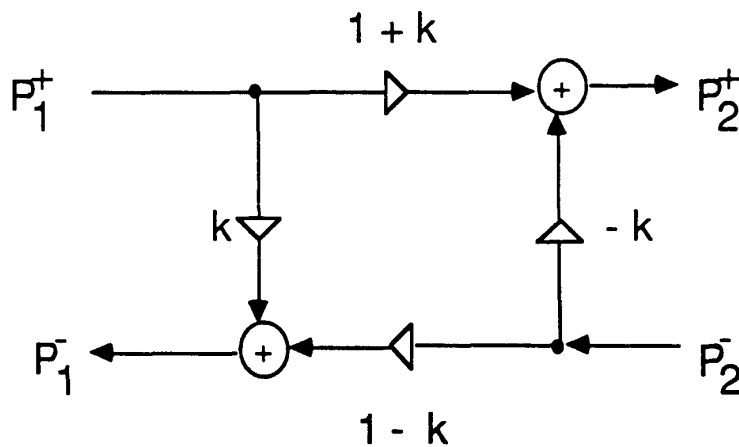
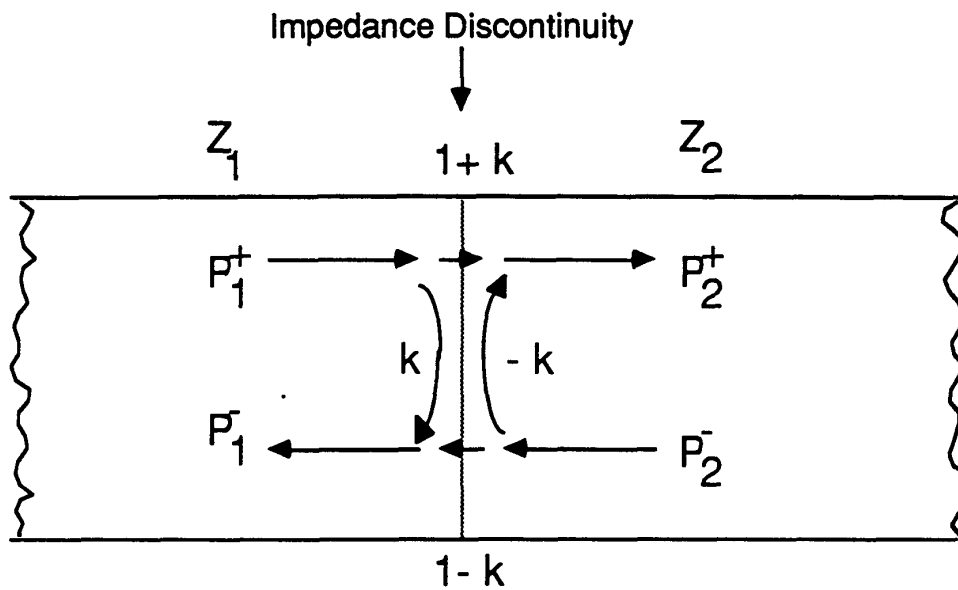
$$P^- = -Z U^-$$

- o Signal Power

$$I = P U = P^+ U^+ + P^- U^- = \frac{|P^+|^2}{Z} - \frac{|P^-|^2}{Z}$$

- o Signal power is INSTANTANEOUS with respect to space and time

Digital Cascade Waveguide Network Simulation



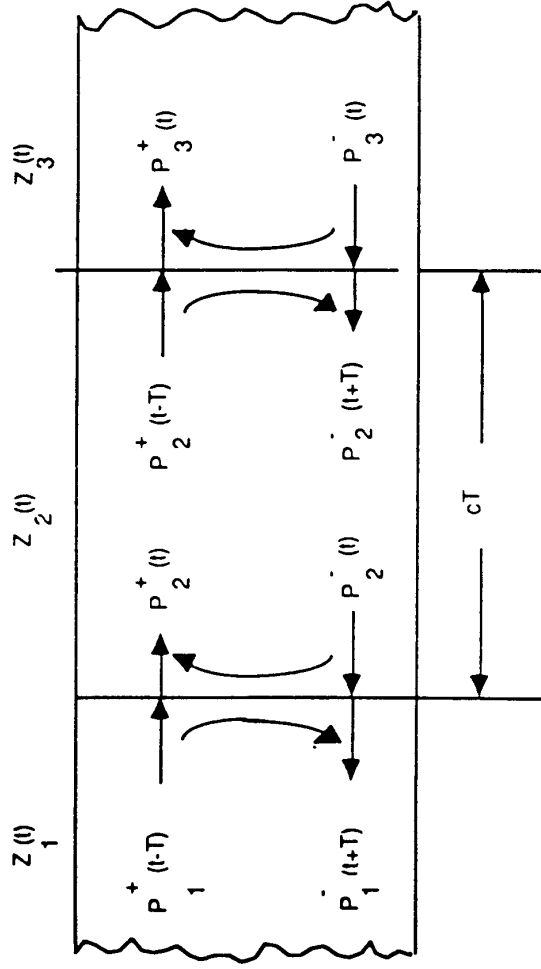
$$k = \frac{Z_2 - Z_1}{Z_1 + Z_2} = \text{Reflection Coefficient}$$

$$P_1 = P_1^+ + P_1^- = \text{Pressure in Section 1}$$

$$I_1 = \frac{|P_1^+|^2 - |P_1^-|^2}{Z_1} = \text{Instantaneous Power in Section 1}$$

Must Bound I_2

WAVEGUIDE VARIABLES



$P_1^+(t)$ = Right-going traveling pressure at left of section i

$P_1^-(t)$ = Left-going traveling pressure at left of section i

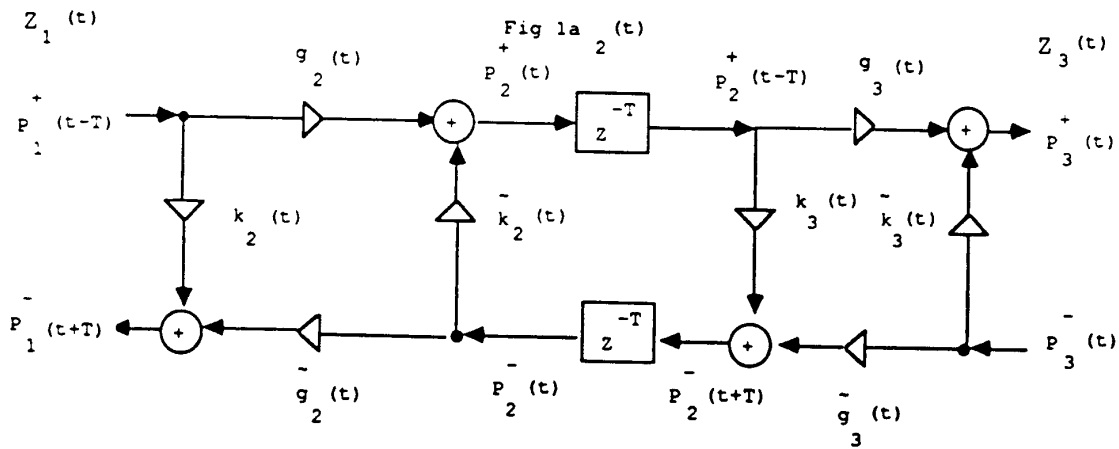
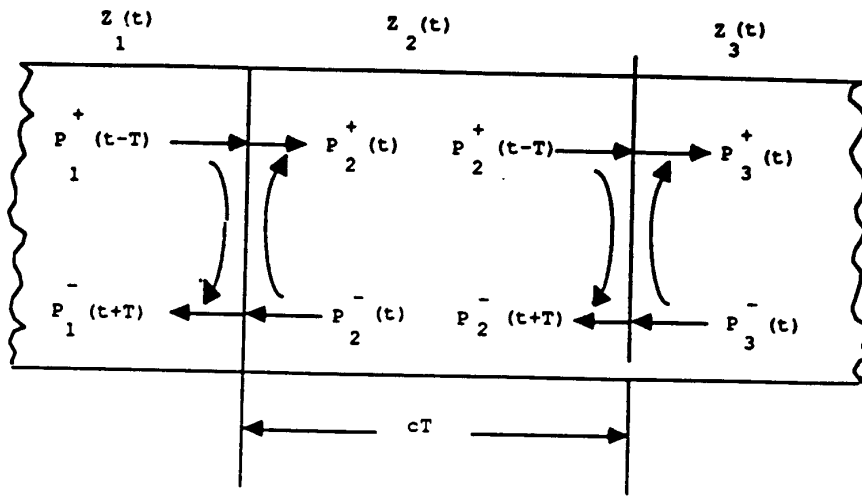
WAVEGUIDE VARIABLES (cont'd)

$$P_i(t) = P_i^+(t) + P_i^-(t) = \text{Physical pressure at left of section } i$$

$Z_i(t)$ = Characteristic impedance of section i

$$k_i(t) = \frac{Z_j(t) - Z_{i-1}(t)}{Z_j(t) + Z_{i-1}(t)} = i \text{ th reflection coefficient}$$

Digital Simulation of Waveguide Section



RELATION TO WAVE DIGITAL FILTERS (WDF)

- o Different only in theoretical derivation
- o WDF digitizes RLC networks
- o WGF digitizes transmission-line networks
- o WDF models system of differential equations at 3 frequencies (0,f,infinity)
- o WGF models wave propagation in lossless media having spatially discrete changes in characteristic impedance
- o WDF digitizes frequency variable via the bilinear transform (Trustin)

RELATION TO WAVE DIGITAL FILTERS (WDF) (continued)

WGF digitizes frequency variable via matched z
(impulse invariant)

o WDF wave variables are $P+ZU$ and $P-ZU$

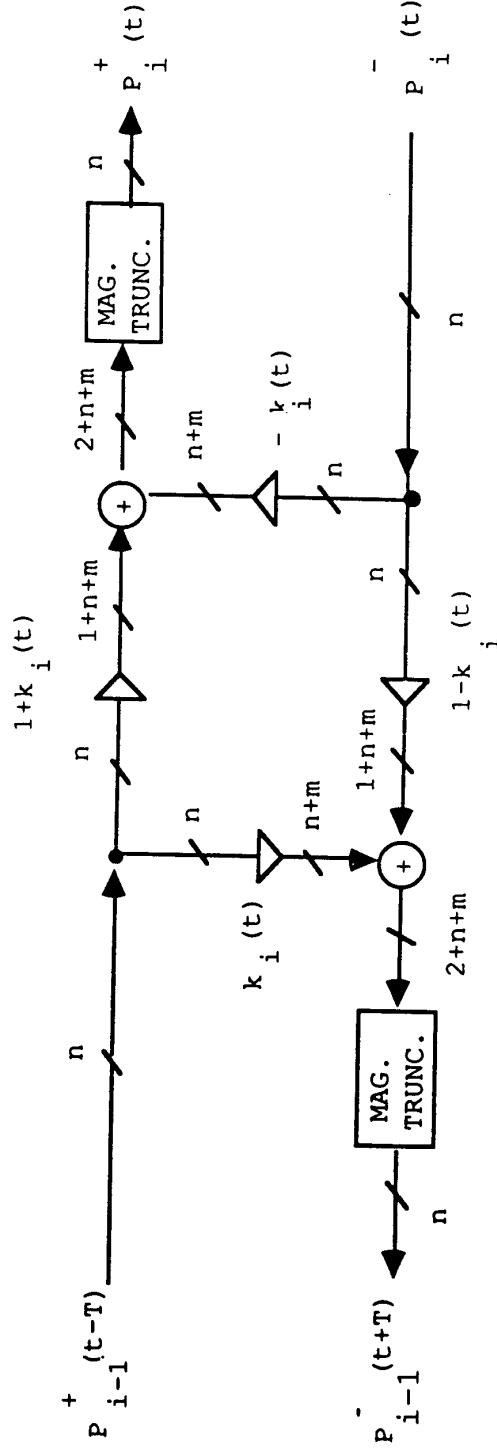
WGF wave variables are P^+ and P^-

o WDF is valuable for utilizing mature literature in
analog filter design

WGF formulation is clearer for physical interpretation

Ensuring Passive Scattering

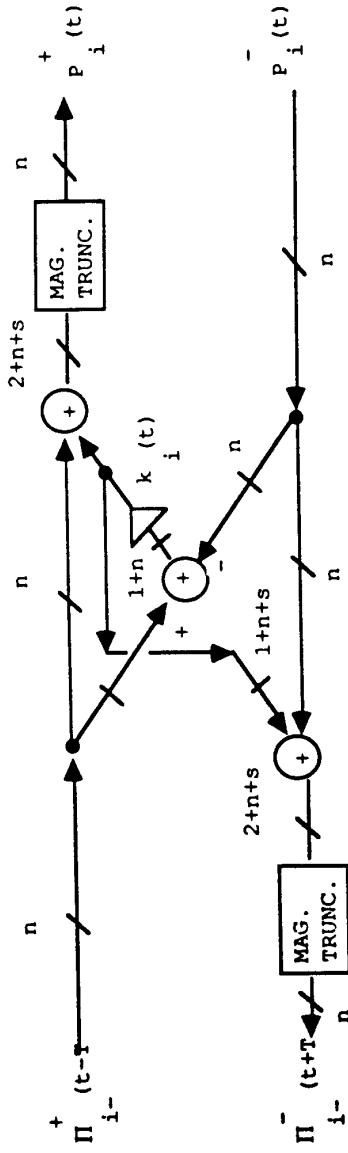
- Sufficient to ensure outgoing waves do not increase in magnitude as a result of round-off or overflow
- Strategy:
 - Extend internal precision
 - Magnitude truncation on outgoing waves



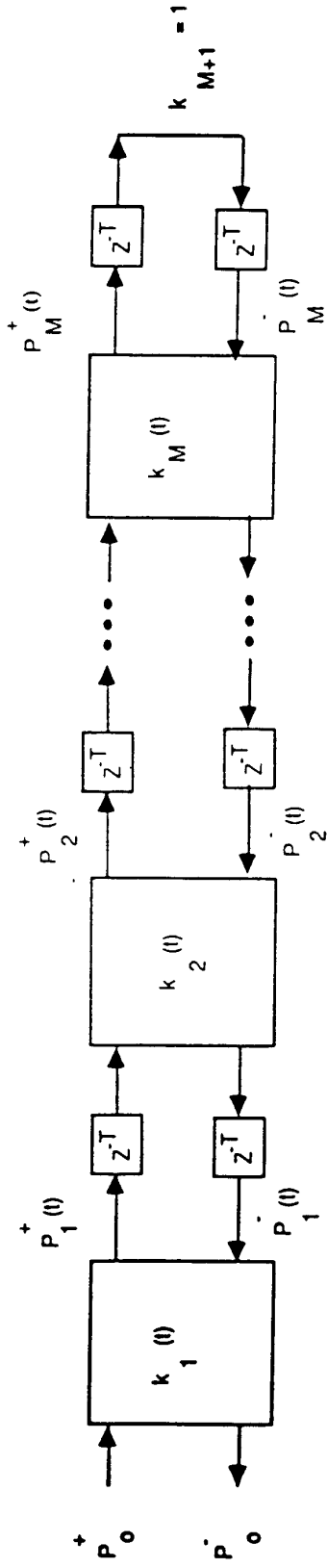
n = number of signal bits

m = number of reflection-coefficient bits

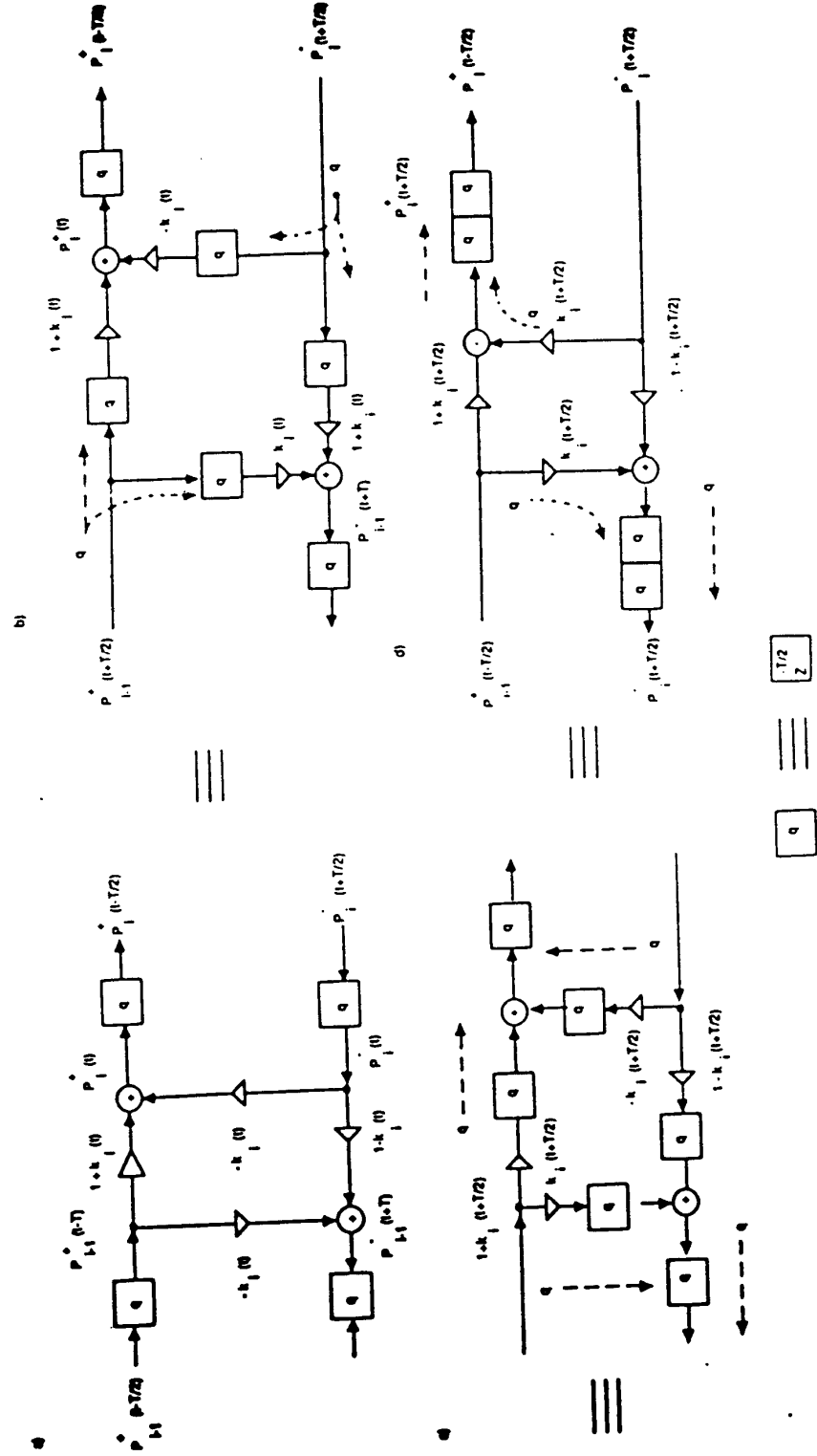
Passive One-Multiply Junction



THE WAVEGUIDE FILTER (WGF) STRUCTURE

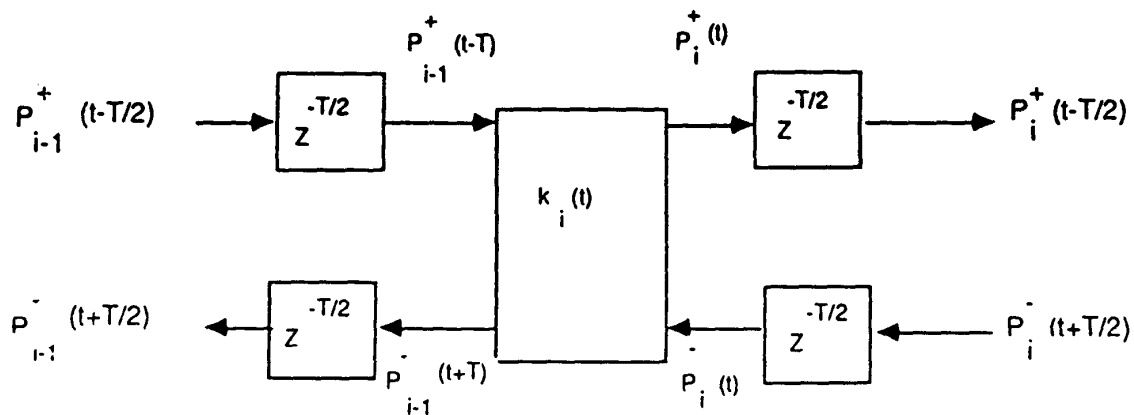


PUSHING DELAYS THROUGH TIME-VARYING JUNCTIONS

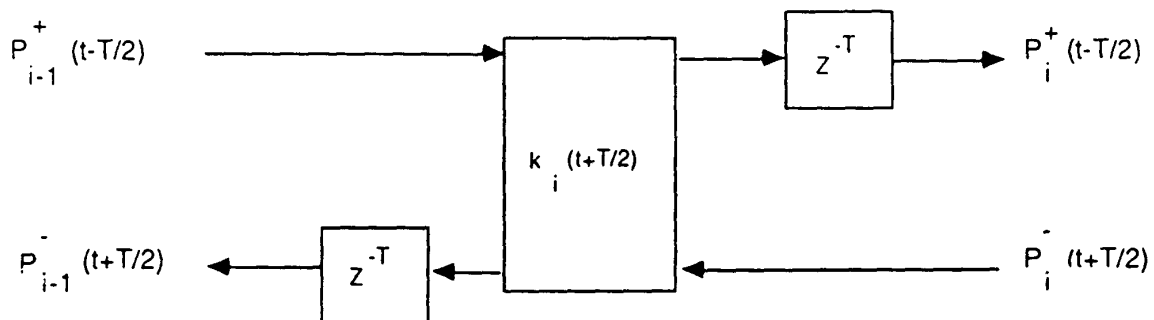


EQUIVALENT SECTIONS

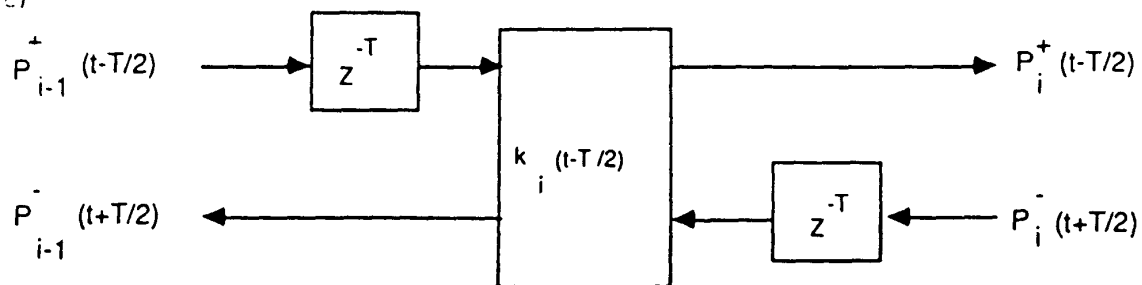
a)



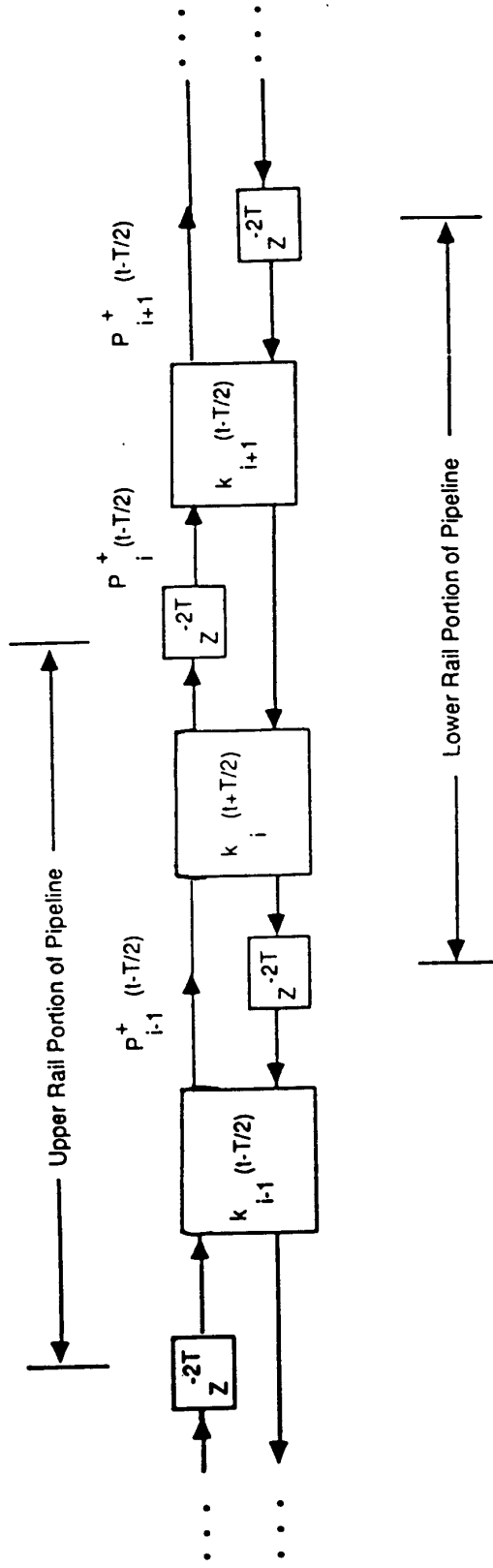
b)



c)

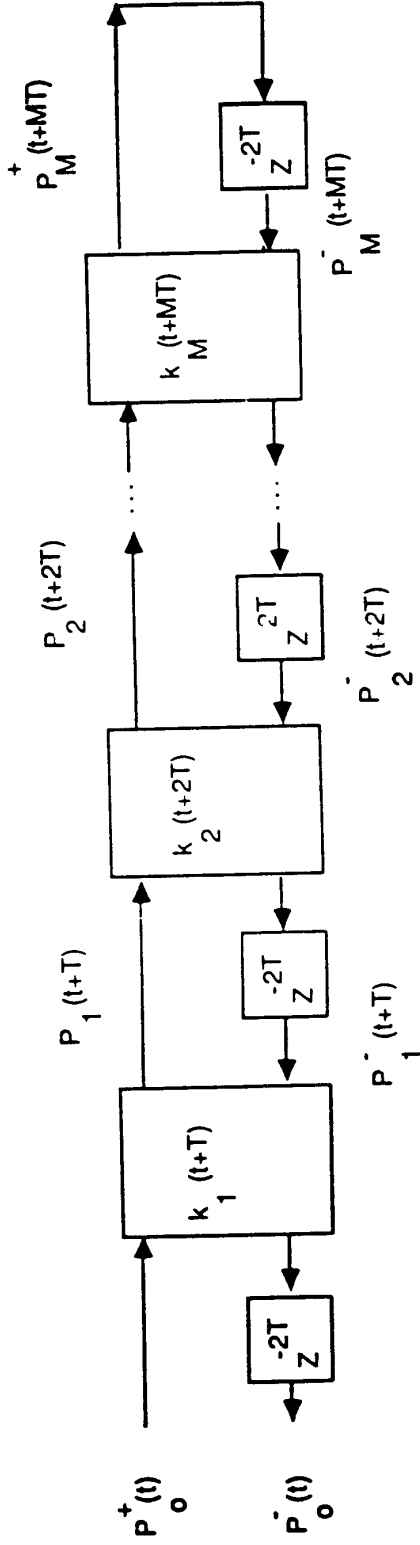


A USEFUL INTERMEDIATE WGF STRUCTURE



- o Number of delays halved as in conventional lattice
- o Reflective termination NOT required (can extend physically)
- o Pipeline segment size is two sections

CONVENTIONAL LADDER/LATTICE STRUCTURE



- o Half as many delays, each a section round-trip time in length
- o No delays along top path => cannot feed output to input
- o Reflective termination REQUIRED (Rightmost impedance = zero or infinity)
(Cannot add sections on the right)
- o Cannot pipeline

Time-Varying Physical Simulation by WGF Structures

1. Impulse Invariant Simulation
 - Physical input signal = linear combination of IMPULSES arriving at multiples of the sampling period T .
 - Characteristic impedance can change any time while an impulse is between scattering junctions (i.e. almost any time).
 - Impulse effectively samples the physical network at the sampling instants.
 - Time-varying physical network is exactly simulated at the sampling instants

TIME-VARYING PHYSICAL SIMULATION BY WGF STRUCTURES (continued)

2. Bandlimited Simulation

- Physical input signal is bandlimited to $1/2T$ Hz. Delay sections are sampled at all multiples of T sec.
- Signal bandwidth is increased by reflection-coefficient modulation.

$$BW(\text{reflection}) = BW(\text{incident signal}) + BW(\text{coefficient})$$

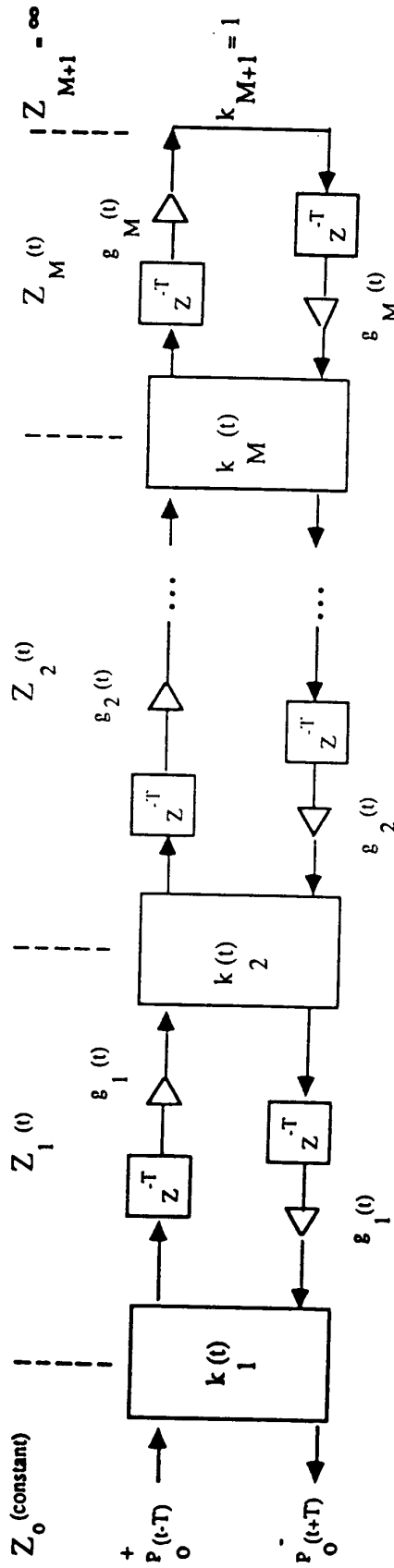
- Persistent time variation yields infinite bandwidth growth!
If stable, bandwidth expansion \Leftrightarrow attenuation
- Bandwidth expansion beyond Nyquist limit \Rightarrow aliasing
- Aliasing does not affect instantaneous signal power accounting

THREE NORMALIZATION STRATEGIES

- 1. Waveguide normalization - Correct for power modulation upon delay exit**
- 2. Wave normalization - Propagate rms-normalized waves**
- 3. Transformer coupling - Change impedance w/o scattering at delay exit**

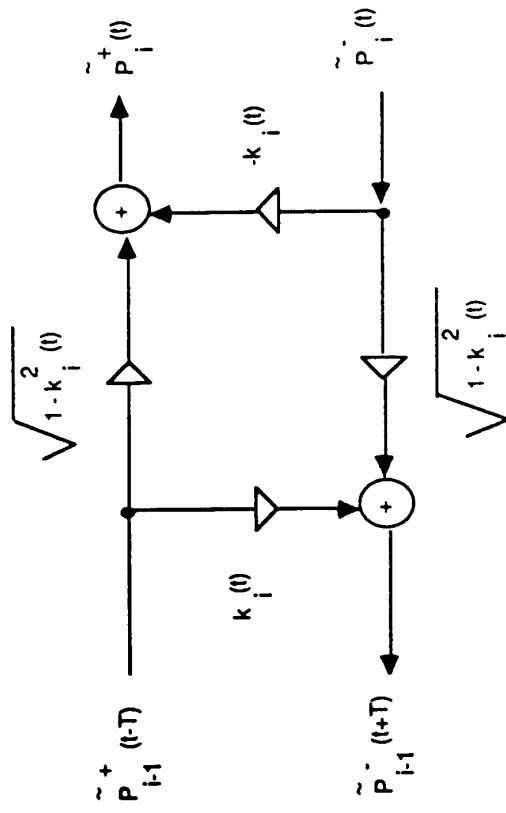
Result: 2 and 3 are equivalent

WAVEGUIDE NORMALIZATION

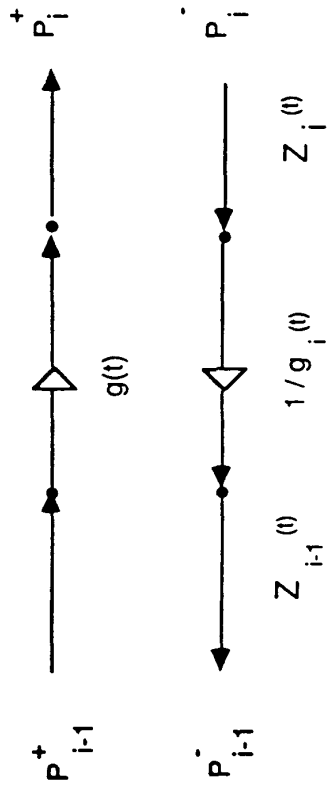


$$P_i^{(-)}(t+T) = \sqrt{Z_i(t) / Z_{i-1}(t-T)}$$

WAVE NORMALIZATION



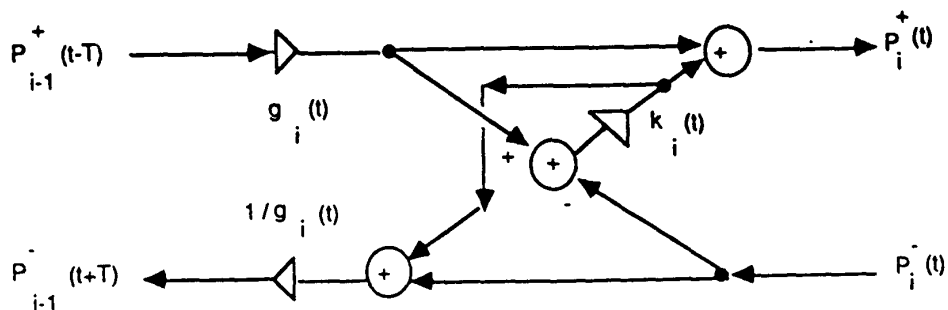
TRANSFORMER COUPLING



$$g_i^{(0)} = \sqrt{Z_i^{(0)} / Z_{i-1}^{(0)}}$$

EQUIVALENCE OF WAVE NORMALIZATION AND TRANSFORMER COUPLING

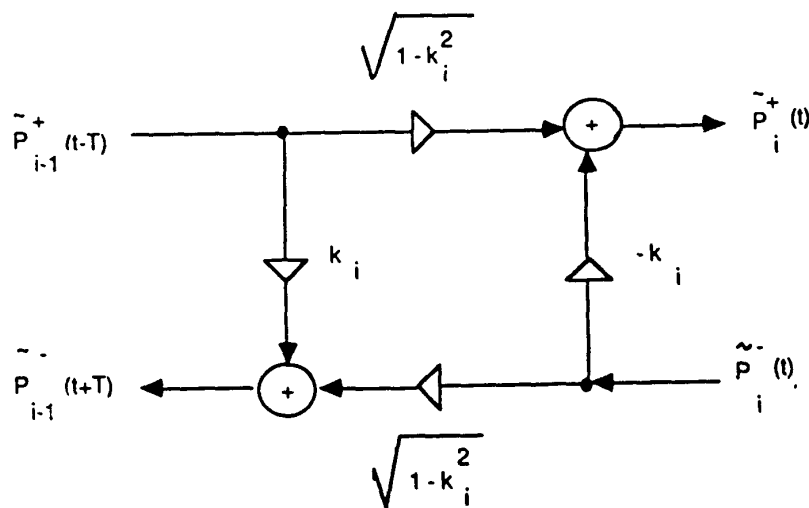
a)



$$g_i(t) = \sqrt{\frac{1 - k_i(t)}{1 + k_i(t)}}$$



b)



DRAFT
5/28/87
108

Waveguide Digital Filters

Julius O. Smith III

*Center for Computer Research in Music and Acoustics (CCRMA)
Department of Music, Stanford University
Stanford, California 94305*

Abstract

Digital filters are derived by sampling lossless propagation through a network of ideal "waveguides." Sampled waveguide networks provide numerically robust time-varying filter structures which we call "WaveGuide Filters" (WGF). After demonstrating the numerous desirable properties of WGF structures, widely used filter structures (such as lattice and ladder filters used in speech modeling) are derived as a special case. It is then clear under what conditions prevalent filter structures inherit these desirable properties.

One desirable property of waveguide filters is that *signal power* can be *decoupled* from changes in the filter parameters. WGF structures can be "balanced" such that decoupling between signal power and time-varying filter coefficients is maintained for each individual section in the structure. (A "section" is a length of ideal waveguide material with a single characteristic impedance.)

Numerical round-off effects are easily controlled in WGF structures. For example, it is simple to *suppress limit cycles and overflow oscillations*, even in the time-varying case. This is accomplished by using "passive" arithmetic; the exact physical interpretation of signals in a WGF makes it clear how define passive arithmetic.

Finally, WGF structures can be *interconnected in cascade or in parallel* without disturbing the signal/coefficient decoupling, signal power balance, or roundoff passivity properties. Thus, waveguide filters are very useful for *modeling physical systems*, and the exactness of their physical interpretation enhances their suitability for the time-varying case. These more elaborate physical modeling networks do not reduce to presently well-known filter structures.

Waveguide Digital Filters

Table of Contents

| | | |
|----|---|----|
| 1. | Introduction | 2 |
| 2. | Related Prior Work | 5 |
| | 2.1. Wave Digital Filters | 5 |
| | 2.2. Ladder and Lattice Filters | 7 |
| | 2.3. Synthesis and Approximation | 10 |
| 3. | Traveling Waves and Lossless Scattering | 10 |
| | 3.1. Three Fundamental Constraints | 11 |
| | 3.2. Reflection at a Junction | 16 |
| | 3.3. α -parameters | 19 |
| | 3.4. Reflection Coefficients | 22 |
| | 3.5. Pure Delays and Multi-Junction Networks | 22 |
| 4. | Cascade Waveguides | 27 |
| | 4.1. The Two-Port Junction | 27 |
| | 4.2. The Scattering Matrix | 29 |
| | 4.3. The Chain-Scattering Matrix | 30 |
| | 4.4. The One-Multiply Scattering Junction | 30 |
| | 4.5. The Normalized Scattering Junction | 32 |
| | 4.6. The Three-Multiply Normalized Scattering Junction | 34 |
| | 4.7. The Two-Port Delay Line | 36 |
| | 4.8. Generalized Delay | 37 |
| | 4.9. The Two-Port Transformer | 37 |
| | 4.10. The Two-Port Dualizer (Gyrator) | 40 |
| | 4.11. The Normalized Time-Varying One-Multiply Junction | 42 |
| 5. | Signal Power in Lossless Waveguides | 43 |
| | 5.1. Instantaneous Propagating Power | 44 |
| | 5.2. Instantaneous Stored Power | 46 |
| | 5.3. Power Conservation at a Junction | 47 |
| | 5.4. Normalized Waves | 48 |
| | 5.5. Effects of Quantization on Scattered Power | 49 |
| | 5.6. Elimination of Limit Cycles | 50 |
| | 5.7. Dynamic Range Conservation | 51 |
| | 5.8. Energy Conservation with Quantization | 53 |
| 6. | Equivalent Forms in General Networks | 54 |
| | 6.1. Power-Equivalent Junctions | 55 |
| | 6.2. Impedance Scaling | 56 |
| | 6.3. Equivalent Chains | 56 |
| | 6.4. Transformer Scaling | 57 |
| | 6.5. Generalized Transformer Equivalences | 57 |
| | 6.6. Delay Equivalences | 57 |
| | 6.7. (π, σ) -Parameters | 58 |

| | | |
|------|--|----|
| 6.8. | Nested Structures | 59 |
| 6.9. | Time Reversal | 59 |
| 7. | Conclusions | 60 |
| 8. | Appendix A—The Wave Equation | 60 |
| 9. | Appendix B—Norms | 61 |
| 9.1. | Discrete Norms | 63 |
| 9.2. | Matrix Norms | 64 |
| 10. | References | 65 |

The WGF structures are derived in the MIMO case (multiple inputs and multiple outputs).

1. Introduction

Digital filtering techniques have often been derived from classical or “analog” techniques [33]. Classical filter design has its roots in “network theory” for describing linear time-invariant systems accessed by means of “ports” [11]. Network theory itself is a body of mathematics built upon certain assumptions [7,14] which become true in the limit at low-frequencies according to Maxwell’s equations for electromagnetic propagation [9]. Thus, the theory of filters grew originally out of the scalar theory of wave propagation.

Since the emergence of digital techniques, little attention has been paid to the close correspondence between filter computations and physical law. In signal processing applications, we normally approximate directly some desired transformation of the signal spectrum, and a true physical modeling is irrelevant. This paper will show that much can be gleaned from taking a physical point of view with respect to digital filtering computations.

Most filtering applications have employed time-invariant filters which approximate an ideal *amplitude response* such as low-pass, high-pass, band-pass, or band-reject characteristics, or which provide a desired *phase response* such as in equalizers for communications channels [33]. In the time-invariant case, the amplitude response and phase response completely determine a linear filter [33]. For time-varying filters, there is no longer a simple description in terms of amplitude and phase response. (A frequency response requires time-invariance.) In many cases, time-varying filters have been developed in an ad hoc manner, being regarded as “quasi-static” in most cases. Such extensions require the assumption that the filter coefficients vary slowly relative to the impulse-response duration of the filter. When the coefficients change too rapidly, unnatural artifacts can occur due to the incompatibility between the

filter state (a function of all prior time in a recursive filter) and the new filter coefficients. The physical formulation of this paper allows precise accounting of stored signal energy even under time-varying conditions.

This Paper

This paper derives the class of linear, finite-order, recursive digital filters starting from structures which exactly simulate physical wave propagation in ideal linear media. We call them "Waveguide Filters" (WGF), because they can be interpreted as networks of intersecting waveguides or transmission lines. The WGF structures are closely related to the "wave digital filters" developed principally by Fettweis [19,32], the lattice filter structures arising in geoscience and speech modeling [54,36], and the "normalized ladder filter" discussed by Gray [34,47]. Waveguide filters have the following characteristics:

- The correspondence to physical wave-propagation systems is exact even though time is discrete. No bilinear transformation is necessary to connect digital quantities with physical quantities as is usual in the wave digital filter (WDF) context [19]. This allows a priori choice of filter structure to obtain precise models for physical processes.
 - The instantaneous power anywhere in the filter structure can be made invariant with respect to time-varying filter coefficient variations.
 - Generalized versions of the "Normalized Ladder," "One-Multiplier Lattice," and other ladder/lattice filters are derived, all having the provision for invariant instantaneous power in the time-varying case. The normalized one-multiplier lattice section turns out to be equivalent to the normalized ladder section yet less expensive computationally.
 - The structures can be coupled at a junction, cascaded, looped, or branched, to any degree of network complexity, and the desirable properties such as stability and power decoupling are retained. Prevalent ladder and lattice
-

filter are a small special case in the sense that they involve only cascaded waveguide sections.

- A synthesis procedure exists for realizing any digital filter transfer function by means of a WGF.
- There is an identification method for determining the coefficients of the WGF structure from measured input/output data. Similarly, there are "linear prediction" modeling techniques for these WGF's which provide ARMA models for time series.
- No overflow oscillations can occur, even in the time-varying case.
- No limit cycles (also called "granularity oscillations") can occur if one of many "passive" numerical round-off strategies is employed, even in the time-varying case. In the simplest case, the passive round-off strategy reduces to magnitude truncation (or truncation toward zero).
- As in the scalar lattice filter and WDF cases, sensitivity of coefficient quantization can be minimized by properly scaling the network to deliver "maximum power transfer" at frequencies where low sensitivity is required [62].
- The desirable structural properties are derived for multi-input, multi-output (MIMO) transfer-function matrices.

The derivation of the WGF is made exceedingly simple by using three simple principles of wave propagation in an ideal linear medium. While such a derivation is highly classical in spirit, its use for deriving present-day digital filter structures appears to be new. We feel that this fundamental reformulation of digital filters is important for its tutorial value and for its impact on numerical issues, time-varying filters, and physical modeling.

2. Related Prior Work

This section reviews some of the most closely related work on digital filter structures. These include the orthogonal-polynomial filters of Szegö [2], the “lumped-distributed” filters analyzed by Youla et al. [23,24], the “wave digital filters” of Fettweis [18,19,22,32], the “ladder and lattice filters” of Markel and Gray [27,34,36,47], the “lossless bounded-real” formulation of Vaidyanathan [62,64,65,67], and the “orthogonal filters” of Dewilde [41,49,51]. Naturally, there are many more related lines of development, in view of the first law of signal processing.* These represent only the major recent areas closest to our point of view.

In the following subsections, some of the closest connections between the above work and waveguide formulation presented here are examined.

2.1. Wave Digital Filters

The wave digital filter (WDF) approach of Fettweis [18,19,22,32] comes closest to the point of view taken in this paper. Fettweis obtains a similar class of structures by use of the classical notion of *wave variables* [14].

For example, if v and i denote the voltage and current at a terminal of an N -port network, the wave variables are defined by $x = v + Ri$ and $y = v - Ri$, where R is an arbitrary “reference impedance” [39]. These wave variables are logically equivalent to the left-going and right-going “pressure traveling waves” considered in this paper, and R plays the role of characteristic impedance in the associated transmission line.

Fettweis describes how to directly model resistors, capacitors, inductors, transformers, gyrators, and circulators using the WDF approach, and he describes the necessary rules for connecting ports together [19]. The modeling of a capacitor, for example, is accomplished by scaling the reference impedance R until the capacitor

* The first law of signal processing is “Everything is equivalent to everything else.”

“reflectance” is exactly a unit-sample delay. (The model is parametrized in frequency so that the wave variables are really phasors.) An inductor also maps to a unit-sample delay but with a sign-change relative to a capacitor. A complete circuit is built out of basic elements by means of “adaptors” [32] which play the role of the junctions or scattering layers described in this paper; the adaptor accomplishes interconnection of ports at different reference impedances.

The WDF modeling of inductors and capacitors is limited because the continuous-time frequency variable is mapped to the discrete-time frequency variable via the bilinear transform. If the points $z = 1$ and $z = -1$ in the complex plane are identified with zero and infinite continuous-time frequencies, respectively, then only one more mapping frequency (say ψ) can be chosen. Thus, the bilinear transformation provides exact modeling only at the three frequencies: 0, ψ , and ∞ .

The WDF formulation models a system of differential equations at three frequencies, while the WGF formulation exactly models wave propagation in lossless media having spatially discrete changes in characteristic impedance. Consequently, in our formulation, a wave variable may be a “voltage” or “current” or a linear combination of the two without incurring realizability problems [39]. This is a considerable conceptual simplification for applications to physical modeling.

Another way of stating the comparison between WDF and WGF formulations is that WDF's are derived from *lumped* circuit elements (R,L,C) while WGF's are derived from *distributed* circuit elements (intersecting waveguide sections). Both formulations employ a scattering theory point of view.

A general result in this paper is that overflow oscillations and limit cycles can be suppressed in *all forms* of scattering-type filter structures simply by using extended numerical precision in each scattering section, saving quantization (toward zero) for the final outgoing waves. The basic principles involved apparently appeared first in the WDF context [30,47]. The level of generality for these results in this paper appear to exceed that in the literature thus far.

2.2. Ladder and Lattice Filters

For some time it has been known that lattice and ladder filtering structures are superior to the so-called direct form in several ways. These include reduced sensitivity to coefficient quantization, less effect of round-off noise on the filter frequency response, ease of stability checking, reduced probability of limit cycles or overflow oscillations, and section-wise orthogonality in the linear prediction context [36]. For a discussion of ladder and lattice filters in adaptive estimation, see [54].

Lattice structures have been in use for decades in directly modeling layered scattering media. The mapping of underground striations in rock density, for example, is a basic diagnostic tool in oil exploration. The interface between two subterranean layers of rock of different densities produces a scattering layer because the characteristic impedance of the medium with respect to sound propagation changes across such a boundary.

Another example of the use of lattice structures for physical modeling is the "acoustic tube" models developed for speech analysis and synthesis. In this case, the vocal tract is modeled as a cascade of coaxial cylindrical tubes with varying cross-sectional areas and equal length. The change in area from one tube section to the next provides a change in the characteristic impedance of the air column for sound propagation, and so a series of equally spaced scattering layers is obtained.

Apparently, the filter structures developed in the above applications are only as general as a single chain of scattering layers with one input and one output, and the input and output sections are terminated in a non-extendable way. Little if any work has explored branching and intersecting chains of scattering layers. In the case of speech, the use of a separate acoustic tube branching off from the vocal tract to model the nasal tract would obviously be very natural. Apart from branching, it is not possible to continue the structures in common use from the output section to a larger section. This is because the typical arrangement is to assume a perfectly reflecting termination at the output. Such a termination cannot be followed by an added termination in a physically meaningful way. Perfectly reflecting terminations

also allow the delays in the scattering network to be moved around and combined in pairs such that the required signal sampling rate is reduced by a factor of 2 (see §3.5). We have found that the cascade scattering chains, which dominate the recent literature, can be immediately extended to general acyclic trees with the same basic properties.

Our formulation is more general than even the acyclic-tree extension of prevalent lattice filters in that arbitrary networks can be constructed (i.e., cycles in the network graph are allowed). Also, there does not seem to be an existing treatment of multi-input, multi-output (MIMO) systems from the acoustic waveguide point of view.

A particularly important antecedent to the normalized WGF in the speech processing literature is the normalized ladder filter (NLF) developed by Gray and Markel [27,34,47]. Gray considered only the single-input, single-output (SISO) all-pole case. (Zeros are obtained in the NLF using “taps,” which leads outside the class of structures considered here.) Their approach was based on orthonormal-polynomial expansion [1,2,6] which is closely connected with *linear prediction* theory [36]. They showed the following to be true:

- The NLF is optimal in the sense that each internal node has unity power gain. This means, for example, that the response to a unit impulse cannot overflow anywhere within a stable NLF filter. Also, if the input signal is white noise with unit variance, the variance of the signal at each internal node is exactly unity [34].
 - The NLF is stable in the case of time-varying filter parameters [34] as long as the “reflection coefficients” $k_i(t)$ are always less than or equal to some $K < 1$ in magnitude. ($|k_i(t)| < 1$ is not sufficient for bounded-input, bounded-output (BIBO) stability unless the input signal energy is finite.) It was derived incidentally that the total energy entering the ladder eventually “exits” through the particular delay element at the entrance to the ladder.
 - The NLF has superior roundoff noise properties, especially when poles are
-

clustered close together and/or close to the unit circle [34].

- The NLF is free of zero-input overflow oscillations [47].
- The NLF is free of zero-input limit cycles [47] in magnitude-truncation arithmetic.

The NLF is obtainable by transformations of a special case of the WGF structures derived here. The most significant difference is in the distribution of delay elements. We will show that delay distribution in the usual NLF is not obtainable from a WGF unless the waveguide is terminated by a pure reflection. This means, for example, that an NLF cannot be connected to another NLF to build a larger waveguide system with finite loading from one stage to the next. Also, the delay distribution chosen for the NLF is such that creating a loop with NLF's yields a degenerate (non-computable) structure because a delay-free loop appears. Another limitation of the NLF is that the concept of instantaneous power becomes artificial for individual sections (although Gray defines a non-physical but similar quantity in [47, eq. (2)]).

A disadvantage of the NLF is that it requires four multiplications per pole of the filter transfer function. The one-multiplier lattice filter, on the other hand [36] requires only one multiplication per pole. Conceptually, the four-multiply NLF results from normalizing the propagated variable, say P^+ , to units of *root-power*, $\tilde{P}^+ = P^+ / \sqrt{Z}$. We will show how to use a (two-multiply) *transformer* to cancel the signal power modulation of an ordinary one-multiplier lattice section (in the time-varying case). By elementary graph manipulations, it is shown that the two forms are equivalent, i.e., the normalized one-multiplier form is in fact a three-multiplier NLF.

This paper describes how power-normalization, perfect energy conservation, and complete suppression of limit cycles and overflow oscillations can be guaranteed for MIMO analogues of *all* ladder and lattice filter structures, with extensions to branching structures and general terminations.

For the case of reflectively terminated, time-varying, MIMO, acyclic trees, (which specialize to ordinary lattice/ladder structures in the SISO single-branch case), we derive efficient equivalent structures in which the delays are moved and combined to yield computational savings without loss of the desired power-invariance or numerical properties.

2.3. Synthesis and Approximation

The synthesis procedure we use for the WGF is based on the Schur algorithm which recursively computes a solution to the Nevanlinna-Pick problem [49,44,52]. The Nevanlinna-Pick problem is to interpolate a rational Schur function* through n complex values at n points in the closed unit disk in the complex plane. The Schur algorithm has also been called the “Nevanlinna recursion scheme” [52]. In other contexts, a special case of the the Schur algorithm, which computes only all-pole digital filters, has been called the “Durbin” [8] or “Levinson” [3] algorithm [41,49,51,46,36]. The complete Schur algorithm constructs a cascade WGF realization of a digital filter containing both poles and zeros.

The estimation problem has been addressed by DeWilde [49,51]. In this context, the Schur algorithm provides an ARMA estimation technique in which the pole estimates are optimal in the mean square sense for the given fixed zeros which are chosen a priori.

3. Traveling Waves and Lossless Scattering

For concreteness of discussion, we will focus on *pressure* and *flow waves* in a lossless, linear, *acoustic tube*. We could just as easily think of the electric and magnetic components of light, voltage and current in a transmission line, or force

* A *Schur function* $S(z)$ is defined as a complex function analytic and of modulus not exceeding unity in $|z| \leq 1$

and transverse velocity on a vibrating string. An analysis of the acoustic tube is discussed by Markel and Gray [36] and Flanagan [21] in the context of vocal-tract modeling. Further details on the acoustics of sound in tubes can be found in Morse [4]. The term “waveguide” will be used interchangeably with “acoustic tube.”

A derivation of traveling waves from the basic *wave equation* is presented in Appendix A. The result is that in a cylindrical acoustic tube, longitudinal[†] pressure and flow waves propagate back and forth with speed c . Let x denote distance along the tube axis and let t denote time in seconds. Then the instantaneous pressure $P(x, t)$ and flow $U(x, t)$ is given by the sum of the left-going and right-going traveling-wave components:

$$P(x, t) = P^+(x, t) + P^-(x, t) \quad (1a)$$

$$U(x, t) = U^+(x, t) + U^-(x, t) \quad (1b)$$

3.1. Three Fundamental Constraints

The behavior of waves traveling unidirectionally in a lossless medium is governed by three laws: (1) the pressure is proportional to flow, (2) the pressure is a continuous function of position, and (3) the flow variable (e.g. mass or charge) is neither created nor destroyed in the medium.

Characteristic Impedance

An ideal linear propagation medium is completely determined by its charac-

[†] We assume the tube radius is much smaller than the wavelength of sound in the tube, so that pressure and flow are constant over any cross-section of the tube normal to the axis. In other words, waves do not propagate up and down but only left and right. For more details on the assumptions involved in acoustic tube models, see Flanagan [21].

teristic impedance[‡] $Z(x, t)$. The *characteristic impedance* is defined as the constant of proportionality between pressure and flow in a unidirectional traveling wave:

$$P^+ = ZU^+ \quad (2a)$$

$$P^- = -ZU^- \quad (2b)$$

In “lumped” circuit theory [7], (2) is called *Ohm's Law*. When the arguments (x, t) are omitted, it is understood that all quantities are written for some constant time t and position x . The minus sign for the left-going wave P^- accounts for the fact that flows in opposite directions subtract while pressure waves passing through each other add.

We will consider initially a more general situation in which $Z = Z(d)$ is a q by q complex matrix function of the complex variable (or unit-delay operator) d . For stability of propagation in the waveguide, we require that $Z(d)$ be analytic for $|d| \leq 1$. The results also extend to the case of vector $\underline{d}^T = [d_1, \dots, d_K]$, but we will treat only one complex argument d for notational simplicity. The pressure and flow variables are q by m matrix complex functions of d . However, keep in mind that the physical analogy we are pursuing is for the case of real scalar Z , P , and U .

[‡] For an acoustic tube, the characteristic impedance is given by $Z = \sqrt{P_0 \gamma_c \rho} / S = \rho c / S$, where ρ is the density (mass per unit volume) of air in the tube, c is the speed of propagation, P_0 is ambient pressure, γ_c is the ratio of the specific heat of air at constant pressure to that at constant volume, and S is the cross-sectional area of the tube. In a vibrating string, $Z = \sqrt{T \rho} = \rho c$, where ρ is string density (mass per unit length) and T is the tension of the string. In an electric transmission line, $Z = \sqrt{L/C} = Lc$ where L and C are the inductance and capacitance, respectively, per unit length along the transmission line. In free space, $Z = \sqrt{\mu_0 / \epsilon_0} = \mu_0 c$, where μ_0 and ϵ_0 are the permeability and permittivity, respectively, of free space.

For lossless propagation in the scalar case, the characteristic impedance Z must be real. In the matrix-delay-operator case, lossless propagation will now be characterized by the requirement that Z be *para-Hermitian*, i.e.,

$$Z_*(d) = Z(d) \quad (3)$$

where

$$Z_*(d) \triangleq \overline{Z(1/\bar{d})}^T \quad (4)$$

denotes the *para-Hermitian conjugate* of $Z(d)$ [14,49], $(\cdot)^T$ denotes transposition, and $(\bar{\cdot})$ denotes complex conjugation. For $d = e^{j\theta}$, $Z_*(e^{j\theta})$ coincides with the Hermitian transpose of $Z(e^{j\theta})$. The para-Hermitian conjugate is the unique analytic continuation (when it exists) of the Hermitian transpose $Z_*(e^{j\theta}) = \overline{Z(e^{j\theta})}^T$ from the unit circle into the complex plane. Thus, a lossless medium in our framework is defined as one in which the characteristic impedance is para-Hermitian. The extension to vector \underline{d} is obtained by regarding $Z(\underline{d})$ as K functions of scalar complex variables d_i . Note that in the scalar case, Z para-Hermitian implies $Z = \bar{Z}$ which implies Z is real. Henceforth, we assume Z denotes a para-Hermitian characteristic impedance. For non-para-Hermitian Z , (2) should be modified to read $P^- = -Z_*U^-$ [14], and a passive medium is one in which $Z + Z_*$ is positive semi-definite.

It is worthwhile to interpret the various levels of extension we are considering for the characteristic impedance Z . When Z is real and scalar, we obtain exactly the ideal behavior of one dimensional traveling waves in a lossless medium. Extending to q by q matrix characteristic impedances facilitates development of multi-input, multi-output (MIMO) systems which have the desired numerical and power-invariance properties. The extension to analytic matrix functions of a complex variable provides a generalized scattering medium whose reflectance and transmission coefficients are themselves rational transfer function matrices. This provides for nesting of the WGF structures. The complex argument d of the characteristic impedance is interpreted as a unit-delay operator, and the meaning of the characteristic impedance is attached to its Laurent series expansion with respect to the unit circle in the d -plane (a polynomial in the delay operator d). Additional

complex variables d_i in the arguments to the characteristic impedance allow the generalized scattering layer to perform filtering in several domains such as time and space. Since the characteristic impedance is assumed stable and para-Hermitian, all delay-operator impedance matrices must be nonrecursive and zero-phase. Therefore, computability, stability, and nonlinear oscillation problems do not arise in the case of multiple domains.

Pressure Continuity and Medium Conservation

We will be interested in the situation wherein the characteristic impedance changes abruptly from one value to another, say from Z_1 to Z_2 . The impedance discontinuity can be a sudden change along x in the acoustic tube, or it can be a change introduced at some time t (as needed for time-varying filters). Consider changes with respect to x . Given the traveling waves impinging on the junction between Z_1 and Z_2 , we seek formulas for the traveling waves leaving the junction. To solve this problem, we need two laws in addition to Ohm's law (2) for an ideal wave medium:

- 1) Pressure cannot change instantaneously across the junction (5a)
- 2) The sum of flows meeting at the junction is zero (5b)

A more general case which we call the "loaded-junction" case, is obtained by replacing the second constraint above by

- 2') The sum of flows meeting at the junction equals the exit flow

where the exit flow is used to perform work on some external dynamic system attached to the junction.

In the context of lumped circuit theory, the constraints (5) are called "Kirchoff's node equations". Equation (5b) expresses *conservation of flow* (the "continuity" equation), and equation (5a) follows from (5b) and *conservation of power*.

For changes in characteristic impedance with respect to time, (5) is not applicable. Time-varying characteristic impedances will be implemented using waveguide *transformers*, and will be used to obtain power-invariant lossless digital filters in the time-varying case.

Kirchoff's constraints (5) and Ohm's law (2) together determine what pressure and flow waves emerge from a junction between waveguide media of differing characteristic impedance, given the incoming waves.

Consider the case of N waveguides meeting at a loaded junction. Kirchoff's laws state that there can be only one resultant pressure P_J at the junction, and the sum of flows entering and leaving the junction must total to the exit flow. Thus, we have the constraints

$$P_1 = P_2 = \dots = P_N = P_J \quad (6a)$$

$$U_1 + U_2 + \dots + U_N = U_L = \Gamma_L P_J \quad (6b)$$

where

$$\begin{aligned} P_i &= P_i^+ + P_i^- & P_i^+ &= Z_i U_i^+ \\ U_i &= U_i^+ + U_i^- & P_i^- &= -Z_i U_i^- \end{aligned} \quad (7)$$

Z_i = Characteristic impedance of the i th waveguide (q by q)

$\Gamma_i = Z_i^{-1}$ = Characteristic admittance of the i th waveguide (q by q)

P_i^+ = Incoming pressure wave along the i th waveguide (q by m)

U_i^+ = Incoming flow wave along the i th waveguide (q by m)

P_i^- = Outgoing pressure wave along the i th waveguide (q by m)

U_i^- = Outgoing flow wave along the i th waveguide (q by m)

P_i = Instantaneous pressure wave in i th waveguide just outside junction (q by m)

U_i = Instantaneous flow wave in i th waveguide just outside junction (q by m)

P_J = Resultant pressure at the junction (q by m)

U_L = Resultant flow at the junction (q by m)

Γ_L = Admittance of the junction load (q by q)

(9)

Pressure Loaded versus Lossless Junctions

In most of what follows, the junction load admittance Γ_L will be taken to be zero, corresponding to a lossless waveguide junction.

An example in which Γ_L would not be zero would be the vibrating-membrane model consisting of a two-dimensional “mesh” of waveguides (propagating transverse velocity waves like ideal strings) on which ideal masses are placed at each mesh intersection to “load” the corresponding waveguide junction.

Note that the load admittance Γ_L is regarded as a *lumped driving-point admittance* [7], and the relation $U_L = \Gamma_L P_J$ is the usual form of Ohm's law. Γ_L would normally be defined over the analog s -plane and carried into the z -plane via the “matched- z ” transformation $z = e^{sT}$.

We should have $\Gamma_L \approx 0$ for frequencies near and above half the sampling rate. In other words, the dynamic response of the continuous-time junction load should be bandlimited to within half the sampling rate. Otherwise, Γ_L will contain aliasing error, and the junction response will not be true.

Γ_L should not vary too fast with respect to time. Time variation can cause aliasing of signals passing through the junction even when the load admittance itself is not aliased.

3.2. Reflection at a Junction

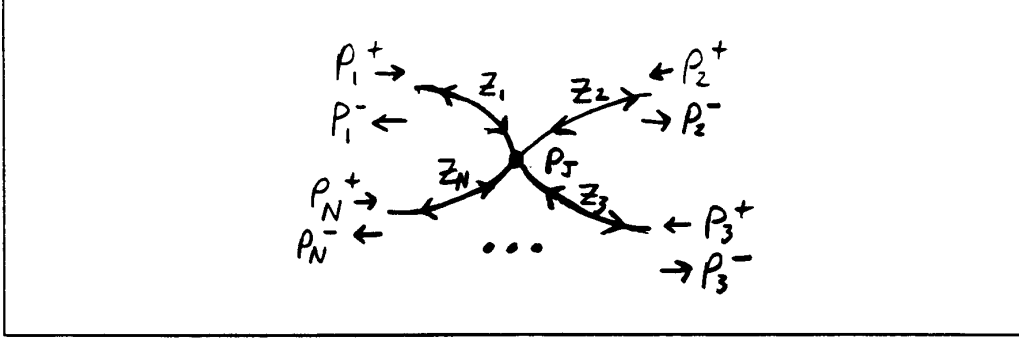


Figure 1. N -way parallel waveguide junction. Each waveguide is a bidirectional signal path (implemented by two “delay lines”).

Consider the “parallel” intersection of N waveguides at a common junction as shown in Fig. 1. Given a set of incoming traveling pressure waves, P_i^+ , $i = 1, \dots, N$, the constraints (2,6) determine the outgoing waves P_i^- as follows. As before, Z_i and hence $\Gamma_i = Z_i^{-1}$ are para-Hermitian positive definite. Substituting (1b), (2) solved for flow, and $P_i^- = P_J - P_i^+$ into (6b) yields the resultant junction pressure:

$$P_J = 2 \left(\Gamma_L + \sum_{i=1}^N \Gamma_i \right)^{-1} \sum_{i=1}^N \Gamma_i P_i^+ \quad (10)$$

From now until certain applications are discussed, we will consider only the unloaded-junction case $\Gamma_L = 0$. Thus, all waveguide junctions will be *lossless*.

Define

$$\Gamma_J \triangleq \sum_{i=1}^N \Gamma_i \quad Z_J \triangleq \Gamma_J^{-1} \quad U_J \triangleq 2 \sum_{i=1}^N \Gamma_i P_i^+ \quad (11)$$

define the *junction admittance*, *junction impedance*, and *junction flow*, respectively.

(In the extension to non-para-Hermitian Z_i , U_J becomes $U_J^+ = \sum (\Gamma_i + \Gamma_{i*}) P_i^+$.)

Relation (10) then reads $P_J = Z_J U_J$, or,

$$\text{Junction Pressure} = \text{Junction Impedance} \times \text{Junction Flow}$$

Since $\Gamma_i P_i^+ = U_i^+$, we have

$$U_J = 2 \sum_{i=1}^N U_i^+ \triangleq 2U^+ \Rightarrow |U_J| = |U^+| + |U^-| \quad (12)$$

where $|\cdot|$ denotes elementwise complex modulus. That is, the junction flow can be interpreted as the magnitude sum of the incoming and outgoing current waves.

Now, given incoming traveling waves P_i^+, U_i^+ and the characteristic impedance Z_i of each branch terminating at the junction, we easily find the outgoing waves P_i^-, U_i^- to be

$$P_i^- = P_J - P_i^+ \quad (13a)$$

$$U_i^- = -\Gamma_i P_i^- \quad (13b)$$

Equations (13) specify the scattering at the junction of N intersecting “waveguides,” given the incoming waves P_i^+ (or U_i^+) and the branch characteristic impedances Z_i .

In view of relations (2), we can consider only left-going and right-going pressure waves, since the flow waves can be readily computed from the characteristic impedance of the propagation medium. At this point, we could instead choose wave variables of the form $x_i = P_i + Z_i U_i$ and $y_i = P_i - Z_i U_i$ and proceed along the lines of classical wave filtering [14]. However, such a path is less fundamental in the present development because we are considering only discrete-time filters.

We have treated only a *parallel junction* of waveguides. A *dual* set of equations is obtained by considering a *series junction*. However, pressure waves intersecting in a parallel junction are equivalent to flow waves intersecting at a series junction. When using flow waves as the primary variables, (13b) can be written

$$U_i^- = U_i^+ - \Gamma_i P_J \quad (14a)$$

$$P_J = 2Z_J \sum_{i=1}^N U_i^+ \quad (14b)$$

The series pressure junction is obtained by taking the dual of (14). That is, replace U_i by P_i and Γ_i by Z_i to obtain

$$P_i^- = P_i^+ - Z_i U_J^s \quad (15a)$$

$$U_J^s = 2\Gamma_J^s \sum_{i=1}^N P_i^+ \quad (15b)$$

$$\Gamma_J^s = Z_J^{s-1} \quad (15c)$$

$$Z_J^s = \sum_{i=1}^N Z_i \quad (15d)$$

The junction impedance for a series junction is the sum of the branch impedances, while for a parallel junction, it is the parallel combination of the branch impedances (inverse of the sum of admittances).

Equations (13a) and (14a) are *computationally efficient* ways to implement an N -port scattering junction. In the case $N = 2$, the well-known one-multiplier lattice filter section (minus its unit delay) is obtained immediately from (13a). More generally, an N -way intersection requires N multiplies and $N-1$ additions to obtain P_J , and one addition for each outgoing wave, for a total of N multiplies and $2N-1$ additions. The dual junction (15) also requires N multiplies and $2N-1$ additions. In the next section, a method for trading one multiplier for another $N-1$ additions [32] is described.

3.3. α -parameters

One parametrization of all passive N -junctions is the set of N branch impedances with positive-definite para-Hermitian parts (cf. §5.1). This section describes another parametrization, analogous to that used in the WDF context [32].

Define

$$\alpha_i = 2Z_J\Gamma_i \quad (16)$$

which is twice the junction impedance times the i th branch admittance. (In the non-para-Hermitian case, $\alpha_i = Z_J(\Gamma_i + \Gamma_{i*})$.) Then the junction pressure can be

written as a linear combination of the incoming pressure waves in terms of the α_i as

$$P_J = \sum_{i=1}^N \alpha_i P_i^+ \quad (17)$$

Since $\sum_{i=1}^N \Gamma_i \triangleq \Gamma_J$,

$$\sum_{i=1}^N \alpha_i = 2I_q \quad (18)$$

where I_q is the q by q identity matrix.

In the case where Z_i hence α_i is diagonal (or scalar), we have

$$0 \leq \alpha_i \leq 2I_q, \quad \alpha_i \text{ diagonal} \quad (19)$$

In matrix form, (13a) can be written

$$\begin{bmatrix} P_1^- \\ P_2^- \\ \vdots \\ P_N^- \end{bmatrix} = \begin{bmatrix} \alpha_1 - I_q & \alpha_2 & \dots & \alpha_N \\ \alpha_1 & \alpha_2 - I_q & \dots & \alpha_N \\ \vdots & \vdots & \ddots & \vdots \\ \alpha_1 & \alpha_2 & \dots & \alpha_N - I_q \end{bmatrix} \begin{bmatrix} P_1^+ \\ P_2^+ \\ \vdots \\ P_N^+ \end{bmatrix} \quad (20)$$

or

$$P^- = \Sigma P^+ \quad (21)$$

where

$$\Sigma \triangleq \mathcal{A} - I_{Nq}, \quad \mathcal{A} \triangleq \begin{bmatrix} I_q \\ I_q \\ \vdots \\ I_q \end{bmatrix} [\alpha_1 \alpha_2 \dots \alpha_N] \quad (22)$$

The matrix Σ is called the *scattering matrix* of the junction.

In the general lossless case, (18) implies

$$\Sigma^2 = I_{Nq} \quad (23)$$

Equation (23) states that lossless junction scattering is *reversible*. In other words, if the output scattering due to a particular input configuration is fed to the junction as input, the original unscattered input is obtained. For example, if all N waveguides are the same length and are terminated with perfect reflecting “mirrors,” then the network returns to its original initial conditions every $4T$ seconds, where T is the travel time from the junction to a mirror.

An N -port network is said to be *reciprocal* if its scattering matrix is *symmetric* [14]. We see that N -way junction is reciprocal if

$$\alpha_i \equiv \alpha \triangleq \frac{2}{N} I_q \quad (24)$$

Equivalently, the characteristic impedances of all intersecting branches must be the same in order to obtain a reciprocal network. Reciprocity is a specialized concept in this context.

Equations (13a,17,18) combine to give

$$P_i^- = P_i^+ + \sum_{\substack{j=1 \\ j \neq i}}^N \alpha_j (P_j^+ - P_i^+) \quad (25)$$

Thus, α_j can be interpreted as the *fraction of the pressure differential* between branches j and i which is reflected back along the i th branch with P_i^+ , for any i . Use of this expression saves one matrix multiply but entails $3N-2$ matrix additions. If one multiply is worth $N-1$ additions or more, then (25) is less expensive to implement than (13a).

3.4. Reflection Coefficients

Since $P_i^- = (\alpha_i - I_q)P_i^+$ when $P_j^+ = 0$ for all $j \neq i$, we define the *reflection coefficient* at the i th port by

$$\rho_i \triangleq \alpha_i - I_q \quad (26)$$

Reflection coefficients are used extensively to parametrize waveguide junctions in the special case where the waveguides are joined end to end in a cascade chain. For more general networks, α -parameters are typically better suited for junction parametrization.

3.5. Pure Delays and Multi-Junction Networks

Up to now we have been concerned only with the scattering of traveling waves at a single impedance-discontinuity junction. We now allow for many such junctions interconnected by lossless, reflectionless waveguide sections. Physically, an interconnection between junctions is a length of material at a single characteristic impedance. It is implemented digitally using a *bi-directional delay line*.

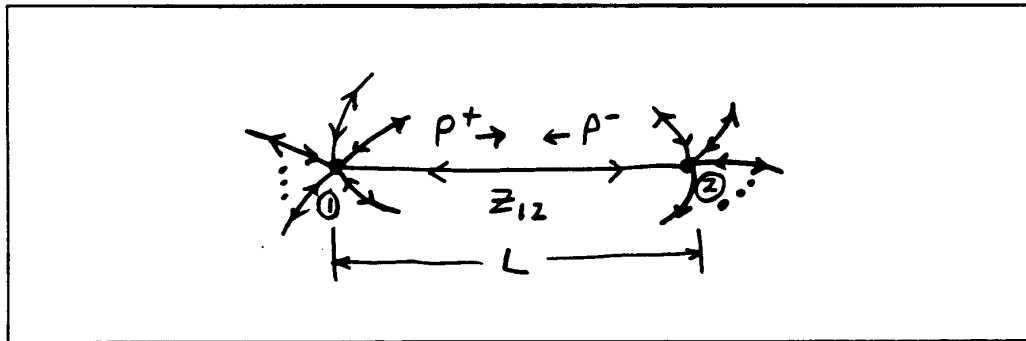


Figure 2. Two N -way junctions joined by a bidirectional delay line.

Consider the interconnection of two N -port junctions, numbered 1 and 2, as shown in Fig. 2. Between the two junctions is a section of pure waveguide which is

a lossless medium having characteristic impedance Z_{12} . Let c denote the speed of propagation in this waveguide section, and suppose the distance between the junctions is L . Then the propagation time from one junction to the other is $T_s = L/c$. Consider a pressure wave impulse $P^+(x - ct) = \delta(x - ct)$ traveling from junction 1 to junction 2 starting at time $t = 0$. At time T_s it reaches junction 2, and a reflection $P^-(x + ct) = \rho_{12}\delta[x + c(t - 2T_s)]$ starts out to the left from junction 2, heading back to junction 1. (ρ_{12} is the reflection coefficient for a pulse incident from junction 1 to junction 2, reflecting back toward junction 1.) A fragment of the pulse is also sent out along all waveguides connected to junction 2, according to the relative branch impedances. At time $t = 2T_s$, the reflected pulse reaches junction 1, and scatters again. A portion of the scattering heads back toward junction 2, and so on.

A section of waveguide joining two junctions by a propagation delay T_s is called a *unit delay*. If the speed of propagation is everywhere the same,* then all unit delays are of the same length $L = cT_s$.

Impulse-Invariant Digital Simulation

If an impulse is injected into a network constructed of length L waveguide sections, scattering takes place every $L/c \triangleq T_s \triangleq 1/F_s$ seconds. Therefore, the network can be precisely simulated (ignoring roundoff errors) by a digital network with sampling rate F_s . In other words, *a digital waveguide network is equivalent to a physical waveguide network in which the input pressure signals are streams of weighted impulses at intervals of T_s seconds.* This equivalence is true also in the case

* Since the characteristic impedance Z of a linear medium is the geometric mean of the "inertia constant" m and the "stiffness constant" k , i.e., $Z = \sqrt{mk}$ (cf. §3.1), and since the phase velocity in the medium is $c = \sqrt{k/m}$, it is physically possible to construct a waveguide network with varying characteristic impedances and uniform propagation speeds. A characteristic impedance can only be modified in such a network by scaling the inertia and stiffness constants equally.

of time-varying characteristic impedances. The impulsive nature of the propagating signals serves to sample the junction scattering coefficients at the digital sampling instants.

Bandlimited Digital Simulation

A more natural correspondence between physical and digital waveguide networks is obtained by assuming the inputs to the physical networks are *bandlimited continuous-time pressure functions*. The signals propagating throughout the physical network are assumed to consist of frequencies less than $F_s/2$ Hz. Therefore, by the well known Nyquist sampling theorem [33], if we record a sample of the pressure at the midpoint of each waveguide section every T_s seconds, the bandlimited continuous pressure fluctuation can be uniquely reconstructed throughout the waveguide network. Saying the pressure variation is bandlimited to $|F_s/2|$ is equivalent to saying the pressure distribution is *spatially bandlimited* to less than $k_s/2$, where $k_s = 1/L$, or, a single section of waveguide is no longer than half a cycle of the shortest cycle contained in a traveling pressure wave. In summary, *a digital waveguide network is equivalent to a physical waveguide network in which the input pressure signals are bandlimited to $|F_s/2|$ Hz*. This equivalence is *not* true in the time-varying case.

Time-Varying Digital Simulation

In the case of time-varying characteristic impedances, the bandlimited physical signal interpretation breaks down because the time-variation of the scattering coefficients applies a continuous amplitude modulation to the continuous propagating signals, thereby generating sidebands. If the signals incident on a junction are bandlimited to $|f_1|$ Hz and the α parameters (not the characteristic impedances!) are bandlimited to $|f_2|$ Hz, then equation (25) shows that the signals emerging from the junction are bandlimited only to $|f_1 + f_2|$ Hz. If the network is nontrivial, a portion of the amplitude-modulated signals eventually comes back to the same

time-varying junction, and the signal bandwidth expands to $|f_1 + 2f_2|$, and so on. A time-varying junction eventually expands the bandwidth of the signals contained in the network to infinity! If we ignore this phenomenon in the physical network and persist with a sampling rate of F_s in the digital network, we can only construct *aliased* [33] versions of the physical signals. The general result is that *time-varying physical waveguide networks cannot be simulated by digital waveguide networks at a fixed sampling rate*. In practice, however, we obtain good approximate digital simulations by working with pressure waves and junction parameters bandlimited to much less than $F_s/2$ and by using sufficient damping in the network so that the aliased signal energy is attenuated below significance.

In the following, we will maintain the impulse-invariant point of view, primarily for its greater simplicity.

General Waveguide Networks

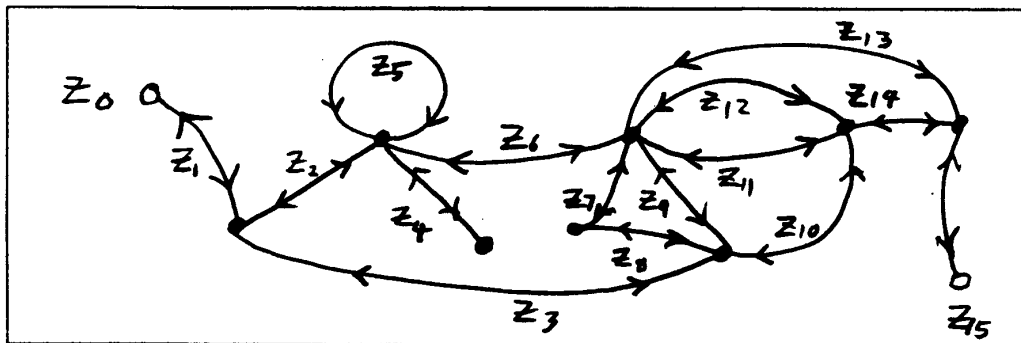


Figure 3. A more general network of waveguide sections.

Consider interconnecting many waveguide sections to form an arbitrary network, as depicted in Fig. 3. In general, the impulse response of the network will be nonzero at all multiples of T_s . Such a case is called *full-rate* waveguide network.

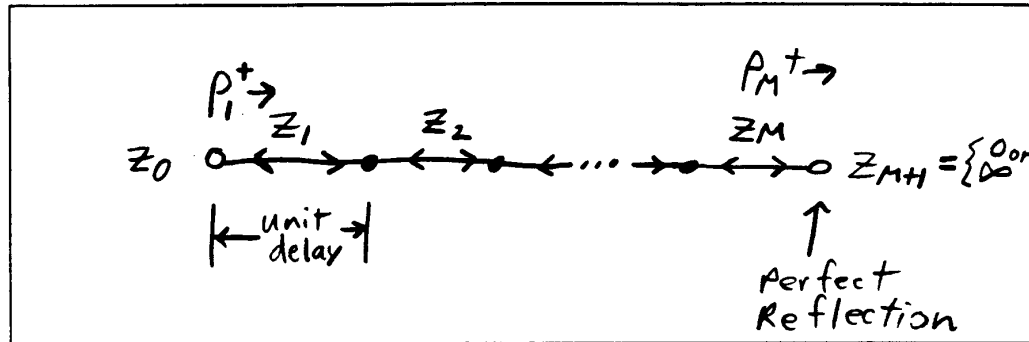
Cascade Waveguide Sections

Figure 4. A cascade of waveguide sections.

Consider a linear chain of M junctions separated by unit delays, as shown in Fig. 4. The input is defined as the pressure entering at the far left (junction 0), and the output is defined as the pressure emerging from the far right (junction M). This special case is the one which reduces to the prevalent ladder and lattice filter structures [36]. Note that the impulse response of structures of this type is zero at every other sampling instant. For this reason, we refer to the cascade chain as an example of a *half-rate* waveguide network. Half-rate structures can be exactly simulated digitally using a sampling rate $F_s' = F_s/2$.

If the input signal to a time-invariant (physical) cascade chain is bandlimited to $|F_s'/2 = F_s/4|$, then the signals in each section can be sampled half as often as in the general case.

In general, a half-rate structure cannot have a self-loop at any node (a *self-loop* is defined as a waveguide section connected to the same junction on both ends), and it must possess an even number of branches on every path from the input to the output, plus possibly a single odd section (which causes a half-sample shift of the output relative to the input). When there is an odd section, we do not allow the resulting structure to be placed in a feedback loop. The principal example of a half-rate structure is when waveguides are connected in a cascade chain. The

cascade waveguide chain reduces in the time-invariant case to the popular ladder and lattice filter structures, as discussed in the next section.

It appears that the more natural full-rate waveguide structures have not been used in digital filtering or modeling applications up to now. At least it can be said that full-rate waveguide structures are not mentioned in the prevailing textbooks on digital filtering and system modeling.

4. Cascade Waveguides

We now specialize discussion to cascade waveguide sections. The junction between two waveguides of differing characteristic impedance will create a scattering junction. The stretch of pure waveguide material between scattering junctions will provide delay lines for the propagation signal. From these structures all digital filters can be built in such a way that they behave nicely with respect to time-varying parameters and numerical roundoff/overflow. Almost all special properties in the cascade case carry over to arbitrary acyclic trees. This section provides a summary of the most important aspects of WGF's for the case of two-port sections; in later sections, these aspects will be generalized to more general waveguide networks.

4.1. The Two-Port Junction

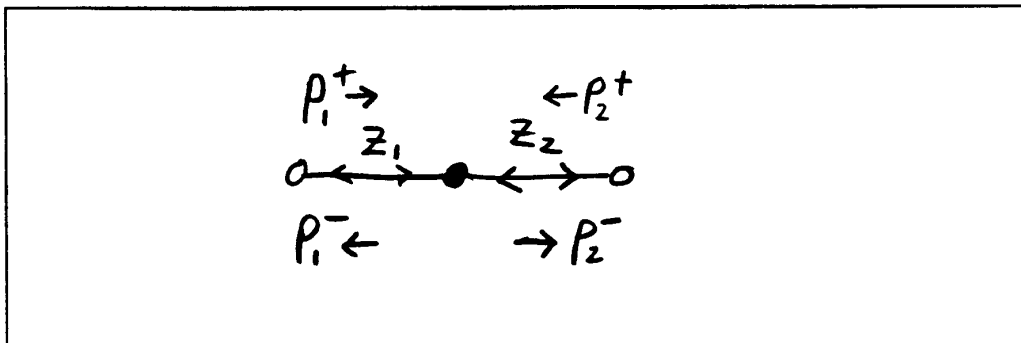


Figure 5. A single junction of two waveguide sections.

If there are only two waveguides meeting at a junction, we obtain the classical “scattering theory” in which an incoming wave is split into a “reflected” and “transmitted” part (Fig. 5). From (16), the α -parameters are

$$\begin{aligned}\alpha_1 &= 2(Z_1^{-1} + Z_2^{-1})^{-1} Z_1^{-1} = 2(\Gamma_1 + \Gamma_2)^{-1} \Gamma_1 = 2(I_q + Z_1 \Gamma_2) \\ \alpha_2 &= 2(Z_1^{-1} + Z_2^{-1})^{-1} Z_2^{-1} = 2(\Gamma_1 + \Gamma_2)^{-1} \Gamma_2 = 2(I_q + Z_2 \Gamma_1)\end{aligned}\quad (27)$$

From (25), the reflected pressure waves are

$$\begin{aligned}P_1^- &= \alpha_2(P_2^+ - P_1^+) + P_1^+ = (\alpha_1 - I_q)P_1^+ + \alpha_2 P_2^+ \\ P_2^- &= \alpha_1(P_1^+ - P_2^+) + P_2^+ = \alpha_1 P_1^+ + (\alpha_2 - I_q)P_2^+\end{aligned}\quad (28)$$

If $P_2^+ = 0$, then the incidence of P_1^+ produces a reflected wave $P_1^- = (\alpha_1 - I_q)P_1^+$. Thus, we define the following *reflection coefficients*:

$$\begin{aligned}\rho_1 &\triangleq \alpha_1 - I_q = (Z_2 - Z_1)(Z_2 + Z_1)^{-1} = (\Gamma_1 + \Gamma_2)^{-1}(\Gamma_1 - \Gamma_2) \\ \rho_2 &\triangleq \alpha_2 - I_q = -\rho_1\end{aligned}\quad (29)$$

It is now apparent that if the reflection coefficient at port 1 is $\rho_1 = \rho$, then at port 2 the reflection coefficient is $-\rho$. Another point of view is that inverting the impedance-step ratio from $Z_1:Z_2$ to $Z_2:Z_1$ merely changes the sign of the reflection coefficient. It is easy to show that for scalar Z_i , exchanging pressure waves for flow waves also toggles the sign of all reflection coefficients in the network. Thus, left is the dual of right as pressure is the dual of flow (and parallel is the dual of series).

In the matrix-impedance case ($q > 1$), however, replacement of pressure by flow changes ρ to $-(\Gamma_1 Z_2 - I_q)(\Gamma_1 Z_2 + I_q)^{-1}$ which equals $-\rho$ only if Z_1 commutes with Z_2 . Two Hermitian matrices commute if they have the same eigenvectors, i.e., their “principal axes of dilation” are aligned. There exists a unitary transformation of any Hermitian matrix which commutes with any other Hermitian matrix; that is,

a Hermitian matrix can be “rotated” until it commutes with any other Hermitian matrix. For waveguides with impedance matrices so aligned (all Z_i have the same eigenvectors on the unit circle), junction reversal is equivalent to wave-variable exchange; either causes a sign reversal in all reflection coefficients.

4.2. The Scattering Matrix

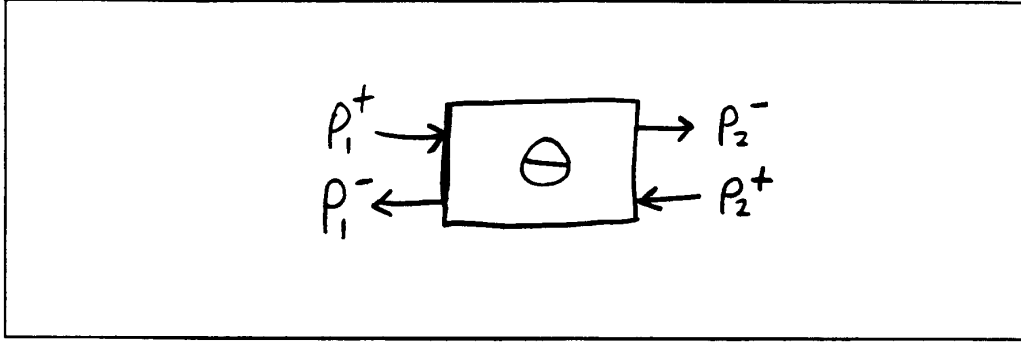


Figure 6. A two-port diagram.

In block-matrix notation, the junction output is given by

$$\begin{bmatrix} P_1^- \\ P_2^- \end{bmatrix} = \begin{bmatrix} \alpha_1 - I_q & \alpha_1 \\ \alpha_2 & \alpha_2 - I_q \end{bmatrix} \begin{bmatrix} P_1^+ \\ P_2^+ \end{bmatrix} = \begin{bmatrix} \rho_1 & I_q + \rho_1 \\ I_q - \rho_1 & -\rho_1 \end{bmatrix} \begin{bmatrix} P_1^+ \\ P_2^+ \end{bmatrix} \quad (30)$$

reciprocal for ρ_1 , or

$$\underline{P}^- = \Sigma \underline{P}^+ \quad (31)$$

This is called the *scattering formulation*, and Σ is called the *scattering matrix*. It is a special case of the N -junction scattering matrix defined in (20). Often we depict a two-port junction as shown in Fig. 6, where Θ is defined in the next subsection.

4.3. The Chain-Scattering Matrix

In the two-port case only, we can also define the *chain-scattering matrix* via

$$\begin{bmatrix} P_1^+ \\ P_1^- \end{bmatrix} = \Theta \begin{bmatrix} P_2^- \\ P_2^+ \end{bmatrix} \quad (32)$$

where

$$\Theta \triangleq \begin{bmatrix} \Theta_{11} & \Theta_{21} \\ \Theta_{12} & \Theta_{22} \end{bmatrix} \quad (33)$$

While the scattering matrix computes outgoing waves from incoming waves, the chain-scattering matrix computes the left-going and right-going waves in section 1 given the left-going and right-going waves in section 2. The relation between the scattering matrix Σ and the chain-scattering matrix Θ is given by

$$\begin{aligned} \Theta_{11} &= \Sigma_{21}^{-1} & \Theta_{12} &= -\Sigma_{21}^{-1} \Sigma_{22} \\ \Theta_{21} &= \Sigma_{11} \Sigma_{21}^{-1} & \Theta_{22} &= \Sigma_{12} - \Sigma_{11} \Sigma_{21}^{-1} \Sigma_{22} \end{aligned} \quad (34)$$

and

$$\begin{aligned} \Sigma_{11} &= \Theta_{21} \Theta_{11}^{-1} & \Sigma_{12} &= \Theta_{22} - \Theta_{21} \Theta_{11}^{-1} \Theta_{12} \\ \Sigma_{21} &= \Theta_{11}^{-1} & \Sigma_{22} &= -\Theta_{11} \Theta_{12} \end{aligned} \quad (35)$$

4.4. The One-Multiply Scattering Junction

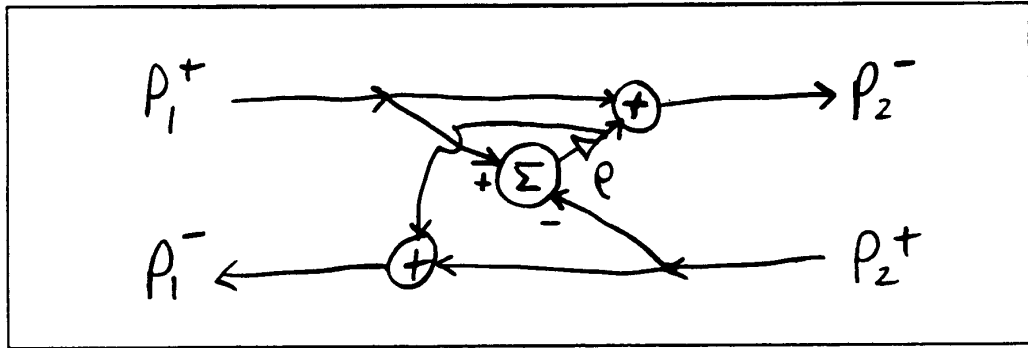


Figure 7. The two-port one-multiply scattering section.

Equations (28) and (29) combine to give

$$\begin{aligned} P_1^- &= P_2^+ + P_\Delta \\ P_2^- &= P_1^+ + P_\Delta \end{aligned} \quad (36)$$

where

$$\begin{aligned} P_\Delta &= \rho(P_1^+ - P_2^+) \\ \rho &= \rho_1 = \alpha_1 - I_q \end{aligned} \quad (37)$$

Thus, only one matrix multiplication is necessary to compute the reflected waves from the incoming waves. In the scalar case, this reduces to the so-called *one-multiplier lattice section* [36] (minus the unit-sample delay ordinarily associated with each section). A system diagram for the one-multiplier section is shown in Fig. 7. It is well-known that any rational digital filter can be built using one-multiplier lattice sections [36]. In fixed-point implementations, the only source of error would typically be in the computation of P_Δ .

In linear fixed-point implementations, to ensure the absence of limit cycles and overflow oscillations, the additions in (36) must be performed before rounding, and the final rounding to obtain P_1^- and P_2^- must be *norm reducing*. (In the scalar case, magnitude truncation is sufficient.) The added expense for postponing round-off until the final outgoing waves are computed is typically negligible, requiring only logic to determine the desired direction of truncation from the signs of P_1^+ and P_2^+ , and the low-order product of P_Δ . In other words, the double precision computations required are only conceptual because the low-order half of the incoming wave P_1^+ is zero.

Another one-multiplier form is obtained by organizing (28) as

$$\begin{aligned} P_1^- &= P_1^+ + \alpha(P_2^+ - P_1^+) = P_1^+ - \alpha\tilde{P}_\Delta \\ P_2^- &= P_1^- + (P_1^+ - P_2^+) = P_1^- + \tilde{P}_\Delta \end{aligned} \quad (38)$$

where $\alpha \triangleq \alpha_2$ to get (28). As in the previous case, only one multiply and three adds are required per section.

In the scalar case, the single section parameter ρ of (38) must lie between -1 and 1 , while in (37), the single section parameter α must lie between 0 and 2 . Otherwise, the junction is not passive. The practical implication of non-passive junctions (ignoring roundoff error) is potential filter instability in the presence of feedback.

In logarithmic fixed-point implementations, multiplication and division are exact (in the absence of overflow or underflow), and roundoff error occurs only upon addition or subtraction [17,37,48]. In this case, limit cycles and overflow oscillations are suppressed if (a) a true zero element ζ is supported such that $x \pm \zeta = x$ and $z\zeta = \zeta$, and (b) the $\log(1 \pm B^x)$ table used in addition and subtraction are truncated toward negative infinity. Normal truncating of the log magnitude of a number yields a contractive quantization in the number itself. While it is not necessary for passivity of overflow, it is preferable that overflow result in the maximum magnitude number, of correct sign.

4.5. The Normalized Scattering Junction

Consider the rescaled quantities

$$\begin{aligned} \bar{P}_i^+ &\triangleq Z_i^{-\frac{1}{2}} P_i^+ & \bar{P}_i^- &\triangleq Z_i^{-\frac{1}{2}} P_i^- \\ \bar{U}_i^+ &\triangleq Z_i^{\frac{1}{2}} U_i^+ & \bar{U}_i^- &\triangleq Z_i^{\frac{1}{2}} U_i^- \end{aligned} \quad (39)$$

for $i = 1, 2$ where

$$Z_{i*}^{\frac{1}{2}} = Z_i^{\frac{1}{2}} \quad (40)$$

is the unique para-Hermitian square root of Z_i . The *para-Hermitian square root* of Z_i is defined as the analytic continuation of the Hermitian square root of $Z_i(e^{j\theta})$. Uniqueness is inherited from uniqueness of both the Hermitian square root and the process of analytic continuation.

In terms of $\tilde{P}_i^+, \tilde{P}_i^-$, the two-port scattering equations (38) become

$$\begin{aligned}\tilde{P}_1^- &= \left[Z_1^{-\frac{1}{2}}(\alpha_1 - I_q)Z_1^{\frac{1}{2}} \right] \tilde{P}_1^+ + \left[Z_1^{-\frac{1}{2}}\alpha_2 Z_2^{\frac{1}{2}} \right] \tilde{P}_1^+ \\ \tilde{P}_2^- &= \left[Z_2^{-\frac{1}{2}}\alpha_1 Z_1^{\frac{1}{2}} \right] \tilde{P}_1^+ + \left[Z_2^{-\frac{1}{2}}(\alpha_2 - I_q)Z_2^{\frac{1}{2}} \right] \tilde{P}_1^+\end{aligned}\quad (41)$$

or, in terms of the reflection coefficient $\rho = \rho_1 = \alpha_1 - I_q = I_q - \alpha_2$,

$$\begin{aligned}\tilde{P}_1^- &= \left[Z_1^{-\frac{1}{2}}\rho Z_1^{\frac{1}{2}} \right] \tilde{P}_1^+ + \left[Z_1^{-\frac{1}{2}}(I_q - \rho)Z_2^{\frac{1}{2}} \right] \tilde{P}_1^+ \\ \tilde{P}_2^- &= \left[Z_2^{-\frac{1}{2}}(I_q + \rho)Z_1^{\frac{1}{2}} \right] \tilde{P}_1^+ - \left[Z_2^{-\frac{1}{2}}\rho Z_2^{\frac{1}{2}} \right] \tilde{P}_1^+\end{aligned}\quad (42)$$

This form will be further generalized in §5.4.

If Z_1, Z_2 are *diagonal*, then each component $Z_i[j]$ is real and positive and ρ is diagonal by (29). In fact, there is very little difference between the case of diagonal Z and scalar Z . In the diagonal case, (42) simplifies to

$$\begin{aligned}\tilde{P}_1^- &= \rho \tilde{P}_1^+ + (I_q - \rho)\sqrt{Z_2/Z_1} \tilde{P}_2^+ \\ \tilde{P}_2^- &= (I_q + \rho)\sqrt{Z_1/Z_2} \tilde{P}_1^+ - \rho \tilde{P}_2^+, \quad (\text{diagonal case})\end{aligned}\quad (43)$$

Recall from (29) that

$$\rho = (Z_2 - Z_1)(Z_2 + Z_1)^{-1} = (\Gamma_1 + \Gamma_2)^{-1}(\Gamma_1 - \Gamma_2) \quad (44)$$

which can be used to show

$$Z_1 Z_2^{-1} = (I_q + \rho)^{-1}(I_q - \rho) \quad (45)$$

This formula further simplifies (43) since

$$\begin{aligned} (I_q - \rho) \sqrt{\frac{Z_2}{Z_1}} &= (I_q - \rho) \sqrt{\frac{I_q + \rho}{I_q - \rho}} = \sqrt{I_q - \rho^2} \\ (I_q + \rho) \sqrt{\frac{Z_1}{Z_2}} &= (I_q + \rho) \sqrt{\frac{I_q - \rho}{I_q + \rho}} = \sqrt{I_q - \rho^2} \end{aligned} \quad (46)$$

Defining $\tilde{\rho} = \sqrt{I_q - \rho^2}$, the normalized scattering section, in the case of *diagonal* characteristic impedance, reduces to

$$\begin{aligned} \tilde{P}_1^- &= \rho \tilde{P}_1^+ + \tilde{\rho} \tilde{P}_2^+ \\ \tilde{P}_2^- &= \tilde{\rho} \tilde{P}_1^+ - \rho \tilde{P}_2^+ \\ \tilde{\rho} &\triangleq \sqrt{I_q - \rho^2}, \quad \rho \text{ diagonal} \end{aligned} \quad (47)$$

which is the well-known *normalized ladder form* (NLF) [36].

4.6. The Three-Multiply Normalized Scattering Junction

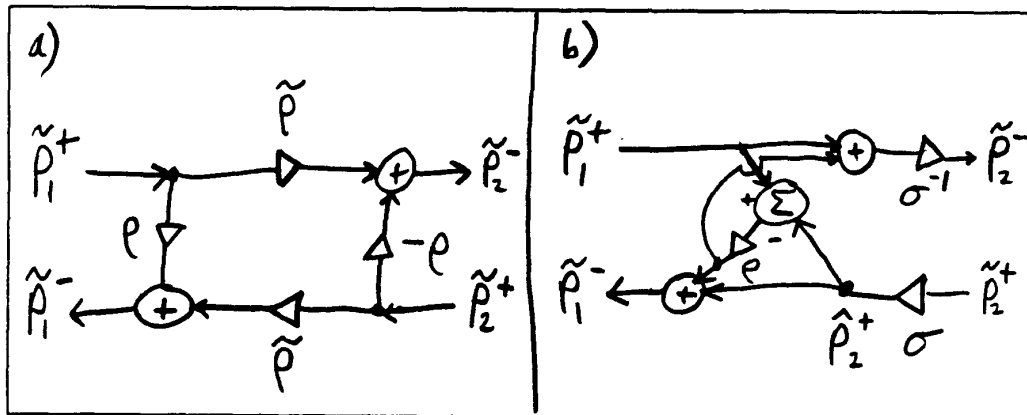


Figure 8. The normalized ladder form (NLF).

- a) The four-multiply NLF.
- b) The three-multiply NLF.

Note that the normalized ladder form (NLF) for the diagonal or scalar case (§4.5) requires four (matrix) multipliers for each scattering junction, as shown in Figure 8a. One of these multipliers can be eliminated as shown in Figure 8b.

The three-multiplier NLF is derived from (43) as follows. Define

$$\begin{aligned}\hat{P}_2^+ &= \tilde{P}_2^+ \sqrt{\frac{Z_2}{Z_1}} \\ \hat{P}_2^- &= \tilde{P}_2^- \sqrt{\frac{Z_2}{Z_1}}\end{aligned}\tag{48}$$

Rewrite (43) so that the second equation becomes

$$\tilde{P}_2^- = \sqrt{Z_1/Z_2} \left[(I_q + \rho) \tilde{P}_1^+ - \rho \sqrt{\frac{Z_2}{Z_1}} \tilde{P}_1^+ \right]\tag{49}$$

and compare to the first equation, recognizing \hat{P}_2^+ in both. The NLF is thus reduced to a one-multiplier junction followed by a transformer (cf. §4.9), as shown in Fig. 8b.

Let

$$\sigma \triangleq \sqrt{\frac{Z_2}{Z_1}} = \sqrt{\frac{I_q + \rho}{I_q - \rho}}, \quad (\text{diagonal case})\tag{50}$$

Then we can write the formulas for the three-multiplier NLF as

$$\begin{aligned}\hat{P}_2^+ &= \sigma \tilde{P}_2^+ \\ \tilde{P}_\Delta &= \rho (\tilde{P}_1^+ - \tilde{P}_2^+) \\ \tilde{P}_1^- &= \hat{P}_2^+ + \tilde{P}_\Delta \\ \tilde{P}_2^- &= \tilde{P}_1^+ + \tilde{P}_\Delta \\ \tilde{P}_2^- &= \sigma^{-1} \hat{P}_2^-, \quad \rho, \sigma \text{ diagonal}\end{aligned}\tag{51}$$

4.7. The Two-Port Delay Line

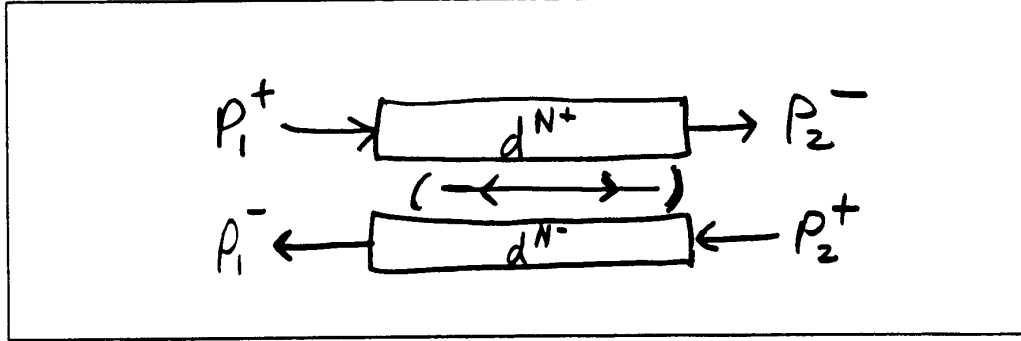


Figure 9. The two-port delay line.

Section §3.5 discusses the use of pure delay lines between scattering junctions. A single section of lossless waveguide material is a two-port as shown in Fig. 9. The input-output equations are

$$\begin{aligned} P_1^- &= d^{N^-} P_2^+ \\ P_2^- &= d^{N^+} P_1^+ \end{aligned} \quad (52)$$

where d is the unit-sample delay operator ($d \leftrightarrow z^{-1}$) defined by $d^k x(t) = x(t - k)$. We will normally consider only the physically meaningful case $N^+ = N^-$, corresponding to equal forward and reverse delays. However, in typical ladder and lattice filter structures [36], $N^+ = 0$ and $N^- = 2N$, where N is the propagation delay (in samples) from one junction to the next.

The *scattering matrix* (cf. §4.2) of a bidirectional delay line is

$$\Sigma = \begin{bmatrix} 0_q & d^{N^-} I_q \\ d^{N^+} I_q & 0_q \end{bmatrix} \quad (53)$$

reciprocal for $N^+ = N^-$, and the *chain scattering matrix* (cf. §4.3) is

$$\Theta = \begin{bmatrix} d^{-N^-} I_q & 0_q \\ 0_q & d^{N^+} I_q \end{bmatrix} \quad (54)$$

4.8. Generalized Delay

By replacing the delay operator by an arbitrary lossless transfer function matrix, we obtain a generalized waveguide section. A transfer function matrix H is said to be *lossless (allpass)* if it is para-unitary, i.e.,

$$H_*H = I \quad (55)$$

Introducing an allpass filter into a delay line can be interpreted as making the length of the waveguide section *frequency-dependent*. This technique has been used to simulate stiffness in models for vibrating strings [56,57,58]. Since the phase velocity along a stiff string increases with frequency [4], an allpass filter with a phase delay which decreases with frequency can capture the most essential effects of stiffness on traveling-wave propagation. A method which can be adapted to design a scalar allpass filter, of any order, approximating a desired phase delay is given in [55,57].

4.9. The Two-Port Transformer

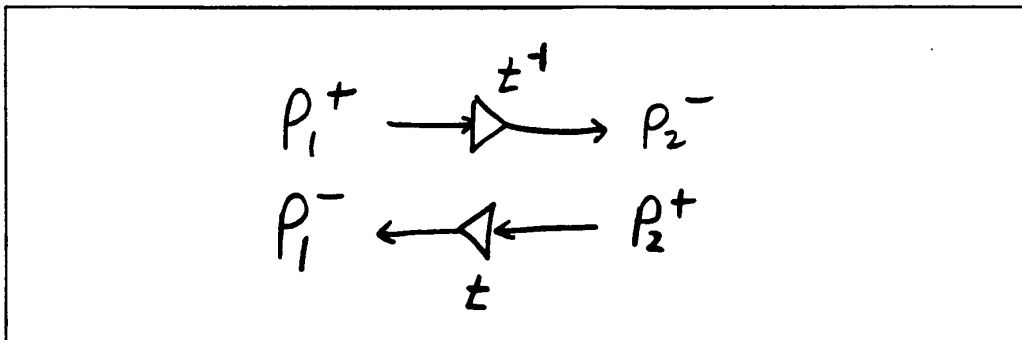


Figure 10. The two-port transformer.

The ideal *cascade transformer* is a *lossless 2-port* which scales up pressure by some factor and scales down flow by the same factor without generating scattering

reflections. This amounts to scaling the characteristic impedance across a waveguide without causing the reflections which normally accompany an impedance discontinuity. Doing this requires violating conservation of flow (cf. (6)). Thus, transformers are non-physical "miracle junctions" which can arbitrarily redistribute the traveling wave between its pressure and flow components such that free propagation is undisturbed. We will use transformers to control time-varying filters. A diagram is shown in Fig. 10.

Recall the fundamental relations

$$\begin{aligned} P_i^+ &= Z_i U_i^+ \\ P_i^- &= -Z_i U_i^- \end{aligned} \quad (56)$$

for $i = 1, 2$. Ordinarily, the impedance step from Z_1 to Z_2 generates a reflection. A transformer suppresses reflections when crossing an impedance step. As discussed in §5, the right-going and left-going signal power in a section of waveguide of impedance Z are given, respectively, by

$$\begin{aligned} p^+ &= P_+^+ U^+ = U_+^+ Z U^+ = P_+^+ \Gamma P^+ \\ p^- &= P_+^- U^- = -U_+^- Z U^- = -P_+^- \Gamma P^- \end{aligned} \quad (57)$$

A two-port transformer, by definition, preserves the right-going and left-going signal power. Thus, we require

$$\begin{aligned} P_{1+}^+ \Gamma_1 P_1^+ &= P_{2+}^+ \Gamma_2 P_2^+ \\ P_{1+}^- \Gamma_1 P_1^- &= P_{2+}^- \Gamma_2 P_2^- \end{aligned} \quad (58)$$

This is arranged if

$$P_2^\pm = Z_2^{1/2} Z_1^{-1/2} P_1^\pm \quad (59)$$

Let

$$t \triangleq Z_2^{1/2} Z_1^{-1/2} \quad (60)$$

where t is not necessarily Hermitian ($Z_i^{1/2}$ is not necessarily Hermitian even if Z_i is Hermitian). Then (58) implies

$$\begin{aligned}
 P_2^+ &= t^{-1}P_1^+ \\
 P_2^- &= t^{-1}P_1^- \\
 \Rightarrow P_2 &= t^{-1}P_1 \\
 U_2^- &= t_*U_2^+ \\
 U_1^- &= t_*U_2^+ \\
 \Rightarrow U_1 &= t_*U_2
 \end{aligned} \tag{61}$$

The pressure scattering equations are

$$\begin{aligned}
 P_1^- &= tP_2^+ \\
 P_2^- &= t^{-1}P_1^+
 \end{aligned} \tag{62}$$

as shown in Fig. 10.

The scattering matrix of an ideal transformer is

$$\Sigma = \begin{bmatrix} 0_q & t \\ t^{-1} & 0_q \end{bmatrix} \tag{63}$$

reciprocal for $t^2 = I_q$, and the chain scattering matrix is

$$\Theta = \begin{bmatrix} t & 0_q \\ 0_q & t \end{bmatrix} \tag{64}$$

Note that the transformer scale factor t can be any stable minimum-phase* q by q transfer function matrix.

* A transfer function t is *minimum-phase* iff its inverse t^{-1} is stable and causal.

The *reflectance transfer function* seen at any port (e.g., P_1^-/P_1^+ at port 1) is not changed by the insertion of a transformer if that port is not connected to anything “downstream” of the transformer. This applies to waveguide chains and to acyclic trees of waveguides. The filtering by t is always canceled in the end by t^{-1} .

4.10. The Two-Port Dualizer (Gyrator)

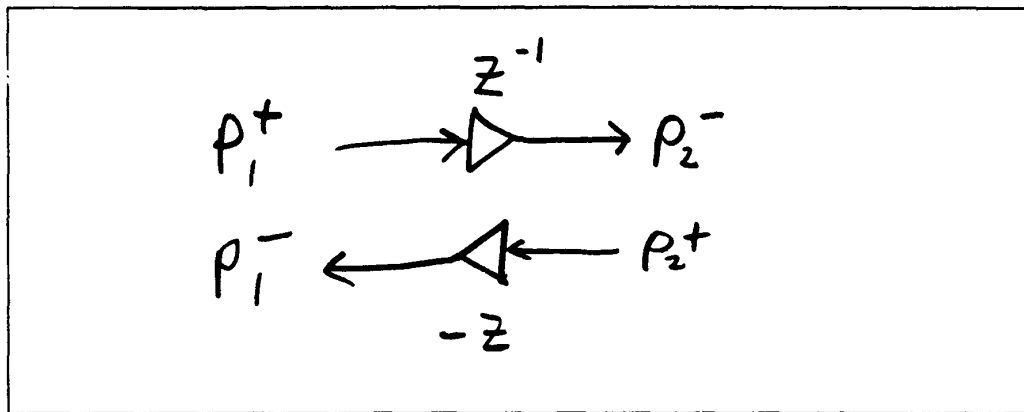


Figure 11. The two-port dualizer.

- a) Pressure to flow.
- b) Flow to pressure.

To minimize dynamic range requirements in fixed-point implementations (see §5.7) it is helpful to be able to switch between pressure and flow as the explicitly computed variable of propagation. Transformation from pressure to flow or vice versa can be accomplished by means of a two-port “dualizer” which is a special case of a *gyrator* [14]. (A gyrator is more generally a dualizer in cascade with any transformer.)

The dualizer merely implements the fundamental relations between pressure and flow:

$$\begin{aligned} P^+ &= ZU^+ \\ P^- &= -ZU^- \end{aligned} \tag{65}$$

This is a flow to pressure dualizer. The pressure to flow dualizer is obtained by solving for flow in terms of pressure.

A two-port junction which converts pressure waves on the left to pressure waves on the right which are equal to the flow waves on the left is obtained by defining $P_2^+ = U_1^-$ and $P_2^- = U_1^+$, and we get

$$\begin{aligned} P_1^- &= -ZP_2^+ \\ P_2^- &= Z^{-1}P_1^+ \end{aligned} \tag{66}$$

Note that we write Z instead of Z_1 or Z_2 in (66) above because $Z_1 = Z_2$. That is, the dualizer converts pressure to flow at the same characteristic impedance.

The dualizer can be seen as a transformer scaling by Z together with a sign reversal in the reflection branch. A gyrator is therefore any transformer modified to have a sign change in the reflection path. The sign change in the reflection is the heart of the dual operation: When pressure reflects in-phase, flow reflects out-of-phase, and vice versa.

When inserting a dualizer into a network, it is necessary to redo the scattering equations "down-stream." In other words, if a pressure waveguide is connected to a junction whose scattering coefficients expect pressure waves as input, changing the wave variable to flow necessitates changing the scattering coefficients. Typically this is done by converting back to pressure at the junction and combining computations.

In the case of cascade two-ports, one easily can change a waveguide from pressure to flow or vice versa by inserting complementary dualizers on either side of the waveguide branch and then absorbing the dualizer coefficients into the adjacent two-port junctions.

The scattering matrix of the pressure to flow dualizer is

$$\Sigma = \begin{bmatrix} 0_q & -Z \\ Z^{-1} & 0_q \end{bmatrix} \tag{67}$$

reciprocal when $Z^2 = -I_q$, and the chain scattering matrix is

$$\Theta = \begin{bmatrix} Z & 0_q \\ 0_q & -Z \end{bmatrix} \quad (68)$$

The flow to pressure versions are obtained by substituting Z^{-1} for Z .

4.11. The Normalized Time-Varying One-Multiply Junction

Suppose we are using a scalar one-multiply scattering junction (§4.4) and wish to vary it over time. The scattering coefficients are completely determined by the relative characteristic impedances in the successive waveguide branches. Therefore, a time-varying filter is created by changing one or more characteristic impedances over time. Two problems appear:

- 1) Changing a single branch characteristic impedance forces not one but *two* scattering junctions to change with respect to time.
- 2) When a branch characteristic impedance is changed, the stored signal power represented by the contents of the bidirectional delay line changes.

The first problem can be solved by varying all characteristic impedances so that only one junction is modified (the characteristic impedance ratios are held fixed at the remaining junctions). For example, suppose we have a cascade of 5 waveguide sections, and we want to vary the junction between Z_2 and Z_3 with an amplitude modulation $\cos(\omega t)$. Then we can leave Z_1 and Z_2 as before and choose $Z_i \leftarrow \cos(\omega t)Z_i$ for $i = 3, 4, 5$. The last section Z_5 must be terminated by either $Z = \infty$ or $Z = 0$ (the so-called *reflectively terminated* case). In the general case of waveguide networks with branches forming *loops*, this trick does not work, and a changing characteristic impedance generally affects at least two branches.

The second problem can be solved by *rescaling* the entire contents of the bidirectional delay line associated with the characteristic impedance in such a way

as to compensate for the stored energy. If Z denotes the characteristic impedance of the branch before time variation begins, then the original signal power represented by each sample $P^+(n)$ is $P^+(n)^2/Z$, where $n = 1, \dots, N$ denotes delay element index in a length N bidirectional delay line ($2N$ total memory cells). Let time be frozen. Suppose now that the characteristic impedance instantaneously changes to \tilde{Z} . Then to hold stored signal power constant, we must rescale the contents of the delay line to

$$\begin{aligned}\tilde{P}^+(n) &\leftarrow P^+(n)\sqrt{\tilde{Z}/Z} \\ \tilde{P}^-(n) &\leftarrow P^-(n)\sqrt{\tilde{Z}/Z}\end{aligned}\tag{69}$$

Then

$$\begin{aligned}\frac{[\tilde{P}^+(n)]^2}{\tilde{Z}} &= \frac{[P^+(n)]^2 \tilde{Z}/Z}{\tilde{Z}} = \frac{[P^+(n)]^2}{Z} \\ \frac{[\tilde{P}^-(n)]^2}{\tilde{Z}} &= \frac{[P^-(n)]^2 \tilde{Z}/Z}{\tilde{Z}} = \frac{[P^-(n)]^2}{Z}\end{aligned}\tag{70}$$

and signal power is held invariant.

This type of power normalization is unnecessarily expensive in most cases. Normally, the samples interior to a waveguide section can be left unnormalized until they reach the end (a junction) or some interior point where a measurement of waveguide pressure or flow is being made.

Both problems can be conveniently solved by using a *transformer* to change the characteristic impedance just before entering a junction, and incorporating normalization in the transformer. Doing this yields the normalized time-varying one-multiply scattering junction shown in Fig. 8.

5. Signal Power in Lossless Waveguides

This section presents basic definitions of signal energy and power in a waveguide. These concepts provide the necessary handles on filter stability, passivity

with respect to numerical round-off and overflow, and energy modulation due to time-varying parameters.

5.1. Instantaneous Propagating Power

The *instantaneous power* in a waveguide containing instantaneous pressure P and flow U is defined as the m by m product of pressure and flow:

$$\mathcal{P} = P_* U \quad (71)$$

The *total instantaneous power* is defined as the *trace* of the instantaneous power:

$$\mathcal{P}_T \triangleq \text{Tr}\{\mathcal{P}\} = \text{Tr}\{P_* U\} \quad (72)$$

The total instantaneous power is a complex scalar measure of power flow. It can be interpreted in a manner similar to the complex power in scalar transmission-line theory in which sinusoidal phasors are propagated in either direction. The instantaneous power can be expanded into four terms as follows:

$$\begin{aligned} \mathcal{P} &= P_* U = (P_*^+ + P_*^-)(U^+ + U^-) = (U_*^+ - U_*^-)Z_*(U^+ + U^-) \\ &= P_*^+ U^+ + P_*^- U^- + P_*^+ U^- + P_*^- U^+ \\ &= P_*^+ \Gamma P^+ - P_*^- \Gamma P^- + P_*^+ \Gamma P^- - P_*^- \Gamma P^+ \\ &= U_*^+ Z U^+ - U_*^- Z U^- - U_*^+ Z U^- + U_*^- Z U^+ \end{aligned} \quad (73)$$

The *right-going* and *left-going* power are defined, respectively, by

$$\begin{aligned} \mathcal{P}^+ &= P_*^+ U^+ = U_*^+ Z U^+ = P_*^+ \Gamma P^+ \\ \mathcal{P}^- &= P_*^- U^- = -U_*^- Z U^- = -P_*^- \Gamma P^- \end{aligned} \quad (74)$$

Since Z is para-Hermitian, \mathcal{P}^+ and \mathcal{P}^- are Hermitian forms, and can be expressed as

$$\begin{aligned}\mathcal{P}^+ &= \sum_{i=1}^m \lambda_i^+ \underline{v}_i^+ \underline{v}_{i*}^+ \\ \mathcal{P}^- &= \sum_{i=1}^m \lambda_i^- \underline{v}_i^- \underline{v}_{i*}^- \end{aligned} \quad (75)$$

where \underline{v}_i^+ is the i th eigenvector of \mathcal{P}^+ , and λ_i^+ is its i th (real) eigenvalue. The m -vectors \underline{v}_i^+ can be chosen orthonormal. Similar remarks apply to the eigenvalues and eigenvectors of \mathcal{P}^- . It can be shown that the waveguide is passive if and only if $\lambda_i^+, \lambda_i^- \geq 0$. Consequently, we will assume in the sequel that

$$\lambda_i^+ > 0, \quad \lambda_i^- > 0, \quad i = 1, 2, \dots, m \quad (76)$$

This implies \mathcal{P}^+ and \mathcal{P}^- are positive definite Hermitian matrices. The orthonormal vectors \underline{v}_i^+ and \underline{v}_i^- (which are vector analytic functions of d), indicate "directions" along which power flows in the m -dimensional manifold determined by U_i (or P_i) and Z .

In the non-para-Hermitian case, the medium is passive if and only if

$$Z(d) + Z_*(d) \geq 0, \quad \forall |d| \leq 1 \quad (77)$$

That is, the para-Hermitian part of the characteristic impedance of a passive medium must be positive definite in the unit circle. It can be shown using the maximum modulus theorem [5] that (77) holds if $Z + Z_* \geq 0$ for $|d| = 1$.

We define the *cross power* by

$$\mathcal{P}^{\times} = U_*^+ Z U^- \quad (78)$$

The instantaneous power (73) can now be written as

$$\mathcal{P} = (\mathcal{P}^+ - \mathcal{P}^-) + (\mathcal{P}^{\times} - \mathcal{P}_*^{\times}) \quad (79)$$

which we interpret as a sum of a net traveling-power term $\mathcal{P}^+ - \mathcal{P}^-$ plus the skew-para-Hermitian part of the cross-power. In the real scalar case, $\mathcal{P}^\times \equiv \mathcal{P}_*^\times$ and the cross power is zero.

Since the eigenvalues of a Hermitian matrix are purely real, we define the difference between the right-going and left-going power $\mathcal{P}^+ - \mathcal{P}^-$ as the *active power*. Similarly, since the eigenvalues of a skew-Hermitian matrix are purely imaginary, we define the skew-para-Hermitian part of the cross-power $\mathcal{P}^\times - \mathcal{P}_*^\times$ as the *reactive power*. These definitions parallel those of scalar transmission-line theory.

5.2. Instantaneous Stored Power

The total energy in a waveguide network is obtained by summing the instantaneous power over all of the storage elements. The storage elements are the memory locations in the bidirectional delay lines. Each bidirectional delay line represents a sampled uniform waveguide section. Let

Z_i = Characteristic impedance of branch i

N_i = Length of delay (samples) along either direction of branch i

n = Time in samples

$Z_i(n)$ = Characteristic impedance of branch i at time n

$N_b(n)$ = Total number of branches in the waveguide network at time n

$P_i^+(m, n)$ = Right-going pressure in branch i , forward delay element m , time n

$P_i^-(m, n)$ = Left-going pressure in branch i , reverse delay element m , time n

$P_i(m, n) = P_i^+(m, n) + P_i^-(m, n)$ = Instantaneous pressure in branch i , element m , time n

$U_i^+(m, n)$ = Right-going flow in branch i , forward delay element m , time n

$U_i^-(m, n)$ = Left-going flow in branch i , reverse delay element m , time n

$U_i(m, n) = U_i^+(m, n) + U_i^-(m, n)$ = Instantaneous flow in branch i , element m , time n

(80)

The instantaneous signal power contributed by each delay element of a pressure network is

$$P_i(m, n) = P_{i*}(m, n)\Gamma_i(n)P_i(m, n) \quad (81)$$

Similarly, in a flow network, the instantaneous power is

$$P_i(m, n) = U_{i*}(m, n)Z_i(n)U_i(m, n) \quad (82)$$

If branch i is a pressure branch, then increasing $Z_i(n)$ with P^\pm, P_i^- fixed *decreases* the stored power in branch i . On the other hand, the power in a flow branch *increases* as $Z_i(n)$ increases. If the i th branch holds normalized waves (cf. §4.5, §4.6, §5.4) the stored signal power is constant as the characteristic impedance varies.

The total power in a waveguide network at time n is given by

$$P(n) \triangleq \sum_{i=1}^{N_b(n)} \sum_{m=1}^{N_i} P_i(m, n) \quad (83)$$

Energy is the summation of power over time. (Power is energy per unit time.) The total energy seen up to time n at a particular element m is

$$\mathcal{E}_i(m) \triangleq \sum_{k=-\infty}^n P_i(m, k) \quad (84)$$

Total energy measurement is useful for computing how much signal energy has been received at the input(s) and how much has been dispatched through the outputs (using matched-impedance waveguide terminations, for example).

5.3. Power Conservation at a Junction

For the N -way waveguide junction, the fundamental constraints $P^\pm = \pm U^\pm$, $P_i = P_J$, and $\Sigma U_i = 0$ yield

$$P_J \triangleq \sum_{i=1}^N P_{i*}U_i = \sum_{i=1}^N P_J U_i = P_J \sum_{i=1}^N U_i = 0 \quad (85)$$

Thus, the N -way junction is *lossless*; no net power, active or reactive, flows into or away from the junction.

5.4. Normalized Waves

We can normalize the pressure and flow variables by the Hermitian square root of the characteristic impedance to obtain propagation waves in units of root power:

$$\begin{aligned}\tilde{P}_i^+ &\triangleq Z_i^{-\frac{1}{2}} P_i^+ & \tilde{P}_i^- &\triangleq Z_i^{-\frac{1}{2}} P_i^- \\ \tilde{U}_i^+ &\triangleq Z_i^{\frac{1}{2}} U_i^+ & \tilde{U}_i^- &\triangleq Z_i^{\frac{1}{2}} U_i^-\end{aligned}\tag{86}$$

where $Z_{i*}^{\frac{1}{2}}$ is the unique para-Hermitian square root of Z_i as discussed in §4.5.

In the non-para-Hermitian case, we normalize the traveling waves by

$$\begin{aligned}\tilde{P}_i^+ &\triangleq R_i^{-\frac{1}{2}} P_i^+ & \tilde{P}_i^- &\triangleq R_i^{-\frac{1}{2}} P_i^- \\ \tilde{U}_i^+ &\triangleq R_i^{\frac{1}{2}} U_i^+ & \tilde{U}_i^- &\triangleq R_i^{\frac{1}{2}} U_i^-\end{aligned}\tag{87}$$

where

$$\begin{aligned}R_i &\triangleq \frac{1}{2}(Z_i + Z_{i*}) \\ R_{i*}^{\frac{1}{2}} &= R_i^{\frac{1}{2}}\end{aligned}\tag{88}$$

That is, $R_i^{\frac{1}{2}}$ is the para-Hermitian square root of the para-Hermitian part R_i of the i th branch impedance Z_i [14].

By restricting all waveguides to normalized waves, we obtain the WGF generalization of the *normalized ladder form* (NLF). As a result of this normalization, the stored power in each WGF section is unaffected by time variation of the characteristic impedance in each waveguide. This means that the signal power is decoupled from time variation in the filter coefficients. This topic is discussed further in [70,69].

5.5. Effects of Quantization on Scattered Power

While the ideal waveguide junction is lossless, finite wordlength effects can make exactly lossless networks unrealizable. In fixed-point arithmetic, the product of two numbers requires more bits (in general) for exact representation than either of the multiplicands. If there is a feedback loop around a junction, the number of bits needed to represent exactly a circulating signal grows without bound. Therefore, some sort of round-off rule must be included in a finite-precision implementation of a WGF.

The sum of power flows entering a junction is given by

$$\begin{aligned}
 P_J &= P_* U \triangleq \sum_{i=1}^N P_{i*} U_i \\
 &\triangleq \sum_{i=1}^N (P_{i*}^+ + P_{i*}^-)(U_i^+ + U_i^-) \\
 &= \sum_{i=1}^N (P_{i*}^+ + P_{i*}^-) \Gamma_i (P_i^+ - P_i^-)
 \end{aligned} \tag{89}$$

where $\Gamma_i = Z_i^{-1}$ is the characteristic admittance of the i th waveguide. From (85), $P_J = 0$ in the absence of quantization error for a lossless junction. Define an *inner product norm* by

$$\begin{aligned}
 \langle \underline{x}, \underline{y} \rangle_{\Gamma} &\triangleq \sum_{i=1}^N x_{i*} \Gamma_i y_i \\
 \|\underline{x}\|_{\Gamma}^2 &\triangleq \sum_{i=1}^N x_{i*} \Gamma_i x_i = \langle \underline{x}, \underline{x} \rangle_{\Gamma}
 \end{aligned} \tag{90}$$

(cf. Appendix B). Since $\Gamma_i > 0$, the quadratic form $\underline{x}_* \Gamma_i \underline{x}$ provides an elliptic

(“weighted root-mean square”) norm for x . By (89),

$$\begin{aligned} p_J &= \left\langle P^+ + P^-, P^+ - P^- \right\rangle_{\Gamma} \\ &= \|P^+\|_{\Gamma}^2 - \|P^-\|_{\Gamma}^2 + \left\langle P^-, P^+ \right\rangle_{\Gamma} - \left\langle P^+, P^- \right\rangle_{\Gamma} \end{aligned} \quad (91)$$

The junction is said to be passive if

$$p_J + p_{J^*} = 2 \left[\|P^+\|_{\Gamma}^2 - \|P^-\|_{\Gamma}^2 \right] \geq 0 \quad (92)$$

or,

$$\|P^+\|_{\Gamma} \geq \|P^-\|_{\Gamma} \quad (93)$$

Note that the definition of passivity (92) ignores the reactive component of the quantization error. While reactive power is in some sense not deliverable, its increase can use up valuable dynamic range in a fixed-point implementation.

5.6. Elimination of Limit Cycles

The guaranteed absence of limit cycles and overflow oscillations is tantamount to ensuring that all finite-wordlength effects result in power *absorption* at each junction, and never power creation.

Let $\hat{P}_i^- = P_i^- - \epsilon_i$ denote the quantized value of P_i^- . Then a sufficient condition for the absence of limit cycles and overflow oscillations in an N -port junction is

$$\|\hat{P}_i^-\|_{\Gamma} \leq \|P_i^-\|_{\Gamma} \quad (94)$$

Condition (94) ensures that roundoff errors result only in energy *absorption*.

Theorem. *In the real vector case (pressure is a real q by 1 propagating vector), a sufficient condition for the absence of overflow oscillations and limit cycles in*

networks built from N -port waveguide junctions is that magnitude truncation be used on each element of the final q by 1 outgoing wave variables P_i^- .

5.7. Dynamic Range Conservation

In finite-precision implementations, it is desirable to minimize dynamic range requirements.

Since the power flowing to the right, say, in a waveguide is given by

$$P^+ = P_*^+ U^+ = U_*^+ Z U^+ = P_*^+ \Gamma P^+ \quad (95)$$

(cf. equation (74)), we have the relations

$$\begin{aligned} \|P^+\| &\leq \|U_*^+\| \cdot \|Z\| \cdot \|U^+\| \\ \|P^+\| &\leq \|P_*^+\| \cdot \|\Gamma\| \cdot \|P^+\| \end{aligned} \quad (96)$$

where $\|\cdot\|$ denotes any matrix norm [20]. For dynamic range purposes, the *uniform norm*, or *Chebyshev norm* is most relevant. Some properties of norms are discussed in Appendix B.

In the case of scalar P, U, Z , we have

$$\|P^+\| = Z |U^+|^2 = \frac{|P^+|^2}{Z} \quad (97)$$

Equations (96) and (97) show that for a given power level, the signal variable P^+ or U^+ with smallest norm (magnitude) is determined by the characteristic impedance. In the scalar case, $Z > 1$ implies flow U is the smaller variable, while if $Z < 1$, pressure P has the smaller dynamic range.

In each branch of a waveguide network, we can independently choose the variable of propagation to be pressure or flow (cf. §4.10). Consequently, the following criterion for this choice can be used to minimize dynamic range in the network:

- If $\|Z\|_\infty > 1$, choose flow as the propagating variable.
- If $\|Z\|_\infty < 1$, choose pressure as the propagating variable.

Such a scheme can even be used adaptively in the time-varying case:

- If $\|Z(t)\|_\infty$ crosses unity from below, switch from pressure to flow.
- If $\|Z(t)\|_\infty$ crosses unity from above, switch from flow to pressure.

Note that by the above rules, if $Z_i < 1$ for all i , every branch will be a pressure branch, and if $Z_i > 1$ for all i , every branch will be a flow branch. In either of these cases, the full dynamic range inherent in the network must be borne by a single variable of propagation.

It is numerically superior to *balance* the dynamic range between pressure and flow. By multiplying all of the characteristic impedances by g such that gZ_i is greater than unity for half the waveguides and less than unity in the other half, the dynamic range is equally shared between the two variables of propagation.

To see the benefits of balancing the characteristic impedance magnitudes about unity, suppose we are given a network scaled such that $Z_i \leq 1$ for all i . Renumber the branches if necessary to obtain them in order of ascending characteristic impedance: $Z_1 \leq Z_2 \leq \dots \leq Z_N = 1$. Since all characteristic impedance magnitudes are less than or equal to 1, pressure is chosen to be the variable of propagation in every branch. Now consider the impedance scaling factor

$$g = \frac{1}{\sqrt{Z_1 Z_N}} \quad (98)$$

such that the characteristic impedance in branch i becomes $Z'_i = gZ_i$. This scaling “balances” the distribution of characteristic impedances such that $Z'_1 Z'_N = 1$, i.e.,

the geometric mean of the extreme characteristic impedances is unity. The characteristic impedances now divide into two groups such that $Z'_M < 1$ and $Z'_{M+1} > 1$ for some M between 1 and N . To minimize the probability of overflow in the scaled network, branches $M + 1$ through N now become flow branches. This way, we still have the property that each signal variable is bounded above by the signal power it represents. At the same time, we have boosted the pressure levels in branches 1 through M by $g > 1$. If $g = 2^K$, then we have effectively added K bits of precision to the signals propagating in the pressure waveguides. This is approximately a $6K$ dB increase in signal-to-noise ratio.

The strategy above reduces the probability of overflow and increases signal to quantization-noise ratio (SNR) from a global perspective. It is a good first pass, but more refinement is possible. Consider, for example, that the pressure in branch 1 and the flow in branch N are potentially much smaller than the powers they represent. It is possible that very little power flows into these branches due to the way they are connected into the network. If so, it may be that the alternative propagation variable would provide a better numerical representation without exhibiting overflow. A more refined scheme would be to measure the average power contained in the waveguide, and use the “best choice” of either pressure or flow. If the power level is below some threshold, we switch to the larger variable of propagation, while if it is above some larger threshold, we switch to the smaller variable of propagation. Thus, pressure or flow can be chosen to trade between quantization noise or probability of overflow, whichever is most important under the circumstances. It is even possible to implement this trade-off in a time-varying manner, based on observed signal characteristics in the various branches. While time-varying filter structures are usually employed to model time-varying systems, they can also be used to implement a time-invariant system with adaptive numerical conditioning.

5.8. Energy Conservation with Quantization

In some applications, energy conservation can be a primary property of the

network. The presence of roundoff in numerical computations converts a perfectly lossless network into one which gains or loses signal energy over time. To suppress limit cycles, magnitude truncation is normally used to ensure that all roundoff errors are “passive” and only decrease the energy stored in the network. However, magnitude truncation can introduce significant energy loss relative to a desired lossless network. Instead, it might be preferable to use another form of *controlled rounding* which sometimes increases and sometimes decreases scattered signal energy in order to achieve constant energy over the long term. In other terms, it is possible to “servo” the direction of energy change caused by roundoff to a desired network energy level.

Roundoff errors are in physical units of signal amplitude. Signal power, on the other hand, is in units of signal amplitude *squared*. As a result, there is no way to use “error feedback” such as that used in delta-modulation waveform coding or line-drawing algorithms in raster graphics. Instead, some measure of the energy increase or decrease due to rounding has to be computed (e.g., the sum of squared roundoff errors), and the sign or value of the net energy error can be used to control the direction of rounding. Since a sum of squares is expensive, simpler alternatives which accomplish the same effect would be useful. For example, the fact that the L_2 norm lies between the L_1 and L_∞ norms can be used to bracket the roundoff energy error between two easily computed bounds.

Note that controlling network parameters as a function of current signal energy is a potentially very rich topic. For example, a “performance gesture” in the context of digital sound synthesis from a waveguide synthesis model can be implemented by providing a servo loop which drives certain parameters of the synthesis based on the error measured between signal power in the model and that desired in the performance. In these applications [69,71], compensation of energy lost via roundoff or magnitude truncation is a free side effect.

6. Equivalent Forms in General Networks

6.1. Power-Equivalent Junctions

By (89) in §5.5, the net power at a scattering junction equals

$$P_J = \underline{P}_* \underline{U} = \underline{P}_* T_*^{-1} T_* \underline{U} \triangleq \tilde{\underline{P}}_* \tilde{\underline{U}} \quad (99)$$

where T is any nonsingular transfer-function matrix (or matrix in the scalar case), and

$$\begin{aligned} \underline{P} &\triangleq T \tilde{\underline{P}} \\ \underline{U} &\triangleq T_*^{-1} \tilde{\underline{U}} \end{aligned} \quad (100)$$

Since $\underline{P} = \underline{P}^+ + \underline{P}^- \equiv T(\tilde{\underline{P}}^+ + \tilde{\underline{P}}^-)$, we must have $\underline{P}^+ = T\tilde{\underline{P}}^+$ and $\underline{P}^- = T\tilde{\underline{P}}^-$. Thus, (21) becomes

$$T\tilde{\underline{P}}^- = \Sigma T\tilde{\underline{P}}^+ \quad (101)$$

or

$$\tilde{\underline{P}}^- = (T^{-1} \Sigma T) \tilde{\underline{P}}^+ \triangleq \tilde{\Sigma} \tilde{\underline{P}}^+ \quad (102)$$

Thus, *the power at a scattering junction is invariant with respect to a similarity transformation on the scattering matrix Σ* . All junctions related by a similarity transformation of their scattering matrices are called *power equivalent junctions*. Power equivalence can be determined by looking at the Jordan form of the scattering matrix. It can be shown that the matrix of q by q block eigenvalues of any lossless scattering matrix Σ is given by $\Lambda = \text{diag}(I_q, -I_q, -I_q, \dots, I_q)$, and the corresponding matrix of eigenvectors is equal to $\Sigma + \Lambda$.

Within a set of power equivalent junctions, junction power is fixed while the detailed scattering behavior varies; this provides one basis for the construction of *power-invariant time varying digital filters* [70].

The power equivalent junctions were obtained by scaling pressure and flow by T^{-1} and T_* , respectively. In classical network theory, T generalizes the *ideal transformer*.

6.2. Impedance Scaling

The general power-equivalence transformations replace each branch at a given junction by a new branch containing a linear combination of *all* pressure waves impinging on the junction. If we specialize to the case in which incoming waves on different branches are not mixed, then the general power-equivalence transformations reduce to *impedance scaling* of the individual incoming branches. In the general case of diagonal T , each branch impedance becomes

$$\tilde{Z}_i = t_i^{-1} Z_i t_i^{-1} \quad (103)$$

where t_i is the i th element along the diagonal of the similarity transform T for the junction scattering matrix.

In a given waveguide structure, the digital filtering characteristics are determined by the network topology and the relative characteristic impedances of the various branches. A filter is made time-varying by changing one or more characteristic impedances. Impedance-scaling provides a way to change the characteristic impedances around a junction *without* modifying the scattering characteristics of the junction. This is valuable for time-varying filter applications because we may wish to vary a reflection coefficient at one junction and not at another [70].

6.3. Equivalent Chains

In the case of *cascade* waveguide interconnection, the impedance-scaling transformations can be chosen to cancel out in the interior of the chain. When this is done, the product of the diagonal similarity transformations appears at the termination end of the chain. In the reflectively terminated case, a certain class of transforms yield equivalent networks. It is this type of transformation which can be used to convert between the so-called one-multiplier lattice (§4.4) and the normalized ladder form. The impedance-scaling transformations are valid in the time-varying

case. Therefore, properties of a given time-varying WGF can be carried over to other WGF structures which differ only by impedance scaling transformations in the time-varying case.

Cascade waveguide equivalences can be extended to all cycle-free networks of junctions and branches. These graphs have the property that there are no loops, and they appear only as "tree" structures.

6.4. Transformer Scaling

We have been concerned up to now with power equivalent junctions and the interpretation of a diagonal similarity transformation of the junction scattering matrix as a scaling of the branch impedances. When such a transformation is applied to a point within a bidirectional delay line, that point being viewed as a lossless two-port junction, the resulting two-port is called a *waveguide transformer*.

6.5. Generalized Transformer Equivalences

If a waveguide is considered as an input/output port of some waveguide network, then the "round-trip" transfer function is unchanged if the forward and reverse branches are cascaded with a pair of transfer functions whose product is the identity*. The argument immediately generalizes throughout a cycle-free tree.

Delay-free transformer equivalences hold in the time-varying case.

6.6. Delay Equivalences

If a waveguide is considered as an input/output port of some waveguide network, then the "round-trip" transfer function is unchanged if the forward and

* Only stable, minimum-phase transfer functions can be used as components of a generalized transformer. For example, allpass filters do not qualify. Allpass filters are generalized delays—not transformers.

reverse delays are redistributed. Progressing through the tree, junction by junction, the same argument can be applied to each subtree of each junction.

Two delay-equivalent trees are not the same if “taps” are allowed. The wave variables are very different in the tree. However, there exists a new set of taps which can provide an arbitrary transfer function numerator up to the network order.

A special case of delay equivalence is when all forward delays are set to zero, and all return delays are twice their original length. In this way, a full-rate tree is converted to a half-rate tree (cf. §3.5). This is how the conventional forms of lattice filter structures can be derived from WGF structures.

Delay equivalences do not provide equivalent trees in the time-varying case. Delay equivalence relies on time-invariance of the branch impedances. In the time-varying case, WGF structures and ladder/lattice structures differ. In [70] it is shown that this difference is a relative time skew of the scattering coefficients. Therefore, by compensating for this time skew, the favorable properties of the WGF can be extended to all half-rate, delay-equivalent trees and hence all ladder and lattice digital filters in the time-varying case.

6.7. (π, σ) -Parameters

It is possible to develop a parametrization of the waveguide in terms of (π, σ) -parameters which are an extension of the π -parameters utilized by Markel and Gray [36]. The (π, σ) -parameters combine the degrees of freedom available from delay and transformer equivalences.

Using (π, σ) -parameters, structural variations can be derived which are multi-dimensional generalizations of the well-known Kelly-Lochbaum, normalized ladder, two-multiplier lattice, and one-multiplier lattice structures discussed by Markel and Gray [36]. Each structure has a set of sign parameters which select between pressure and flow as the wave variable. The sign parameters can be used to optimize dynamic range or signal-to-noise ratio in any of the structures except the NLF.

(The NLF is invariant with respect to sign parameters.) The Kelly-Lochbaum form is the most direct physical model. The one-multiplier lattice is essentially the same as the Kelly-Lochbaum section. The NLF is energy normalized in the time-varying case.

6.8. Nested Structures

It is possible to generalize the WGF in such a way that each reflection coefficient is replaced by a general transfer function. This formulation is convenient for modeling physical systems having frequency-dependent scattering.

6.9. Time Reversal

As a direct result of fact that waveguide networks conserve energy, they can be run *backwards* in time. The junctions are invertible in the sense that if the scattered waves are fed to the junction, the output is the incident waves which generated the scattered waves in the first place. Therefore, a WGF can have a “reverse” switch. Flipping this switch causes the direction of propagation in each delay line to reverse. Input and output exchange at each junction port. The reverse bit can be flipped at any time.

There are many possible applications for time reversal. Some of these include:

- Inverse filtering requires nothing more than time reversal.
 - Upon overflow, the computation can be run backwards far enough so that moving forward again with a slowly increasing loss will be sufficient to prevent the overflow and not disrupt the signal too much.
 - Time can be run forward to *encode* a signal and backward to *decode* it.
 - Artificial sustain of a pulsed, lossy, waveguide network can be implemented by moving forward and backward in time, either periodically or randomly.
-

(Usual end-point conditioning techniques needed for forward-backward looping in “sampling synthesis” should be employed.)

7. Conclusions

We have derived a general framework for recursive digital filtering, based on “waveguide” theory, which has many desirable properties resulting from the physical interpretation and the definition of instantaneous power with respect to space and time. Waveguide digital filters are natural for implementing physically meaningful or time-varying recursive networks, or when it is desired to eliminate limit cycles and overflow oscillations. The computational complexity of a waveguide digital filter need not be greater than that of competing digital filter structures. They can be viewed as a generalization of ladder digital filters in several directions: traveling waves are (optionally) generalized to complex nonsquare matrices, the signal delays are “balanced” between the upper and lower ladder “rails,” and a richer set of physical models can be built using multiway branching of waveguide sections.

8. Appendix A—The Wave Equation

For an ideal acoustic waveguide, we have the following *wave equation*.

$$P_{tt}(x, t) = c^2 P_{xx}(x, t), \quad (104)$$

where $P(x, t)$ denotes longitudinal pressure displacement in the tube at the point x along the tube at time t in seconds. If the length of the tube is L , then x is taken to lie between 0 and L . The partial derivative notation used above is defined by

$$P_{xy} \triangleq \frac{\partial}{\partial x} \left(\frac{\partial P}{\partial y} \right). \quad (105)$$

The constant c is given by $c = \sqrt{\tau/\rho}$ where τ is the “tension” of the gas in the tube (cf. §3.1) and ρ is the mass per unit length of the tube. An elegant derivation of the wave equation is given by Morse [4].

The general *traveling-wave* solution to (104) is given by

$$P(x, t) = P^+(x - ct) + P^-(x + ct). \quad (106)$$

This solution form is interpreted as the sum of two fixed wave-shapes traveling in opposite directions along the tube. The specific waveshapes are determined by the initial pressure $P(x, 0)$ and flow $U(x, 0)$ throughout the tube.

9. Appendix B—Norms

Definition 1. Let P be a vector in the vector space \mathbf{P} [15]. A real-valued function of P is called a *norm*, denoted $\|P\|$, if it satisfies the following three properties:

- (1) $\|P\| \geq 0$, and $\|P\| = 0 \Leftrightarrow P = 0$.
- (2) $\|cP\| = |c| \cdot \|P\|$, c a scalar.
- (3) $\|P_1 + P_2\| \leq \|P_1\| + \|P_2\|$.

The functional $\|P_1 - P_2\|$ serves as a distance function on \mathbf{P} , so a normed linear space is also a metric space.

Definition 2. A *pseudo-norm* is a real-valued function of $P \in \mathbf{P}$ satisfying the following three properties:

- (1) $\|P\| \geq 0$, and $P = 0 \Leftrightarrow \|P\| = 0$.
- (2) $\|cP\| = |c| \cdot \|P\|$, c a scalar.
- (3) $\|P_1 + P_2\| \leq \|P_1\| + \|P_2\|$.

A pseudo-norm differs from a norm in that the pseudo-norm can be zero for nonzero vectors (functions).

In this paper, \mathbf{P} is the space of continuous complex matrix functions on the unit circle in the complex plane. For cases of practical importance, the analytic

continuation of $P \in \mathbf{P}$ exists and is analytic in the closed unit disk. The norm is not changed by multiplication by any function of modulus 1 on the unit circle. In signal processing terms, we can say that the norm is unchanged by multiplication by a unity-gain allpass filter (also known as a Blaschke product).

The L_p norms are defined on \mathbf{P} by

$$\|P\|_p \triangleq \left(\frac{1}{2\pi} \int_{-\pi}^{\pi} \left[\text{Tr} \left\{ P_*(e^{j\omega}) P(e^{j\omega}) \right\} \right]^{p/2} \frac{d\omega}{2\pi} \right)^{1/p}, \quad p \geq 1 \quad (107)$$

where $\text{Tr}\{P\}$ denotes the trace of P , and $P_*(e^{j\omega}) = \overline{P(e^{j\omega})}^T$ is the transpose complex conjugate of $P(e^{j\omega})$ (Hermitian conjugate). The analytic continuation of $P_*(e^{j\omega})$ is called the para-Hermitian conjugate of $P(z)$.

L_p norms are technically pseudo-norms; if each function in L_p is replaced by an equivalence class containing all functions equal to the given function almost everywhere, then a true norm is obtained.

The *weighted* L_p norms are defined by

$$\|P\|_p \triangleq \left(\frac{1}{2\pi} \int_{-\pi}^{\pi} \left[\text{Tr} \left\{ P_*(e^{j\omega}) P(e^{j\omega}) \right\} \right]^{p/2} W(e^{j\omega}) \frac{d\omega}{2\pi} \right)^{1/p}, \quad p \geq 1 \quad (108)$$

where $W(e^{j\omega})$ is real, positive, and integrable. Typically, $\int W = 1$. If $W(e^{j\omega}) = 0$ for a set of nonzero measure, then a new pseudo-norm results.

Definition 3. A matrix function $P(e^{j\omega})$ is said to belong to the space L_p if

$$\int_{-\pi}^{\pi} \left[\text{Tr} \left\{ P_*(e^{j\omega}) P(e^{j\omega}) \right\} \right]^{p/2} \frac{d\omega}{2\pi} < \infty$$

Definition 4. A matrix function $P(e^{j\omega})$ is said to belong to the space H_p if it is in L_p and if its analytic continuation $P(z)$ is analytic for $|z| < 1$. $P(z)$ is said to be in H_{-p} if $P(z^{-1}) \in H_p$.

The case $p = 2$ gives the popular *root mean square* norm, and $\|\cdot\|_2^2$ can be interpreted as the square root of the total energy of P in many physical contexts.

An advantage of working in L_2 is that the norm is provided by an *inner product*,

$$\langle P, U \rangle \triangleq \int_{-\pi}^{\pi} P_*(e^{j\omega})U(e^{j\omega})\frac{d\omega}{2\pi}$$

The norm of a vector $P \in L_2$ is then given by

$$\|P\| \triangleq \sqrt{\text{Tr}\langle P, P \rangle}$$

As p approaches infinity in (107), the norm is dominated by the largest values of $P(e^{j\omega})$. Accordingly, we define the *Chebyshev* or *uniform* norm by

$$\|P\|_{\infty} \triangleq \max_{-\pi < \omega \leq \pi} |P(e^{j\omega})| \quad (109)$$

where

$$|P| \triangleq \sqrt{\text{Tr}\{P_*(e^{j\omega})P(e^{j\omega})\}} \quad (110)$$

is called the *absolute value* of P .

9.1. Discrete Norms

A *discrete norm* is a norm defined on a finite-dimensional vector space. An element \underline{P} of such a space has a finite number of components $\underline{P} = [P_0, P_1, P_2, \dots, P_{N-1}]$.

The *discrete L_p norm* is defined by

$$\|P\|_p \triangleq \left(\sum_{n=0}^{N-1} \|P_n\|^p \right)^{1/p}, \quad p \geq 1 \quad (111)$$

where $\|P_n\|$ is any norm suitable for the object P_n . For example, P_n can be a rational transfer function matrix.

The *normalized discrete L_p norm* is defined by

$$[[P]]_p \triangleq \left(\frac{1}{N} \sum_{n=0}^{N-1} \|P_n\|^p \right)^{1/p}, \quad p \geq 1 \quad (112)$$

As before, the case of $p = \infty$ reduces to the maximum element:

$$\|P\|_\infty = [[P]]_\infty = \max_n \{\|P_n\|\} \quad (113)$$

For discrete norms we have the following.

Theorem 5.

$$[[P]]_1 \leq [[P]]_2 \leq [[P]]_\infty = [[P]]_\infty \leq [[P]]_2 \leq [[P]]_1 = N[[P]]_1 \quad (114)$$

9.2. Matrix Norms

The *Frobenius norm* of an $m \times n$ matrix A is defined as

$$\|A\|_f \triangleq \sqrt{\sum_{i=1}^m \sum_{j=1}^n |a_{ij}|^2}$$

That is, the Frobenius norm is the L_2 norm applied to the elements of the matrix. For this norm there exists the following.

Theorem 6. The unique $m \times n$ rank k matrix B which minimizes $\|A - B\|_f$ is given by $U\Sigma_k V^*$, where $A = U\Sigma V^*$ is a singular value decomposition of A , and Σ_k is formed from Σ by setting to zero all but the k largest singular values.

Proof. See Golub and Kahan [13].

The *induced norm* of a matrix A is defined in terms of the norm defined for the vectors P on which it operates,

$$\|A\| \triangleq \sup_P \frac{\|AP\|}{\|P\|}$$

For the L_2 norm, we have

$$\|A\|_2^2 = \sup_P \frac{P^T A^T A P}{P^T P}$$

and this is called the *spectral norm* of the matrix A .

The *Chebyshev induced norm* is defined in this case for

$$\|A\|_\infty \triangleq \max_P \frac{\|AP\|}{\|P\|} \quad (115)$$

where A is a q by m matrix of analytic functions, P is an m by 1 vector of analytic functions, and

$$\|P\|_\infty \triangleq \max_i \max_{-\pi < \omega \leq \pi} |P_i(e^{j\omega})| \quad (116)$$

The Chebyshev induced norm reduces to the “maximum row sum” for square matrices [20, p. 23], that is, for $m = q$,

$$\|A\|_\infty = \max_{i=1, \dots, q} \sum_{j=1}^q \|A[i, j]\|_\infty$$

Similarly, the L_1 norm reduces to the maximum column sum.

10. References

- [1] G. Szegő, “Ein Grenzwertsatz über die Toeplitzischen Determinanten einer Reellen Positiven Funktion,” *Math. Ann.*, vol. 76, pp. 490–503, 1915.

- [2] G. Szegő, *Orthogonal Polynomials*, Amer. Math. Soc., Colloq. Publ. no. 23, New York, 1939.
 - [3] N. Levinson, "The Wiener RMS (Root-Mean-Square) Error Criterion in Filter Design and Prediction," *J. Math. Physics*, vol. 25, pp. 261–278, 1947.
 - [4] P. M. Morse, *Vibration and Sound*, published by the American Institute of Physics for the Acoustical Society of America, 1976 (1st ed. 1936, 2nd ed. 1948).
 - [5] Z. Nehari, *Conformal Mapping*, Dover, New York, 1952.
 - [6] U. Grenander and G. Szegő, *Toeplitz Forms and their Applications*, University of California Press, Berkeley and Los Angeles CA, 1958.
 - [7] M. E. Van Valkenburg, *Introduction to Modern Network Synthesis*, John Wiley and Sons, Inc., New York, 1960.
 - [8] J. Durbin, "The Fitting of Time Series Models," *Rev. L'Institut Intl. de Statistique*, vol. 28, pp. 233–243, 1960.
 - [9] R. Plonsey and R. E. Collin, *Principles and Applications of Electromagnetic Fields*, McGraw-Hill, New York, 1961.
 - [10] *Banach Spaces of Analytic Functions*, Prentice-Hall Inc., Englewood Cliffs, NJ, 1962.
 - [11] V. Belevitch, "Summary of the History of Circuit Theory," *Proc. IRE*, vol. 50, no. 5, pp. 848–855, May 1962.
 - [12] N. I. Achieser, *The Classical Moment Problem*, Oliver and Boyd, Edinburgh, 1965.
 - [13] G. Golub and W. Kahan, *Calculating the Singular Values and Pseudo-Inverse of a Matrix*, *J. SIAM Numer. Anal. (Ser. B)*, vol. 2, no. 2, pp. 205–224, 1965.
 - [14] V. Belevitch, *Classical Network Theory*, Holden Day, San Francisco, CA, 1968.
 - [15] B. Noble, *Applied Linear Algebra*, Prentice-Hall Inc., Englewood Cliffs, NJ, 1969, 1977.
-

- [16] V. M. Adamjan, D. Z. Arov, and M. G. Krein, "Analytic Properties of Schmidt Pairs for a Hankel Operator and the Generalized Schur-Takagi Problem," *Math. USSR Sbornik*, vol. 15, pp. 31-73, 1971.
 - [17] N. G. Kingsbury and P. J. W. Rayner, "Digital Filtering using Logarithmic Arithmetic," *Electron. Lett.*, vol. 7, pp. 56-58, Feb. 1971.
 - [18] A. Fettweis, "Digital Filters Related to Classical Structures," *AEU: Archive für Elektronik und Übertragungstechnik*, vol. 25, pp. 79-89, Feb. 1971.
 - [19] A. Fettweis, "Some Principles of Designing Digital Filters Imitating Classical Filter Structures," *IEEE Trans. on Circ. Theory*, vol. CT-18, pp. 314-316, March 1971.
 - [20] J. M. Ortega, *Numerical Analysis*, Academic Press, New York, 1972.
 - [21] J. L. Flanagan, *Speech Analysis, Synthesis, and Perception*, Springer-Verlag, New York, 1972.
 - [22] A. Fettweis, "Pseudopassivity, Sensitivity, and Stability of Wave Digital Filters," *IEEE Trans. on Circ. Theory*, vol. CT-19, pp. 668-673, Nov. 1972.
 - [23] D. C. Youla, J. D. Rhodes, and P. C. Marston, "Driving-Point Synthesis of Resistor-Terminated Cascades Composed of Lumped Lossless Passive 2-Ports and Commensurate TEM Lines," *IEEE Trans. on Circ. Theory*, vol. CT-19, pp. 648-664, Nov. 1972.
 - [24] D. C. Youla, J. D. Rhodes, and P. C. Marston, "Recent Developments in the Synthesis of a Class of Lumped-Distributed Filters," *Int. J. Circuit Theory Appl.*, vol. 10, pp. 159-70, 1973.
 - [25] A. Sedlmeyer and A. Fettweis, "Digital Filters with True Ladder Configuration," *Int. J. Circuit Theory Appl.*, vol. 1, pp. 5-10, 1973.
 - [26] A. Fettweis, "Reciprocity, Inter-Reciprocity, and Transposition in Wave Digital Filters," *Int. J. Circuit Theory Appl.*, vol. 1, pp. 323-337, 1973.
 - [27] A. H. Gray and J. D. Markel, "Digital Lattice and Ladder Filter Synthesis," *IEEE Trans. on Audio Electroacoust.*, vol. AU-21, pp. 491-500, Dec. 1973.
-

- [28] A. Fettweis, "Wave Digital Lattice Filters," *Int. J. Circuit Theory Appl.*, vol. 2, pp. 203–211, 1974.
 - [29] A. Fettweis, "Wave Digital Filters with Reduced Number of Delays," *Int. J. Circuit Theory Appl.*, vol. 2, pp. 319–330, 1974.
 - [30] K. Meerkötter and W. Wegener, "A New Second-Order Digital Filter without Parasitic Oscillations," *AEU: Archive für Elektronik und Übertragungstechnik*, vol. 29, pp. 312–314, Feb. 1975.
 - [31] A. Fettweis and K. Meerkötter, "Suppression of Parasitic Oscillations in Wave Digital Filters," *IEEE Trans. Circ. and Sys.*, vol. CAS-22, No. 3, pp. 239–246, Mar. 1975.
 - [32] A. Fettweis and K. Meerkötter, "On Adaptors for Wave Digital Filters," *IEEE Trans. on Acoust., Speech, and Signal Proc.*, vol. ASSP-23, pp. 516–525, Dec. 1975.
 - [33] L. R. Rabiner and B. Gold, *Theory and Application of Digital Signal Processing*, Prentice-Hall Inc., Englewood Cliffs, NJ, 1975.
 - [34] A. H. Gray and J. D. Markel, "A Normalized Digital Filter Structure," *IEEE Trans. on Acoust., Speech, and Signal Proc.*, vol. ASSP-23, pp. 268–277, June 1975.
 - [35] E. E. Swartzlander, Jr., and A. G. Alexopoulos, "The Sign/Logarithm Number System," *IEEE Trans. Computers*, vol. C-24, pp. 1238–1242, Dec. 1975.
 - [36] J. D. Markel and A. H. Gray, *Linear Prediction of Speech*, Springer-Verlag, New York, 1976.
 - [37] S. C. Lee and A. D. Edgar, "The Focus Number System," *IEEE Trans. Computers*, vol. C-26, pp. 1167–1170, Nov. 1977.
 - [38] S. C. Lee and A. D. Edgar, "Focus Microcomputer Number System," in *Microcomputer Design and Applications*, S. C. Lee, ed., Academic Press, New York, 1977.
 - [39] S. S. Lawson, "On a Generalization of the Wave Digital Filter Concept," *Int. J. Circuit Theory Appl.*, vol. 6, pp. 107–120, 1978.
-

- [40] P. H. Delsarte, Y. V. Genin, and Y. Kamp, "Orthogonal Polynomial Matrices on the Unit Circle," *IEEE Trans. Circ. and Sys.*, vol. CAS-25, pp. 145-160, 1978.
 - [41] P. DeWilde, A. C. Vieira, and T. Kailath, "On a Generalized Szegő-Levinson Realization Algorithm for Optimal Linear Predictors Based on a Network Synthesis Approach," *IEEE Trans. Circ. and Sys.*, vol. CAS-25, No. 9, pp. 663-675, September 1978.
 - [42] L. V. Ahlfors, *Complex Analysis*, McGraw-Hill, New York, 1979.
 - [43] Digital Signal Processing Committee, ed., *Programs for Digital Signal Processing*, IEEE Press, New York, 1979.
 - [44] P. H. Delsarte, Y. V. Genin, and Y. Kamp, "The Nevanlinna-Pick Problem for Matrix-Valued Functions," *Soc. for Indust. and Appl. Math.*, vol. 36, no. 1, pp. 47-61, Feb. 1979.
 - [45] A. D. Edgar, "Focus Microcomputer Number System," *Comm. of the ACM*, vol. 22, pp. 166-177, March 1979.
 - [46] A. Bultheel and P. Dewilde, "On the Relation between Padé Approximation Algorithms and Levinson/Schur Recursive Methods," *Sig. Proc.: Th. and Appl.*, M. Kunt and F. de Coulon, eds., North-Holland, (EURASIP), pp. 517-523, 1980.
 - [47] A. H. Gray, "Passive Cascaded Lattice Digital Filters," *IEEE Trans. Circ. and Sys.*, vol. CAS-27, No. 5, pp. 337-344, May 1980.
 - [48] T. Kurokawa, J. A. Payne, and S. C. Lee, "Error Analysis of Recursive Digital Filters Implemented with Logarithmic Number Systems," *IEEE Trans. on Acoust., Speech, and Signal Proc.*, vol. ASSP-28, pp. 706-715, Dec. 1980.
 - [49] P. DeWilde and H. Dym, "Schur Recursions, Error Formulas, and Convergence of Rational Estimators for Stationary Stochastic Estimators," *IEEE Trans. on Info. Theory*, vol. IT-27, pp. 446-461, July 1981.
 - [50] A. Fettweis, "Principles of Complex Wave Digital Filters," *Int. J. Circuit Theory Appl.*, vol. 9, pp. 119-134, 1981.
-

- [51] P. DeWilde and H. Dym, "Lossless Chain Scattering Matrices and Optimum Linear Prediction: The Vector Case," *Int. J. Circuit Theory Appl.*, vol. 9, pp. 135-175, 1981.
 - [52] P. H. Delsarte, Y. V. Genin, and Y. Kamp, "On the Role of the Nevanlinna-Pick Problem in Circuit and System Theory," *Int. J. Circuit Theory Appl.*, vol. 9, no. 2, pp. 177-187, April 1981.
 - [53] P. DeWilde, *Orthogonal Filters*, class notes, EE702, Stanford University, Stanford CA, Fall 1982.
 - [54] B. Friedlander, "Lattice Filters for Adaptive Processing," *Proc. IEEE*, vol. 70, pp. 829-867, Aug. 1982.
 - [55] B. Yegnanarayana, "Design of Recursive Group-Delay Filters by Autoregressive Modeling," *IEEE Trans. on Acoust., Speech, and Signal Proc.*, vol. ASSP-30, pp. 632-637, Aug. 1982.
 - [56] J. B. Allen, private communication.
 - [57] J. O. Smith, "Techniques for Digital Filter Design and System Identification with Application to the Violin," Ph.D. Dissertation, Elec. Eng. Dept., Stanford University, June 1983.
 - [58] D. Jaffe and J. O. Smith, "Extensions of the Karplus-Strong Plucked String Algorithm," *Computer Music J.*, vol. 7, no. 2, pp. 56-69, 1983.
 - [59] B. Friedlander, "Efficient Computation of the Covariance Sequence of an Autoregressive Process," *IEEE Trans. Automat. Contr.*, vol. AC-28, No. 1, pp. 97-99, Jan. 1983.
 - [60] A. Fettweis, "Digital Circuits and Systems," *IEEE Trans. Circ. and Sys.*, vol. CAS-31, No. 1, pp. 31-48, Jan. 1984.
 - [61] B. Friedlander and J. O. Smith, "Analysis and Performance Evaluation of an Adaptive Notch Filter," *IEEE Trans. on Info. Theory*, vol. IT-30, pp. 283-295, March 1984.
-

- [62] P. P. Vaidyanathan and Sanjit K. Mitra, "Low Passband Sensitivity Digital Filters: A Generalized Viewpoint and Synthesis Procedures," *Proc. IEEE*, vol. 72, pp. 404-423, April 1984.
 - [63] W. A. Schneider, "The Common Depth Point Stack," *Proc. IEEE*, vol. 72, pp. 1238-1254, Oct. 1984.
 - [64] P. P. Vaidyanathan, "The Doubly Terminated Lossless Digital Two-Pair in Digital Filtering," *IEEE Trans. Circ. and Sys.*, vol. CAS-32, No. 2, pp. 197-200, Feb. 1985.
 - [65] P. P. Vaidyanathan and S. K. Mitra, "Passivity Properties of Low-Sensitivity Digital Filter Structures," *IEEE Trans. Circ. and Sys.*, vol. CAS-32, No. 3, pp. 217-224, March 1985.
 - [66] M. L. Frey and F. J. Taylor, "A Table Reduction Technique for Logarithmically Architected Digital Filters," *IEEE Trans. on Acoust., Speech, and Signal Proc.*, vol. ASSP-33, pp. 718-719, June 1985.
 - [67] P. P. Vaidyanathan, "The Discrete-Time Bounded-Real Lemma in Digital Filtering," *IEEE Trans. Circ. and Sys.*, vol. CAS-32, No. 9, pp. 918-924, Sep. 1985.
 - [68] S. Basu and A. Fettweis, "On the Factorization of Scattering Transfer Matrices of Multidimensional Lossless Two-Ports," *IEEE Trans. Circ. and Sys.*, vol. CAS-32, No. 9, pp. 925-934, Sep. 1985.
 - [69] J. O. Smith, "A New Approach to Digital Reverberation using Closed Waveguide Networks," *Proc. 1985 Int. Conf. Computer Music, Vancouver Canada*, Computer Music Assoc., 1985. Music Dept. Tech. Rep. STAN-M-31, Stanford University, July 1985.
 - [70] J. O. Smith, "Elimination of Limit Cycles and Overflow Oscillations in Time-Varying Lattice and Ladder Digital Filters," Music Dept. Tech. Rep. STAN-M-35, Stanford University, May 1986. Shorter version, "Elimination of Limit Cycles in Time-Varying Lattice/Ladder Filters," in *Proc. IEEE Conf. Circuits and Systems*, San Jose, May 1986.
-

- [71] J. O. Smith, "Efficient Simulation of the Reed-Bore and Bow-String Mechanisms,"
Proc. 1986 Int. Conf. Computer Music,, The Hague, Netherlands.
-

